Charles University in Prague, Faculty of Science
Institute of Geology and Palaeontology

Climatic, tectonic and provenance record of the Permian non-marine deposits of the Krkonoše Piedmont Basin

PhD Thesis

Author: Mgr. Karel Martínek
Supervisor: Assoc. Prof. RNDr. Stanislav Opluštil, Ph.D.
Consultant: Prof. RNDr. Jiří Pešek, DrSc.

Prague 2008
Czech Republic

Motto:

Blessed is the man who finds wisdom,
the man who gains understanding,

for she is more profitable than silver
and yields better returns than gold.

She is more precious than rubies;
nothing you desire can compare with her.

Long life is in her right hand;
in her left hand are riches and honour.

Her ways are pleasant ways,
and all her paths are peace.

Proverbs 3 : 13 – 17

Many thanks to Marta, Julie, Adéla and many others
for patience and inspiration.

Summary

The PhD thesis covers three main research topics: 1) palaeoclimatology of the lacustrine deposits of Rudník member based on sedimentology and geochemistry; 2) facies analysis, architectural analysis and stratigraphy of the alluvial deposits of Trutnov Formation, using also heavy minerals and gamma-ray logging; 3) provenance study based on the heavy mineral assemblages and composition of detrital garnets of Permian and Pennsylvanian sandstones. All case studies were done in the Krkonoše Piedmont Basin (KPB) which formed in the northern part of the Bohemian Massif as a post-Variscan basin of inferred extensional/transtensional regime and records a history of continental sedimentation between the Late Carboniferous and Early Triassic.

The Lower Permian Rudník member is the most extensive lacustrine deposit in the KPB. Grey to black and variegated lacustrine mudstones, laminites and carbonates of the Rudník member have a lateral extent of more than 400 km^2. In the studied sections four facies associations were recognised: A) anoxic offshore, B) suboxic to oxic offshore, C) nearshore and mudflat, and D) slope deposits. In the northern part of the E – W elongated basin, anoxic to suboxic organic-rich offshore lacustrine facies dominate and form a succession up to 130 m thick. Fan-delta and turbidite facies occur locally along the faulted northern basin margin. The central part of the basin is occupied by anoxic to oxic offshore facies interfingering with nearshore carbonate and mudflat facies of the low-gradient lacustrine margin. In the central part of the basin, the thickness of the lacustrine deposits of the Rudník member reaches up to 60 – 70 m. In the southern part of the basin fluvial and alluvial plain facies dominate and alternate with minor lacustrine nearshore facies. The lateral facies distribution indicates that subsidence along the northern basin fault was the main mechanism generating the asymmetric infill geometry in the basin's half-graben setting.

The $\delta^{18}O$ values of primary and early diagenetic calcite range between -11.0 and +1.3‰ (V-PDB) and $\delta^{13}C$ values between -5.1 and +3.7‰; most of the data fall within the range of freshwater limestones. Coarser-grained pure microspar laminae show more positive $\delta^{13}C$ values in comparison to clayey organic-rich micrite laminae, and are interpreted as a record of bioinduced precipitation during seasonal eutrophication. The obtained $\delta^{13}C_{TOC}$ values range from -29.0 to -24.0‰, the total organic carbon (TOC) content from 0.26 to 23%. Maceral analysis and Rock Eval pyrolysis indicate that most of the samples contain a mixture of aquatic and terrestrial organic matter, but two minor, distinctive groups of samples with algally-dominated and terrestrially-dominated organic matter composition, respectively, were also found. The study of vertical changes in boron content in the clay fraction of the lacustrine mudstones shows that high lake level stages were periods of lower salinity with the lowest boron contents (from 73 to 268 ppm), and periods of falling lake level were followed by significant increases in salinity with much higher boron values (293 – 603 ppm).

Lake-level fluctuations of the Rudník lacustrine system, which are recorded by shallowing-up units of sedimentary facies within most of the sections throughout the basin, can also be traced within the monotonous black shale dominated sections, where no sedimentological evidence of these lake level changes exists. Good indicators for such changes seem to be the $\delta^{18}O$ and $\delta^{13}C$ values of primary calcite, $\delta^{13}C_{TOC}$ and HI. These lake level fluctuations are interpreted as driven by climatic oscillations in the order of tens of thousands years, which could reflect climatic changes connected with the last glaciation event of Gondwana.

The second study interprets the characteristics of a depositional system of the Trutnov Formation in the KPB and the controls on its deposition. The Trutnov Náchod subbasin (TNSB), which contains the Trutnov Formation, is probably a pull-apart structure superimposed on the eastern part of the KPB during the Permian – Triassic period. The identification of basin-wide tectonic events and the climatic record in continental deposits and changes in fluvial style in basin and meso-scale was enabled by integration of several methods, despite of unsatisfactory outcrop and borehole coverage. This study integrates recognition of smaller-scale sedimentary features observed in outcrops with basin-scale features, which can be identified by correlation of individual outcrops to well-logs using heavy mineral data and outcrop gamma-ray logging.

Based mainly on well-log data, the Trutnov Formation is divided into three main genetic stratigraphic units. Well-log data also give an insight to the relationships between the southern and northern parts of the basin. Unit 1 is represented by alluvial conglomerates in the south, passing to alluvial mudstones and siltstones in the central and playa lake calcareous mudstones with gypsum in the northern parts of the basin. Overlying Units 2 and 3 record the onset of fluvial conglomerates' deposition in the north, fluvial sandstones in the centre and a continuous alluvial fan – fluvial conglomerate sedimentation in the south of the TNSB. The unconformity at the base of Unit 2 is a basin-wide correlative erosional surface, which marks an important palaeogeographic change.

The detailed outcrop study focused on the conglomerates and sandstones of Units 2 and 3, which are exposed. Most of the conglomerates are situated along the northern and southern basin margins and are interpreted as fluvial-dominated, distal alluvial fan deposits. Sandstones occur mainly in the central part of the basin. Channel-fill sandstones, crevasse splay deposits, and calcretes/dolocretes are interpreted in the sandstone facies. The strata are interpreted to have been deposited by a low-sinuosity river system with the dominant paleocurrent direction being to

the SE. The high variation in discharge, observed in individual measured sections 10-15 m thick and indicated by the variations in bedform type and grain size, preservation of highly unstable rock fragments, as well as the abundance of calcretes/dolocretes, suggest seasonal to ephemeral flow and arid/semiarid climatic conditions.

Distinct heavy mineral assemblages were used to correlate up to 15 km distant outcrops scattered across the basin, and allowed a larger-scale vertical trend within Units 2 and 3 to be seen. The lower part is characterized by thicker stratal units, finer-grained moderately sorted material, a low proportion of calcretes/dolocretes and bioturbation and low carbonate cementation of most of the sandstones. The upper part is characterized by generally thinner stratal units, poor sorting, a higher proportion of rip-up clasts, abundant calcretes and bioturbation, and pronounced erosional features. This vertical trend is probably a record of transition to generally lower and ephemeral discharge caused by more arid climatic conditions.

The main changes in basin fill architecture are interpreted as major tectonic events. The onset of the Trutnov Formation deposition is interpreted as a major tectonic reactivation at the Autunian/Saxonian (Lower/Upper Rotliegend) boundary, when the extensional regime changed to a strike-slip regime accompanied by a transpressional uplift of the central part of the KPB. The unconformity between Units 1 and 2 and the onset of high sandy sedimentation at the central part of the basin is interpreted as a later progradation of the coarse-grained material during the period of mostly inactive faults. The deposition of low-sinuosity sandstone dominated fluvial sediments over the mudstone dominated playa deposits must have been caused by a steepening of the depositional gradient and was probably accompanied by a change of climate to more humid conditions, which can most easily explain the increase in sediment supply to the basin. This interpretation is supported by the arid/semiarid conditions of Unit 1, the perennial character (more humid) of the lower part of Unit 2 and an ephemeral fluvial system (back to arid/semiarid) of the top of Unit 2. The TNSB is interpreted as a pull-apart basin in which deposition was governed by two major north-west oriented dextral strike-slip faults, Hronov-Poříčí FZ and Pilníkov FZ, which formed releasing stepover pull-apart basin.

The third study focuses on identifying major source areas in several intervals mainly in the Permian of the Krkonoše Piedmont Basin and integrates it with existing sedimentological data. Pebbles in Asselian – Guadalupian conglomerates of alluvial fan, nearshore lacustrine and lacustrine fan-delta deposits, which were deposited close to the northwestern and southeastern basin margin, respectively, correspond almost exclusively to local material from adjacent crystalline complexes.The heavy mineral associations of the sandstone matrix of these conglomerates support this interpretation. Crystalline units of the south-western part of the Krkonoše-Jizera Crystalline Complex and Orlice-Sněžník Crystalline Complex, respectively, are considered as the most favourable source.

Two main possible source areas for the fluvial Asselian deposits (Vrchlabí Formation) of the south-western part of the basin were found. Pebbles of late Devonian – early Carboniferous marine limestones probably come from the central part of the hypothetical Jítrava Hradec Basin. The garnet composition in sand detrital material points to leucogranites and pegmatites of the north-eastern Moldanubian Zone, the Přibyslavice area, as the possible source areas.

Guadalupian fluvial deposits reveal a wide range of sources, which can be attributed to the recycling of detrital material from Cisuralian and Carboniferous deposits. Garnet compositions indicate Moldanubian granulites, garnet clinopyroxenites, leucogranites and pegmatites as a possible source. We infer that Moldanubian granulites and garnet clinopyroxenites were exposed to an erosion level in the Early Permian at the latest.

Keywords: Krkonoše Piedmont Basin, Permian, Bohemian Massif, half-graben, lacustrine facies, lake level changes, stable isotopes, maceral analysis, hydrogen index, boron, climate change, fluvial facies, fluvial architectures, well-logs, tectonic and climatic controls, provenance, heavy minerals, pebble composition, detrital garnet composition.

Contents:

Introduction

This PhD thesis is a result of my research in the Krkonoše Piedmont Basin, which comprises three main projects: 1) „Environmental changes at the Carboniferous/Permian boundary and their impact on the floral and faunal assemblages of the fossiliferous lacustrine horizons of the Krkonoše Piedmont Basin.“ project of the Grant Agency of the Czech Republic to Martin Blecha (GAČR 205/94/0692, 1994 – 1996), 2) „Tectonic and climatic controls on the Permo-Triassic evolution of the Krkonoše-piedmont and Intra-Sudetic basins: early post-orogenic history of the NE part of the Bohemian Massif.“ project GAČR to David Uličný (205/99/0739, 1999 – 2001), and 3) „Spatial and temporal changes of sandstone provenance in the Krkonoše Piedmont Basin and their tectonosedimentary implications.“ project of the Grant Agency of the Czech Academy of Sciences to Karel Martínek (GAAV B3111305, 2003 – 2005). In this thesis my work on those projects is presented, it includes: 1) palaeoclimatological study of the Rudník member based on sedimentology and geochemistry (published by Martínek et al., 2006), 2) facies analysis, architectural analysis and stratigraphy of the Trutnov Formation (using also heavy minerals and gamma-ray logging, manuscript Martínek and Uličný in preparation), and 3) provenance study based on the heavy mineral assemblages and composition of detrital garnets (Martínek and Štolfová in review). Work done largely by other people is not included in the thesis: palaeontological studies of fossiliferous horizons (Šimůnek, Drábková, Zajíc in Blecha et al. 1997), sedimentology of Triassic deposits (Uličný 2004), U-Pb dating of detrital zircons (Martínek and Košler 2004), basin structure and deformation (Uličný et al. 2002), and apatite fission-track study (Svojtka et al. in prep., Martínek et al. 2006, Martínek et al. 2008).

Krkonoše Piedmont Basin

The Krkonoše Piedmont Basin (KPB, Fig. 1) is an intramontane basin covering the area of about 1100 km^2 (including the parts overlapped by the Upper Cretaceous). The basin was formed as a part of a system of extensional/transtensional basins which opened in the Bohemian Massif during the late phases of the Variscan orogeny. It is situated at the north-east of the Bohemian Massif between the crystalline complex of the Krkonoše – Jizerské hory Mts. in the north (forming also the most of crystalline basement of the basin) and the Orlice – Sněžník Crystalline Unit in the south-east.

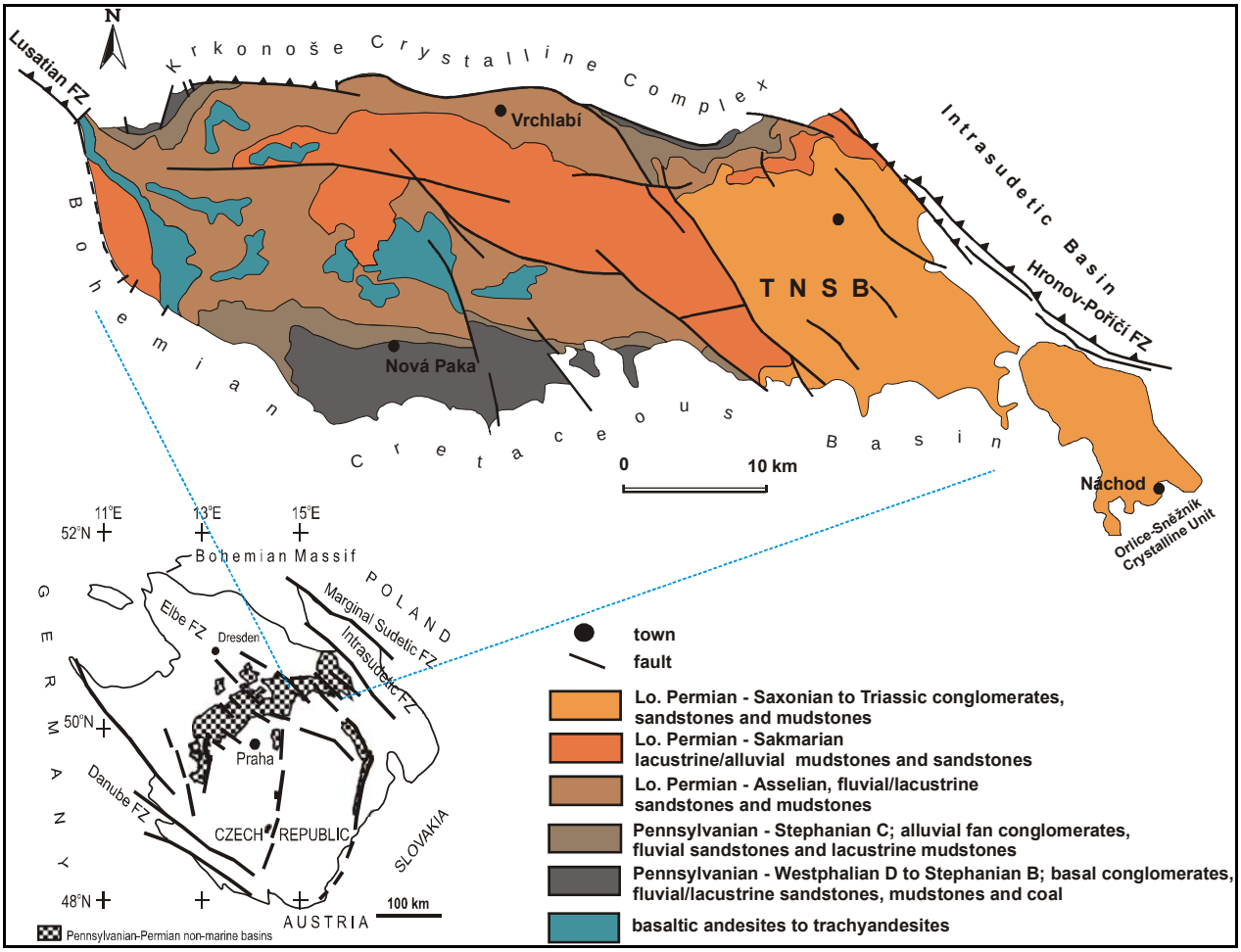

Figure 1. Geological sketch map of the Krkonoše Piedmont Basin

The maximum thickness of the volcanosedimentary basin fill in central part of the basin is nearly 1800 m. The deposition within the basin started in Asturian or Cantabrian. The large portion of deposits (in central part of the basin and especially of the Stephanian C and Autunian age) are claystones and mudstones of lacustrine and flat alluvial plain origin; arkoses, some sandstones and conglomerates are of fluvial origin. Also thick alluvial fan deposits - conglomerates and breccias - occur mainly at the northern and southeastern basin margins and are of important extent and volume.

The youngest (Saxonian to Triassic) units (Trutnov, Bohuslavice and Bohdašín formations) have been preserved in the eastern part of the basin (Trutnov – Náchod subbasin, TNSB) only. They are characteristic by red alluvial deposits and absence of fauna, flora and volcanics.

Substantial portion of the basin fill is formed by volcanics. The Carboniferous and especially Permian (Autunian) volcanic activity of the Krkonoše Piedmont and Mnichovo Hradiště basins was the most intensive all over the whole Bohemian Massif. It started within Asturian, culminated in Lower Autunian and ceased at the end of Autunian. More than 90 % of volcanics are of basic to intermedial nature (mostly andezitoids, formerly called melaphyres), while rhyolites (predominantly ignimbrites) form the lesser part.

The Permo – Carboniferous rocks are in the southern part of the basin and in the Hronov – Poříčí Graben SE of Trutnov covered by marine sediments of the Late Cretaceous age. The volcanic activity in the basin was renewed in Tertiary, when bazaltoidic lava flows were deposited in surroundings of Kozákov, western part of KPB. The relics of Tertiary (Neogene) gravels were preserved in the same area and between Bohuslavice nad Úpou and Chvalkovice, and at Dolní Brusnice in the Trutnov – Náchod subbasin.

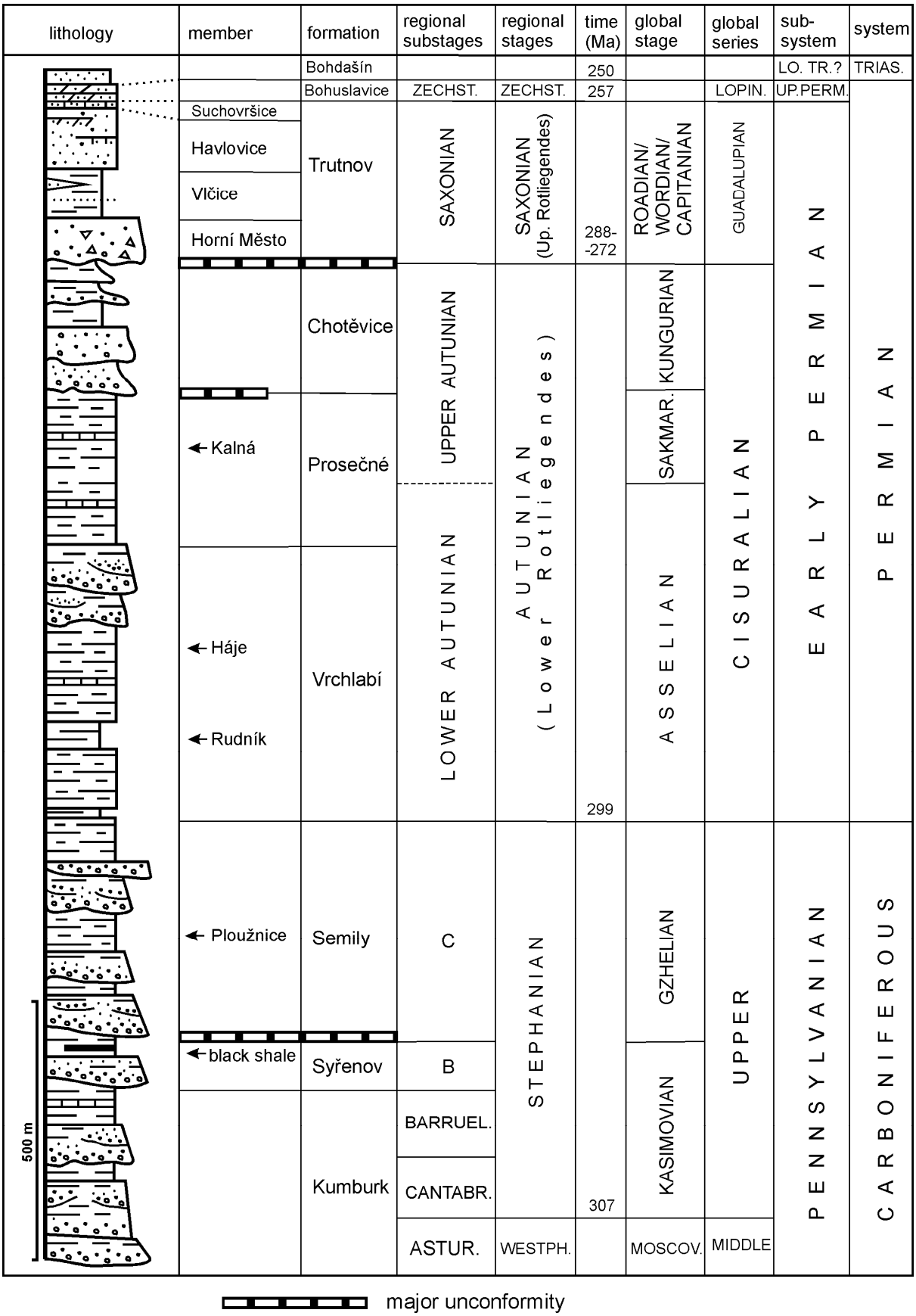

Figure 2. Schematic stratigraphic section of the Krkonoše Piedmont Basin based on the well core Pé-1, located in the central part of the basin, lithology of Saxonian-Triassic succession is based on well cores in Trutnov-Náchod subbasin.

References

Blecha M., Martínek K., Drábková J., Šimůnek Z. and Zajíc J. (1997): Environmental changes at the Carboniferous/Permian boundary and their impact on the floral and faunal assemblages of the fossiliferous lacustrine horizons of the Krkonoše Piedmont Basin. (in Czech). - Final report, project GAČR 205/94/0692, pp. 1-177, Praha.

Martínek K. and Košler J. (2004): Detrital zircon and heavy mineral provenance study of non-marine sediments from the Krkonose Piedmont Basin: evidence for late- to post-orogenic tectonic evolution in the northern Bohemian Massif. Abstracts Book of the 23rd IAS Meeting of Sedimentology, Coimbra – Portugal, 15-17 September 2004.

Martínek and Štolfová (in review): Provenance study of Permian non-marine sandstones of the Krkonoše Piedmont Basin: exotic marine limestone pebbles, heavy minerals and garnet composition. Submitted to Bulletin of Geosciences.

Martínek K. and Uličný D. (in preparation): Climatic vs. tectonic controls on the fluvial/alluvial Trutnov Formation, Upper Rotliegend, Bohemian Massif: an integrated well-log, outcrop and heavy mineral study.

Martínek K., Blecha M., Daněk V., Franců J., Hladíková J., Johnová R. and Uličný D. (2006): Record of palaeoenvironmental changes in a Lower Permian organic-rich lacustrine succession: Integrated sedimentological and geochemical study of the Rudník member, Krkonoše Piedmont Basin, Czech Republic. Palaeogeography, Palaeoclimatology, Palaeoecology, 230, 1-2 , pp. 85-128.

Martínek K., Svojtka M. and Filip J. (2006): Reconstructing Post-Carboniferous History of the Krkonoše Piedmont Basin Using Detrital Apatite Fission-Track Data. Proceedings of the 4th Meeting of the Central European Tectonic Studies Group/11th Meeting of the Czech Tectonic Studies Group, pp. 91-92, Zakopane, Poland, April 19-22, 2006.

Martínek K., Svojtka M. and Filip J. (2008): Multiphase cooling and exhumation of the Krkonoše Piedmont Basin during Mesozoic - Cenozoic basin inversion based on apatite fission track analysis. Abstracts of The 33rd International Geological Congress, Oslo, August 6 – 14th. CD-ROM.

Svojtka M., Martínek K. and Filip J. (in prep.): Multiphase cooling and exhumation of the Krkonoše Piedmont Basin during Mesozoic - Cenozoic basin inversion based on apatite fission track analysis.

Uličný D. (2004): A drying-upward aeolian system of the Bohdašín Formation (Early Triassic), Sudetes of NE Czech Republic: record of seasonality and long-term palaeoclimate change. Sedimentary Geology, 167, pp. 17–39.

Uličný D., Martínek K. and Grygar R. (2002): Syndepositional Geometry and Post-Depositional Deformation of the Krkonoše Piedmont Basin: A Preliminary Model. Proceedings of the 7th Meeting of the Czech Tectonic Studies Group, Zelazno, Poland, May 9-12, 2002, Geolines, vol.14, pp. 101-102.

Chapter 1

Record of palaeoenvironmental changes in a Lower Permian organic-rich lacustrine succession: integrated sedimentological and geochemical study of the Rudník member, Krkonoše Piedmont Basin, Czech Republic

Karel Martínek[a], Martin Blecha[b], Vilém Daněk[a], Jiří Franců[c], Jana Hladíková[d], Renata Johnová[e], David Uličný[f]

[a] *Institute of Geology and Palaeontology, Charles University in Prague, Albertov 6, 128 43 Prague 2, Czech Republic, ph. +420 2195 1464, fax: +420 2195 1452, <karel@natur.cuni.cz>*
[b] *HYDROTECH SG, s.r.o., Přemyslova 6, 128 00 Praha 2, Czech Republic*
[c] *Energy and Geoscience Institute, University of Utah, Salt Lake City, USA*
[d] *Czech Geological Survey, Klárov 3, P.O.Box 85, 118 21 Prague 1, Czech Republic*
[e] *Department of Geochemistry, Mineralogy and Mineral Resources, Charles University, Albertov 6, 128 43 Prague 2, Czech Republic*
[f] *Dept. of Earth Sciences, The University of Western Ontario, London, Ontario, N6A 5B7, Canada*

published in Palaeogeography, Palaeoclimatology, Palaeoecology, 230, 1-2 , 2006, pp. 85-128.

Motto:
To those who are awake, there is one world in common, but of those who are asleep, each is withdrawn to a private world of his own.
Heraclitus of Ephesus, B 89

Abstract

This study presents an integrated sedimentological and geochemical analysis of the Lower Permian Rudník member – the most extensive lacustrine deposits in the Krkonoše Piedmont Basin. Grey to black and variegated lacustrine mudstones, laminites and carbonates of the Rudník member have a lateral extent of more than 400 km^2. In the studied sections four facies associations were recognised: A) anoxic offshore, B) suboxic to oxic offshore, C) nearshore and mudflat, and D) slope deposits. In the northern part of the E – W elongated basin, anoxic to suboxic organic-rich offshore lacustrine facies dominate and form a succession up to 130 m thick. Fan-delta and turbidite facies occur locally along the faulted northern basin margin. The central part of the basin is occupied by anoxic to oxic offshore facies interfingering with nearshore carbonate and mudflat facies of the low-gradient lacustrine margin. In the central part of the basin, the thickness of the lacustrine deposits of the Rudník member reaches up to 60 – 70 m. In the southern part of the basin fluvial and alluvial plain facies dominate and alternate with minor lacustrine nearshore facies. The lateral facies distribution indicates that subsidence along the northern basin fault was the main mechanism generating the asymmetric infill geometry in the basin's half-graben setting.
The $\delta^{18}O$ values of primary and early diagenetic calcite range between -11.0 and +1.3‰ (V-PDB) and $\delta^{13}C$ values between -5.1 and +3.7‰; most of the data fall within the range of freshwater limestones. Coarser-grained pure microspar laminae show more positive $\delta^{13}C$ values in comparison to clayey organic-rich micrite laminae, and are interpreted as a record of bioinduced precipitation during seasonal eutrophication. The obtained $\delta^{13}C_{TOC}$ values range from -29.0 to -24.0‰, the total organic carbon (TOC) content from 0.26 to 23%. Maceral analysis and Rock Eval pyrolysis indicate that most of the samples contain a mixture of aquatic and terrestrial organic matter, but two minor, distinctive groups of samples with algally-dominated and terrestrially-dominated organic matter composition, respectively, were also found. The study of vertical changes in boron content in the clay fraction of the lacustrine mudstones shows that high lake level stages were periods of lower salinity with the lowest boron contents (from 73 to 268 ppm), and periods of falling lake level were followed by significant increases in salinity with much higher boron values (293 – 603 ppm).
Lake-level fluctuations of the Rudník lacustrine system, which are recorded by shallowing-up units of sedimentary facies within most of the sections throughout the basin, can also be traced within the monotonous black shale dominated sections, where no sedimentological evidence of these lake level changes exists. Good indicators for such changes seem to be the $\delta^{18}O$ and $\delta^{13}C$ values of primary calcite, $\delta^{13}C_{TOC}$ and HI. These lake level fluctuations are interpreted as driven by climatic oscillations in the order of tens of thousands years, which could reflect climatic changes connected with the last glaciation event of Gondwana.

Keywords: Lower Permian, Bohemian Massif, half-graben, lacustrine facies, lake level changes, stable isotopes, maceral analysis, hydrogen index, boron, climate change

1. Introduction

Understanding the mechanisms driving stratigraphic architecture in continental deposits remains a matter of controversy and active research (e.g. Shanley and McCabe, 1994; Blair and Bilodeau, 1988; Sweet, 1999; Csato et al., 1997; Liro, 1993). The tectonic setting of the basin is one of the main factors determining basin-scale distribution of sedimentary facies within the basin (e.g. Alexander and Leeder, 1987; Soreghan and Cohen, 1996; Sánchez-Moya et al., 1996; Soreghan et al., 1999; Wells et al., 1999; Gawthorpe and Leeder, 2000). The interplay between tectonics, base level changes and climatically driven sediment supply can be very complex.
Lacustrine deposits are considered good palaeoenvironmental archives, which can record even high-frequency climatic changes. In the Dead Sea Basin, alluvial – lacustrine architecture can directly respond to lake-level changes (Csato et al. 1997). Sediment supply and lake-level variations have been closely coupled in Lakes Malawi and Tanganyika during the Quaternary (Scholz and Rosendahl 1990). Significant climatic changes in the order of icehouse/greenhouse transitions are shown by the sedimentary and palaeontological record in the Upper Carboniferous and Lower Permian in different parts of Pangea (Gastaldo et al., 1996). Changes in the depositional environment can also be driven by tectonics. In the half-graben lake Tanganyika four structural basin margin types with characteristic facies associations were recognised (Soreghan and Cohen 1996). Sánchez-Moya et al. (1996) linked the facies architecture of red beds in a Triassic half-graben to episodically changing rates of basin subsidence. In thick lacustrine successions of cyclically stacked transgressive/regressive lithofacies, Milankovitch periodicities can be a good indicator of orbitally forced climate changes (Olsen and Kent, 1996; Fredriksen et al., 1998). However, in relatively thin successions dominated by monotonous offshore facies, the geochemistry of stable isotopes and organic matter must be taken in consideration in order to detect changes in lake-level and lake metabolism and to decipher their causes (Talbot, 1990; Talbot and Livingstone, 1989; Janaway and Parnell, 1989; Johnson et al., 1991; Gasse et al., 1989; Talbot and Johannessen, 1992; Ricketts and Johnson, 1996; Neumann et al., 2002; Stager et al., 2002; Johnson et al., 2000; Trauth et al., 2001; Bush et al., 2002). Such geochemical parameters can be good indicators of lake-level, hydrology and bioproductivity changes. Nevertheless in relatively thin

successions, where time series analysis of the sedimentary and geochemical record cannot be done, the mechanisms causing lake-level and lake metabolism changes remain poorly understood. For example, during the last glacial maximum (~18 kyr BP) tropical African lakes contain evidence of major dry periods and low lake-levels, which are ascribed to weakening Afro-Asian monsoons (Stager et al., 2002). A similar pattern was found by Benson et al. (1998) in the mid-latitude Mono Lake (California). Lake Tanganyika water-level fluctuation is in phase with glacio-eustatic sea-level changes and Gasse et al. (1989) hypothesised that water bound in ice caps resulted in low atmospheric moisture as a mechanism for the dry glacial periods. This explanation remains problematic, because equatorial lakes of northern Amazonia also show orbital forcing of lake-level but in the opposite phase relative to glacio-eustasy. The last glacial maximum 18 – 22 kyr BP was a wet time here and low lake-levels correlate with maximum insolation (Bush et al., 2002). This contradiction can be resolved by considering local changes in ocean and atmospheric circulation as the main mechanisms driving changes in local climate.
This paper discusses the sedimentary and geochemical record of a large lacustrine system of the earliest Permian age. The aim is to reconstruct the palaeogeography of the basin based on the lateral distribution of facies associations and to show the response of the large lake basin to different climatic and tectonic changes. To understand the interplay between changes in the hydrological regime, bioproductivity and palaeosalinity, which can show whether climate or tectonics were the main controlling factors, an integrated geochemical study of lacustrine carbonates, mudstones and organic matter was also carried out.

2. Geological background and lithostratigraphy

The Krkonoše Piedmont Basin (KPB) belongs to a system of post-orogenic extensional/transtensional basins which formed in the Bohemian Massif in the early post-orogenic phase, during the Westphalian and Saxonian times (about Moscovian to Sakmarian, c. 310 – 280 Ma) (Fig.1). The basin was filled with non-marine red-beds of a total thickness of about 1800 m during the Upper Carboniferous and Lower Permian (Asturian – Sakmarian) late Variscan extension/transtension (Fig. 2). There are several relatively thin grey to black shale, coaly, or variegated mudstone and carbonate interbeds penetrating the red bed infill, which are usually several tens of metres thick.
In the northern part of the basin the Lower Vrchlabí Formation of the Asselian age reaches a thickness of 350 m and is formed mainly by red brown alluvial/lacustrine mudstones with a lacustrine black shale interbed of the Rudník member (Fig. 2). In contrast, the basin's southern part is occupied by a much thinner succession (about 200 m) of red-brown alluvial/fluvial coarse-grained arkosic sandstones with minor interbeds of mudstones and conglomerates of the Stará Paka Sandstones (Prouza and Tásler, 2001). In the central part of the basin, the presence of interfingering variegated claystones, siltstones, carbonates and sandstones is typical and show common facies interfingering (Fig. 3).
The Rudník "Horizon" (=member in this paper) is defined by Tásler et al. (1981) and Prouza and Tásler (2001) as a 40 – 60 m thick succession of lacustrine grey mudstone with minor interbeds of black claystone, carbonate, sandstone and conglomerate, exposed mainly in the northern part of the basin. We use the term Rudník Lake deposits to describe deposits of the larger lacustrine system, which comprise suboxic and anoxic black, grey to variegated deposits of the Rudník member, and also the surrounding oxic red-brown lacustrine nearshore and alluvial facies closely related to lacustrine sedimentation. The Rudník Lake deposits cover an area of approximately 300 – 500 km^2 and along the northern basin margin deposits can reach a thickness of up to 130 m of grey to black shales. The areal extent is derived from the location of present-day outcrops, but could have been much larger, in the order of 1000 km^2. This estimate is based on postsedimentary basin shortening, the assumption of occurence in the eastern part of the basin, where the Vrchlabí Formation is covered by younger strata, and the finds of Rudník member equivalents in the adjacent Mnichovo Hradiště Basin, west of KPB (Prouza et al., 1997).

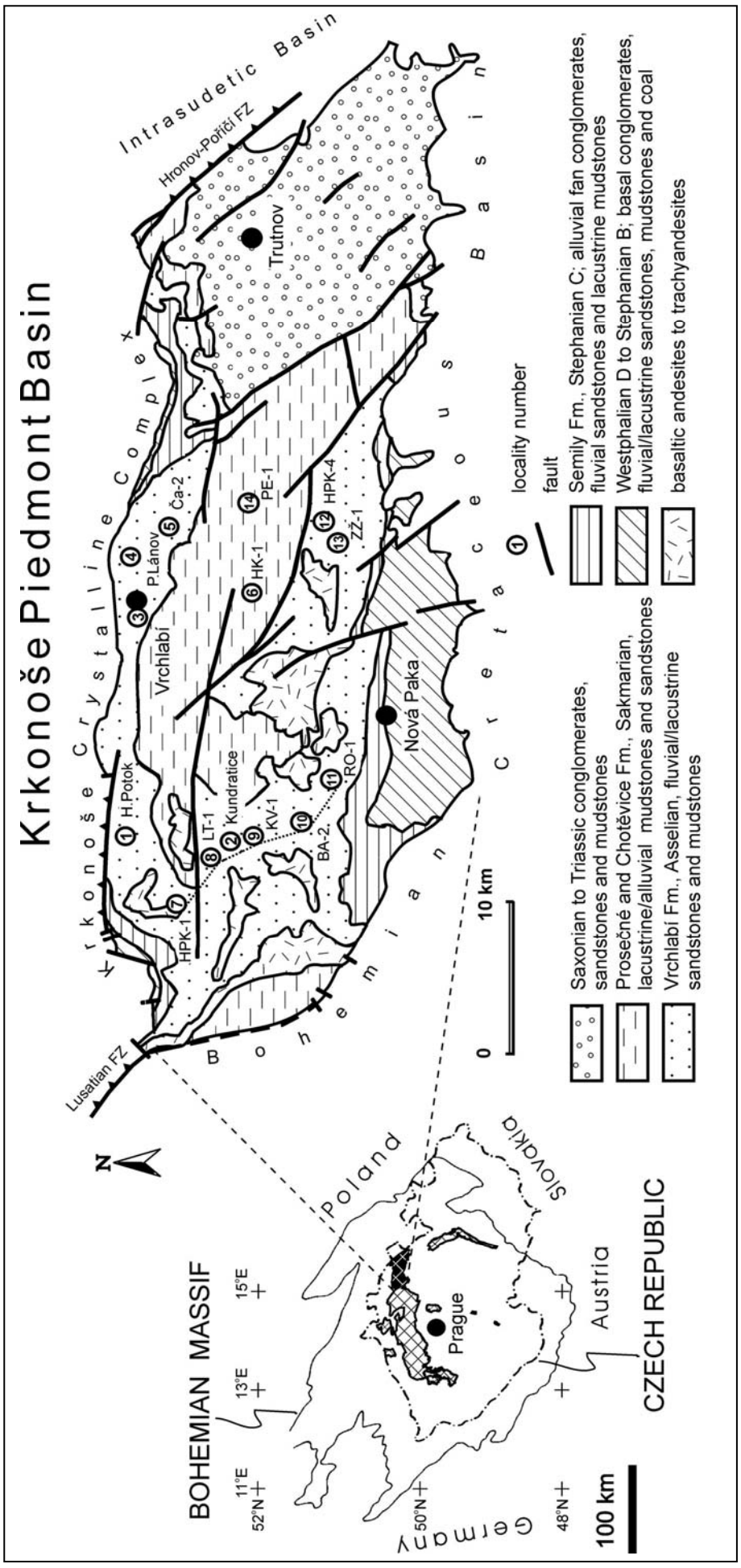

Figure 3. Sketch map (left) showing the position of the Krkonoše Piedmont Basin on the NE part of the Bohemian Massif and other non-marine Upper Carboniferous and Permian basins. Simplified geological map (right) shows the location of the studied sections: 1) Honkův Potok, 2) Kundratice, 3) Vrchlabí, 4) Prostřední Lánov, 5) Čistá (Ča-2) and boreholes 6) HK-1, 7) HPK-1, 7) Kv-1, 8) Lt-1, 9) Kv-1, 10) Ba-2, 11) Ro-1, 12) HPK-4, 13) ZŽ-1, 14) Pe-1; line 7-8-9-10-11 is cross section of Fig.3; FZ – fault zone.

3. Sedimentary record

3.1. Approach and methods

Sedimentary facies of the Rudník Lake deposits were studied in detail in eight outcrop sections and five well cores; in this paper, four selected outcrop sections and one well core, representative of the main facies associations, are shown (Figs. 4 – 7; for locations see Fig. 1). Understanding the local sedimentological picture in a broader, basinwide stratigraphic framework was made possible by correlating gamma-ray and resistivity well logs, combined with the archive documentation of core material (Fig. 3). The use of geophysical logs, enabled the lacustrine offshore and nearshore facies and fluvial facies to be correlated.

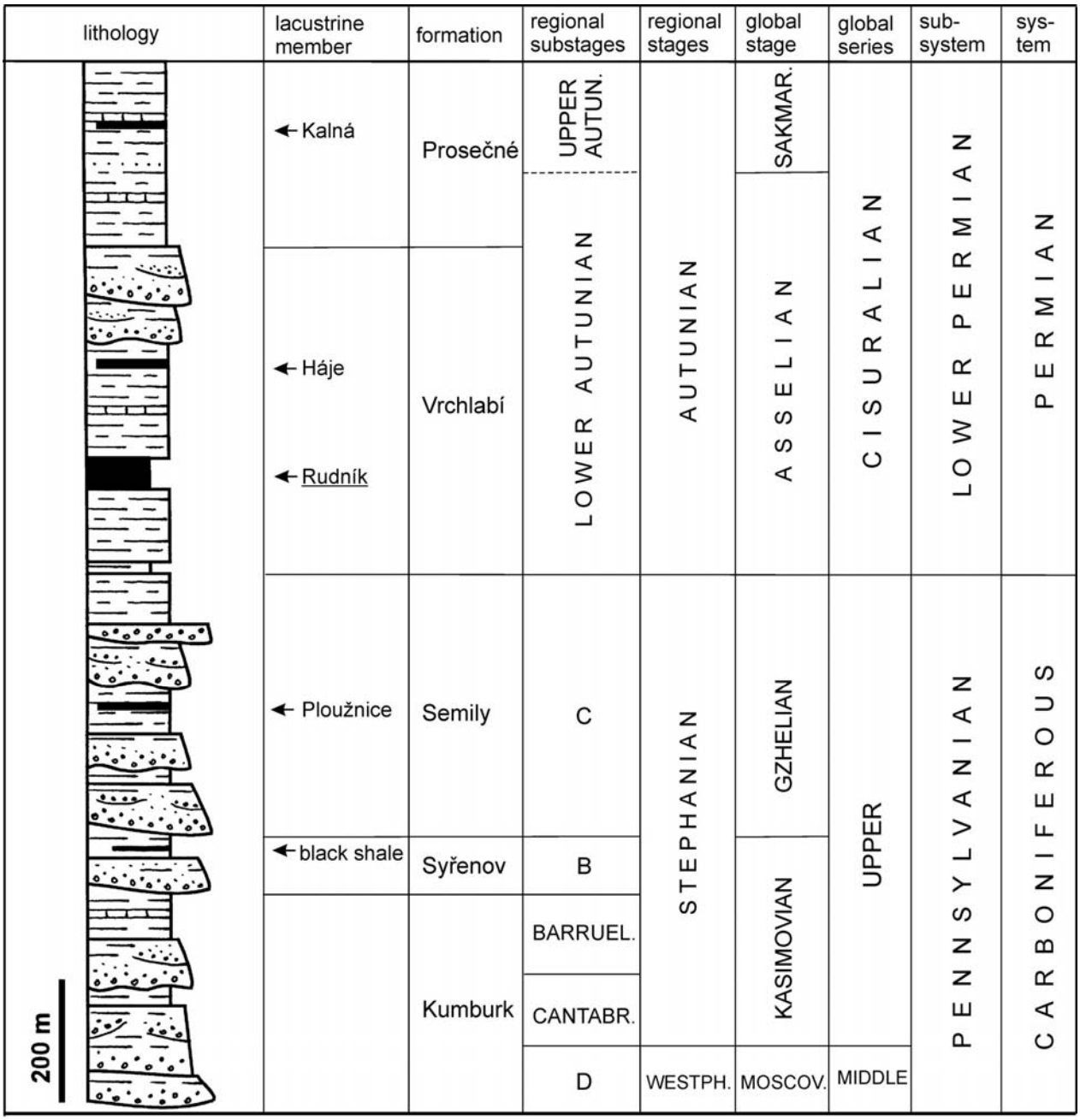

Figure 4. Lithology and stratigraphy of the central part of the Krkonoše Piedmont Basin based on the borehole HK-1.

3.2. Well-log correlation and basin-scale facies architecture

In order to document a basin-scale stratigraphic architecture, relevant for understanding the detailed sedimentological aspects, a N – S cross section showing correlation of well-log and core data is presented (Fig. 3; for location of boreholes see Fig. 1). The well-log correlation in Figure 3 represents a transect across a range of depositional systems that form the Semily and Vrchlabí Formations. The general decrease in grain size towards the north is interpreted as a transition from fluvial and deltaic-dominated palaeoenvironments in the south to lacustrine offshore-dominated palaeoenvironments in the north (cf. Prouza and Tásler, 2001). Schematic lithological variations and facies interfingering are shown only for the uppermost part of the Semily Formation and lower part of the Vrchlabí Formation (Fig. 3).

The well-log patterns are dominated, especially in the upper parts (eg. Fig. 3) by a serrated pattern typical of alluvial/delta plain and some lacustrine deposits (cf. Rider, 1996; Posamentier and Allen, 1999), with occasional blocky log motifs corresponding to sand-dominated alluvial channels (especially logs Ro-1, Ba-2). Maxima in the gamma-ray curves and minima in the resistivity curves correspond to maximum mud contents, as confirmed by core documentation. Vertical variations in sand and mud content become more apparently cyclical further down in the logs, where a repetitive bow-like log motif becomes typical in places in the Semily Formation (e.g. Ro-1 100 – 200 m, Ba-2 100 – 300 m). In the mud-dominated, lacustrine facies of the northern part of the cross-section, only occasional intercalations of sandy strata occur.

The correlations of well-logs across several tens of kilometres are based on the application of the accommodation/supply (A/S) ratio concept (Martinsen et al., 1999). The lithological variations reflected in the varying sand/mud content show similarities for boreholes spaced several kilometres apart, and are interpreted here as a response to cyclical changes in the ratio between accommodation and clastic supply, reflected in both the fluvial-dominated system in the south and the linked lacustrine system in the north. Pronounced maxima in gamma-ray curves are interpreted as flooding surfaces in the lacustrine system, corresponding to expansion surfaces in the coeval alluvial plain (cf. Martinsen et al. 1999). Maxima probably represent a response to a relative rise of lake level in the lacustrine (borehole Kv-1 and Lt-1) and deltaic (Ba-2) settings, accompanied by the expansion of the lake and consequently retrogradation of coarser-grained facies (cf. Sweet 1999). Similar well-log curve patterns can also be observed in borehole Ro-1 in the red-brown sandstones and mudstones, interpreted as predominantly fluvial facies (Fig. 3). The higher mud contents in some intervals can be explained by lower topographic gradients and lower stream energy during the base level rise. An interpreted maximum flooding surface (MFS) of the Rudník Lake succession lies at the base of a significant black shale and carbonate bed with very high TOC content (up to 23%) and is used as a correlation datum (Fig. 3). The MFS correlates to the south with the base of a grey lacustrine mudstone and carbonate bed (borehole Ro-1). The flooding surfaces are commonly sharply overlain by fining-upward, coarser clastic successions. This feature can be seen in both distal and proximal delta/lacustrine facies as well as in fluvial facies. Consequently such an incision is interpreted as being connected with an abrupt relative drop of lake-level followed by a gradual rise of lake-level. Similar interpretations, although with slightly different terminology, are presented from the Eromanga Basin, Australia (Posamentier & Allen, 1999, their Figs. 4.25 and 4.69), from Newark Basin (Olsen, 1986), Schlische, 1992; 1993) or from East Greenland (Dam and Surlyk, 1993).

The syn-depositional basin geometry can be interpreted, taking into account the significant differences in pre-compaction thickness of the facies present (Fig. 3). The post-compaction thickness of the Rudník Lake succession increases from 130 m in the south (Ro-1) to at least 150 m in central part of the basin (Kv-1). In the northern part of the basin it may reach 300 m, as reported by Prouza and Tásler (2001), although direct evidence from subsurface data is missing in this part of the basin. Using decompaction equations (Allen and Allen, 1990) and the porosity coefficients of Sclater and Christie (1980), the difference in pre-compaction thickness was estimated, with input data as follows: 70% of sandstone, 30% of mudstone in Ro-1 and 90% of mudstone and 10% of sandstone lithologies in Kv-1 borehole. An overburden of 1 km of younger deposits is considered although this may be underestimated. Based on these assumptions, an approximate pre-compaction thickness of Ro-1 of 186 m and Kv-1 of 255 m was calculated, representing an increase towards the north of 37%. This significant increase in thickness towards the main boundary fault and the basin-fill style suggests an original half-graben morphology for the basin (e.g. Gawthorpe et al., 1994; Gawthorpe and Leeder, 2000).

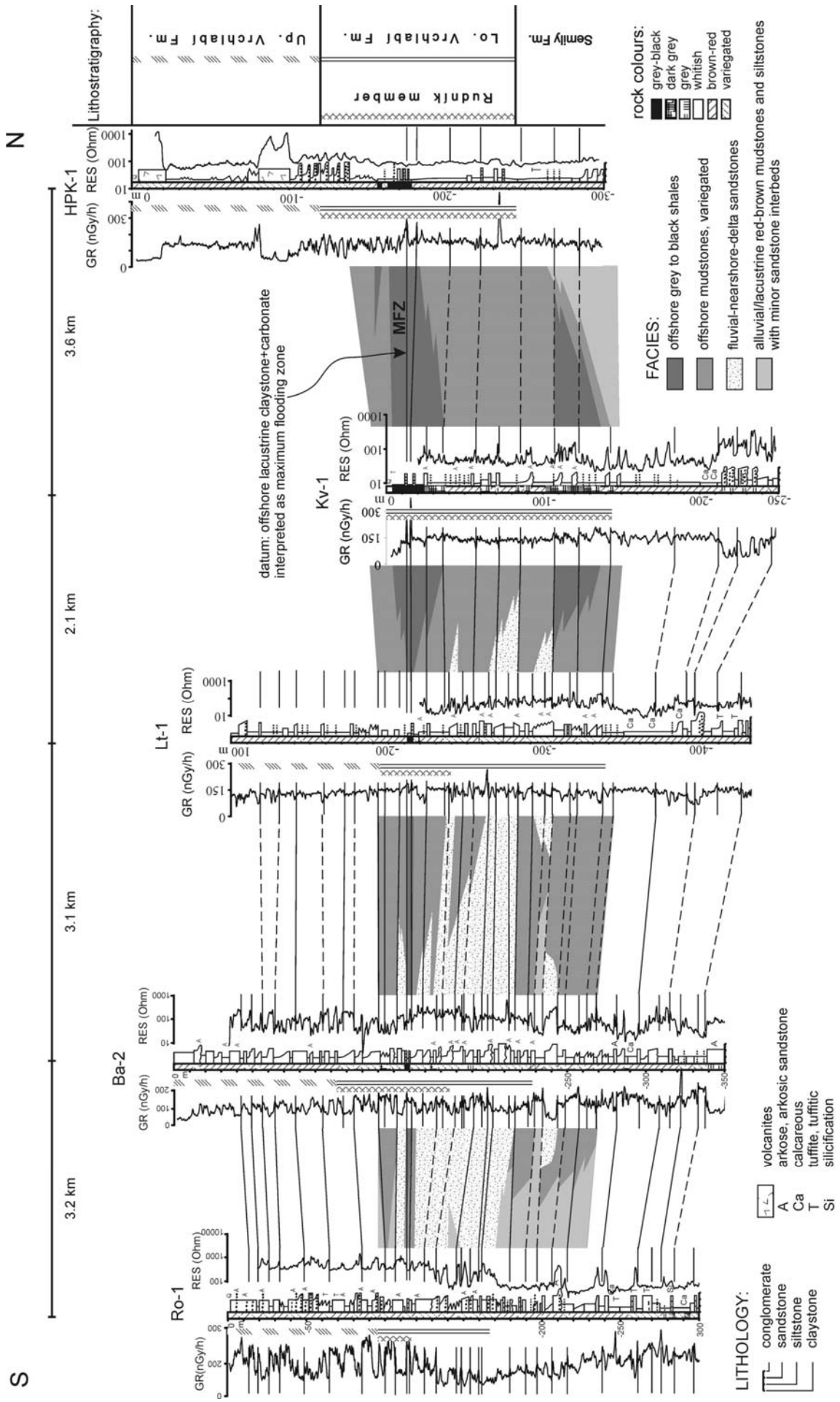
N
S
Lithostratigraphy:
Up. Vrchlabí Fm.
Lo. Vrchlabí Fm.
Semily Fm.
Rudník member
rock colours:
grey-black
dark grey
grey
whitish
brown-red
variegated
HPK-1
RES (Ohm)
GR (nGy/h)
MFZ
datum: offshore lacustrine claystone+carbonate
interpreted as maximum flooding zone
FACIES:
offshore grey to black shales
offshore mudstones, variegated
fluvial-nearshore-delta sandstones
alluvial/lacustrine red-brown mudstones and siltstones
with minor sandstone interbeds
Kv-1
Lt-1
Ba-2
Ro-1
3.6 km
2.1 km
3.1 km
3.2 km
LITHOLOGY:
conglomerate
sandstone
siltstone
claystone
volcanites
arkose, arkosic sandstone
calcareous
tuffite, tuffitic
silicification
A
Ca
T
Si

Figure 5. Cross section of the Lower Vrchlabí Formation, showing asymmetry of the basin fill during the accumulation of Rudník Lake deposits. The datum used is an interpreted maximum flooding surface (MFS) associated with black shale and a carbonate bed with very high TOC content (up to 23%) in the central part of the basin. This can be correlated to the south to grey lacustrine mudstone and carbonate beds. Generalized sedimentary facies transitions are shown for Rudník Lake deposits only. f – highly faulted and jointed rocks. The high gamma peak in HPK-1 234 m is ascribed to a volcanogenic admixture. Horizontal distances not to scale; for location of boreholes see Fig.1.

3.3. Sedimentary facies

3.3.1. Facies and facies associations

A total of 17 sedimentary facies are recognised within the Rudník Lake deposits on the basis of the lithology, colour, sedimentary and biogenic structures, mineral composition and total organic matter content. These facies record specific sedimentary depositional processes, interpreted from the hydrodynamic and biogeochemical point of view (Table 1). The sedimentary facies are grouped into four facies associations interpreted as: A) Anoxic offshore, B) Suboxic to oxic offshore, C) Nearshore and mudflat and D) Slope deposits. Their main descriptive features and interpretations are briefly summarized below.

3.3.1.1. Facies association A – anoxic offshore

The anoxic offshore facies association is composed of black shales (facies Bs, Fig. 8a, Table 1), grey to black mudstones (facies Mo – pelagic unit, Fig. 8d) and carbonate/black shale laminites (facies La), which are characterised by fine laminations, a high organic matter content and a lack of bioturbation. Alternating 1) dark, organic rich laminae and clay minerals with low carbonate content and 2) light laminae rich in carbonate and with lower organic matter and clay content usually form lamination. Fish fossils, amphibians and terrestrial flora can also be present.

3.3.1.2. Facies association B – suboxic to oxic offshore

Finely laminated grey, variegated, to red-brown mudstones and carbonates with low or no organic matter content form facies association B in which bioturbation, amphibians and terrestrial flora can be present. Facies association B comprises laminated mudstone (Ml, Fig. 9b) and laminated limestone (Ll) facies (Table 1).

3.3.1.3. Facies association C – nearshore and mudflat

Facies association C comprises seven carbonate and siliciclastic facies, mostly red-brown in colour: Cm, Ct, Dm (Fig. 9a), Mm, Mss, Sr and Shcs (Table 1). The main characteristics are the presence of desiccation cracks, bioturbation, current and oscillation ripples. The evidence of oscillatory and traction currents indicate shallow water and/or nearshore conditions. The mudflat facies, Mc, comprises mudstones with evidence of repeated desiccation and flooding such as abundant desiccation cracks, pedogenic carbonate nodules.

3.3.1.4. Facies association D – slope deposits

Facies association D is characterised by sharp- to erosionally-based beds of siltstones, sandstones and conglomerates showing slump, graded or massive structures and, rarely, tool marks at the base of beds. Facies Ms, Sg (Fig. 8e), Gm and Mo (silty unit, Fig. 8d) are interpreted as products of turbidites, debris flows and slumps deposited offshore on the lake slope.

3.3.2. Vertical facies pattern and environmental interpretation

Particular sedimentary facies and facies associations form different stacking patterns in different lateral basin settings. Typical sections are presented in Figs. 4 to 7, each representing a particular part of the lacustrine sedimentary systems interpreted as: 1) the offshore mudstone-dominated central part of the lake; 2) sandstone turbidites; 3) fan-delta; 4) sandy nearshore; 5) mudstone-dominated low-gradient lake margin. The studied sections record lacustrine sedimentation of the upper black shale unit of the Rudník member closely associated with bituminous carbonates (0 to -40 m in Kv-1 on Fig. 3; the lower black shale unit, -100 to -140 m in Kv-1, is not exposed).

Table 1. Sedimentary facies of the Rudník Lake deposits.

facies	colour, lithology, structures, mineralogy	biogenic structures, fossils, TOC, X-Ray	interpretation
mudstone	**facies**		
black shale **Bs**	black to grey-black finely laminated (0.2 mm to 2 mm) organic matter very rich claystones and silty claystones; 0.1 to 0.5 m thick beds low carbonate content (0 – 5% normally, 30% max.), mostly calcite mm thick lenses of bitumen can be present as well as bitumen filling tectonic fractures; interbedded carbonate layers 0.5 – 10 cm thick pyrite on bedding planes in places; Figs. 8a, b	5 – 23% TOC fish scales, bones, fish fossils; terrestrial plant fragments Q, F > I, K > C, D, A, H C > F, H, D, I, Q C > D, F, Q > I, K, H calcite dominated carbonate fraction	sedimentation from suspension anoxic bottom high bioproductivity ± seasonal lamination (Fig. 8 a, b) **offshore**
organic-rich mudstone **Mo**	dark-grey to black-grey; dolomitic organic matter rich laminated mudstones; mm to cm lamination; 0.1 m to 9 m thick beds pyrite on bedding planes in places; rhythmic alternation of mm to 5 cm thick units of clay mudstone and silty mudstone to siltstone units **clay mudstone unit** is formed by 0.2 – 2 mm thick laminae composed mainly of dolomicrospar, clay, organic matter; lamination: alternating laminae rich by dolomicrospar or organic matter and clay minerals; **silty unit** is formed by one or several amalgamated laminae; main components are : dolosparite, highly corroded quartz silt grains, carbonate intraclasts (micritic or microsparitic, silt sized); two types of silty laminae are present: 1) sharp-based with graded bedding or massive and with gradual top contact, and 2) with gradual transition at the base as well as at the top; see Fig. 8d	usually 1 – 4% TOC terrestrial plants, plant fragments D >> Q, I, F F > D > I, Q, H D > F > I, H, Q entirely dolomitic, no calcite found	anoxic bottom high bioproductivity clay mudstone unit: sedimentation from suspension silty unit: underflows and interflows **offshore**
laminated mudstone **Ml**	grey , variegated, brown; laminated dolomitic or calcareous mudstones mm to cm lamination; 0.1 – 1.5 m thick beds; different proportion of clay, silt, organic matter and carbonate in particular laminae; 5 – 10 mm thick silty laminae occur in places usually sharp-based and graded bedding in places	max. 0.2 – 1% TOC; terrestrial plants, plant fragments; coprolites, fish fossils bioturbation can be present D, F > C > I, K, Q D >> F > Q, I, C, K both dolomite as well as calcite can be present	suboxic bottom sedimentation from suspension with occasional underflows (gravity flows); lamination can be driven either by climate or by sediment supply **offshore**
mudcracked mudstone **Mc**	red-brown, brown, grey calcareous mudstone 0.1 m to several metres thick beds; cm or disturbed lamination or massive; abundant mudcracks disturb original lamination; pedogenic mottling and claystone rip up clasts can be present; cm to 0.5 m interbeds of heterolithic clayey silty sandstones with rare mudcracks in some places	0.2 – 1% TOC can be present; plant fragments in some places; (Kundratice section: C, Q, A > I, D > F, K; Q, C, A > I, F, H, K; Q, C > I, D > K, F, H calcite dominated carbonate fraction)	frequent alternations of flooding periods with sedimentation from suspension and desiccation with subaerial exposure; **mudflat**
mottled mudstone **Mm**	red-brown, brown, grey-brown, grey calcareous mudstones to siltstones 0.2 m to several metres thick beds pedogenic mottling, mixed up clayey/silty material or crude lamination in some places; rare lensy bedding with silty lenses	bioturbation can be present	primary possibly laminated structures disturbed by later processes - pedogenesis, bioturbation **nearshore / alluvial plain**
carbonate	**facies**		

carbonate / black shale laminite La	carbonate and organic matter rich mudstone laminite; 0.2 – 2 mm thick laminae; alternating of 3 types of laminae: 1) micritic organic matter rich mudstone laminae, **grey;** 2) organic matter very rich mudstone laminae, **black;** 3) pure microspar laminae with dispersed organic matter, **whitish**, silty Q grains can be present microspar laminae are lensy in some places; 1 – 2 cm nodules of bitumen can be present; 0.1 – 0.5 m thick beds	2 – 12 % TOC plant detritus high carbonate content – approx. 50% D > F > C > I, Q, H D >>> F, C, A C > F, D > I dolomite as well as calcite are present	sedimentation from suspension anoxic bottom seasonal bioinduced carbonate precipitation high bioproductivity **offshore**
organic-rich carbonate Co	grey to dark-grey laminated limestones and dolomitic limestones; 0.5 m thick bed; organic matter rich; clayey microspar (Fe calcite and Fe dolomite); dark and light laminae with different proportion of organic matter, clay and carbonate content; low lithological contrast between dark and light laminae; lower part with higher organic matter content is finely laminated – 0.2 – 2 mm; upper part with lower organic matter content have milimetre-scale lamination; highly corroded silt quartz grains or peloids can be present occasionally	0.3 – 8% TOC high carbonate content – 50 – 70%	anoxic to suboxic bottom increasing upwards carbonate precipitation rate high bioproductivity **offshore**
massive (organic-rich) carbonate Cm	grey to dark grey massive carbonate 20 cm thick bed; microspar to spary with relics of clayey micrite matrix; micrite peloids (up to 30%) or highly corroded silt quartz grains can be present; organic matter in the form of dispersed opaque grains; mudcracks on the top		shallow water carbonate precipitation high bioproductivity **nearshore**
laminated limestone Ll	violet-red laminated limestone; 0.5 m thick bed; fine lamination: 0.2 – 2 mm; dark laminae: clayey microspar with dispersed organic matter or Fe pigment; light laminae: pure microspar to sparite; clayey organic matter rich laminae in some places; rare peloids	fish and amphibian fossils, coprolites, terrestrial plants	suboxic to oxic bottom high bioproductivity lamination probably seasonal **nearshore** (low energy)
muddy dolostone Dm	grey muddy limy dolostone; cm to 0.5 m thick lensy or nodular beds, massive to concentric zonal fabric (higher carbonate content in the centre, higher organic matter content in outer rim); clayey dolomicrospar, silty quartz grains admixture, dispersed opaque grains of organic matter; mudcracks on top bedding plane in some places; secondary porosity filled by drusy and blocky sparite calcite cement; Figs. 9a, b	D >> Q > F, C, I	1) shallow water carbonate precipitation; ***palustrine;*** **nearshore** 2) precipitation from saline lake water - Coorong model; **nearshore**
carbonate microbial mat Ct	grey green, grey violet, grey red, mottled; laminated muddy carbonate undulose lamination (Fig. 9c); alternation of clayey microspar laminae with laminae rich in partly oxidised organic matter; lamination is often disturbed, mixed up material, mudcracks in some places; horizons of cm-sized calcareous nodules		shallow water precipitation and sedimentation on microbial mats; followed by subaerial exposure and pedogenesis **nearshore**
sandstone /	**conglomerate facies**		

mudstone, siltstone and sandstone interlamination Mss	red-brown to grey alternation of mm to cm laminae of mudstone, siltstone and fine-grained sandstone; proportion of particular laminae is highly variable transition of lamination to lensy or flaser bedding can be present heterolithic, carbonatic fine to coarse-grained sandstone interbeds 3 – 10 cm thick , massive or rippled or flaser bedded, good to poorly sorted; occasionally with plant debris, mudstone or coal intraclasts and mudcracks	bioturbation in some mudstone-rich horizons (Kundratice: D, Q, F > I, K, C)	higher siliciclastic input alternation of different hydrodynamical regimes shallow water (where desiccation cracks are present) **nearshore** (mud to sand flats) **to distal prograding sand bodies**
sandy mudstone Ms	greenish-grey to reddish; sandy limy silicified mudstone; clayey (zeolites ?) matrix with microspar, quartz silt and fine-grained sand grains, diffused opaque grains of organic matter; volcanogenic material (angular quartz grains with fluid inclusions, felsitic grains); 1 – 2 m thick beds, thickness laterally highly variable; slump structures, plastic deformations or massive, sharp to erosional base; claystone intraclasts and plastically deformed underlying mudstone rip up clasts (facies Bs or Ml) near the base; Fig. 8.c)		rapid sedimentation probably driven by volcanic activity: volcanogenic fall and seismic activity (Semily volcanic centre is 10 to 25 km away) slump **offshore**, lake slope
rippled sandstone Sr	grey, whitish; fine to medium-grained sandstones; 0.1 – 0.6 m thick beds horizontal bedded, laminated, isolated ripples, rarely oscillation ripples medium to well sorted, well rounded; thicker beds can be amalgamated and show planar or trough cross bedding	plant fragments or bioturbation in some places	sedimentation from traction and/or oscillation currents
hummocky cross stratified sandstone Shcs	grey, whitish; medium-grained sandstone; 0.1 – 0.5 m thick lensy beds; sharp base and top; well sorted; form interbeds within sandstones of Sr facies; hummocky cross stratification		sedimentation from storm currents and waves
graded and massive sandstone Sg	grey, whitish; fine to coarse grained sandstones; 5 cm to 0.7 m thick beds poorly to moderately sorted; sharp or erosional based; rarely with flute casts and groove marks on the base; coarse to medium grained sandstones with graded bedding often overlain by fine-grained sandstones with ripples, flaser and lensy bedding (gradually passing up to the grey mudstones); sometimes massive with no graded bedding; beds could be also amalgamated or alternate with black shales (Bs facies)		deposits of turbidity currents
matrix-supported conglomerate Gm	fine-grained conglomerates (mm pebbles, max. 3 cm), rarely medium; grained (cm pebbles, max. 20 cm); 0.2 – 0.4 m thick beds; massive, matrix supported; subangular to well rounded pebbles; medium to coarse grained clayey sandstone matrix; two types: 1) tabular beds, sharp planar base, planar or undulose top; 2) lensy trough-like beds with erosional base		1) cohesive debris flow 2) non-cohesive debris flow

Symbols used for mineralogical composition obtained by X-Ray diffraction: C – calcite, D – dolomite, Q – quartz, A – analcite, I – illite, F – feldspars (both K- and Ca-feldspars are present), K – kaolinite, H – hematite; D>C means that dolomite content is significantly higher than calcite content; C>>D means that calcite content is much higher than dolomite content; C, D means that calcite content is of similar percentage than dolomite content; minerals are sorted from left to right by decreasing content in the sample; relative portion of

individual minerals in the sample was obtained by comparing the three highest peaks in the X-Ray difractogram; detection limit is approximately 5% of mineral phase in the sample. All X-Ray diffraction data are from Kundratice and Vrchlabí sections only. TOC – total organic carbon.

3.3.2.1. Vrchlabí section: offshore black shales and laminites

The Vrchlabí road-cut is situated on the present northern basin margin (Fig. 1), where a monotonous 130 m thick succession of dark-grey to black laminated mudstones with rare intercalations of black shales and carbonates crops out (Drábková et al., 1990). The determination of thickness is only approximate, because the outcrop is deformed by several small thrust faults. The section (corresponding to Section 4 of Drábková et al., 1990) represents only a small part of this outcrop, but is the most diverse lithologically: offshore anoxic black shales and laminites are present as well as shallow-water carbonates and microbial mat deposits.

Two distinctive units are recognised (Fig. 4). At the base of the section, mottled mudstones with carbonate nodules of probably pedogenic origin occur. The interpretation of these mudstones remains problematic, because the original structures are disturbed by jointing and fluid migration along a nearby fault. The base of the overlying Unit V1 is marked by a flooding surface at the base of finely laminated offshore mudstones of facies Ml. These mudstones show a gradual upward increase of organic matter content, accompanied by a gradual decrease in iron oxides, reflected by a gradual change of colour from red-brown at the base through grey-brown to dark grey at the top. These trends are interpreted as a record of the lake bottom waters' increasing oxygen depletion, which could be caused by a rise of lake level and the establishment of a stratified water column as well as by an increase in bioproductivity. The overlying anoxic offshore facies Bs, La and Mo probably represent the period of highest lake level with permanent stratification and high bioproductivity. Beds characterised by alternations of well-defined black clayey laminae and white microspar laminae (similar to the anoxic facies of the Kundratice section, Fig. 7 b) are common within this succession and are interpreted as reflecting seasonal variations of bioproductivity, sediment input and water chemistry. Mudstones of facies Mo containing rhythmic alternations of pelagic mudstone laminae and silty laminae (Table 1, Fig. 8d) are interpreted as products of occasional underflows and interflows triggered by hyperpycnal inflows. No periodicity was found in the thickness of both types of packets. They could have been driven by seismicity caused by tectonic activity on the northern marginal basin fault zone. The presence of turbidity underflows can indicate a higher topographic gradient along the northern basin margin. A gradual upward decrease in organic matter content and increase of iron oxides within the overlying offshore facies Ml is interpreted to record an increase in lake bottom oxygenation, which may be caused by a drop in lake level. Alternatively oxygenation of deep water can be caused by water mixing, which is primarily controlled by surface wind stress in deep tropical lakes. Thus apparent fluctuations in bottom-water oxygen supply could also be a result of changes in wind intensity. The top of unit V1 is a finely laminated nearshore carbonate Ll, which is characterised by alternations of dark grey, organic matter-rich laminae and red-violet iron oxides pigmented submilimetre-thick laminae. This unusual feature can be caused by seasonal/annual changes of bioproductivity and a relatively high carbonate accumulation. Rapid precipitation of carbonate could prevent black shale laminae oxygenation during later oxic conditions. The presence of amphibian fossils provides evidence of relatively shallow water conditions. The lower part of the overlying Unit V2 is formed by a sandy mudstone slump bed (Ms) overlain by anoxic to suboxic offshore mudstones Ml. The upper part of unit V2 is formed by muddy microbial mat carbonate with mudcracks and pedogenic nodules at the top. Slump and anoxic offshore facies are interpreted as a record of a significant rise in lake level and lake highstand, where a subsequent drop in lake level is indicated by the overlying microbial mat facies.

The absence of coarser clastic deposits, even in nearshore facies, implies a relatively low sediment input, suggesting that the Vrchlabí section was located near the depocentre. In this case substantial changes in lake level, causing large lateral shifts of coastline, seem to be necessary in order to explain the vertical facies transitions from anoxic offshore black shales and distal silty turbidites to shallow water carbonates or microbial mats (Dam and Surlyk, 1993).

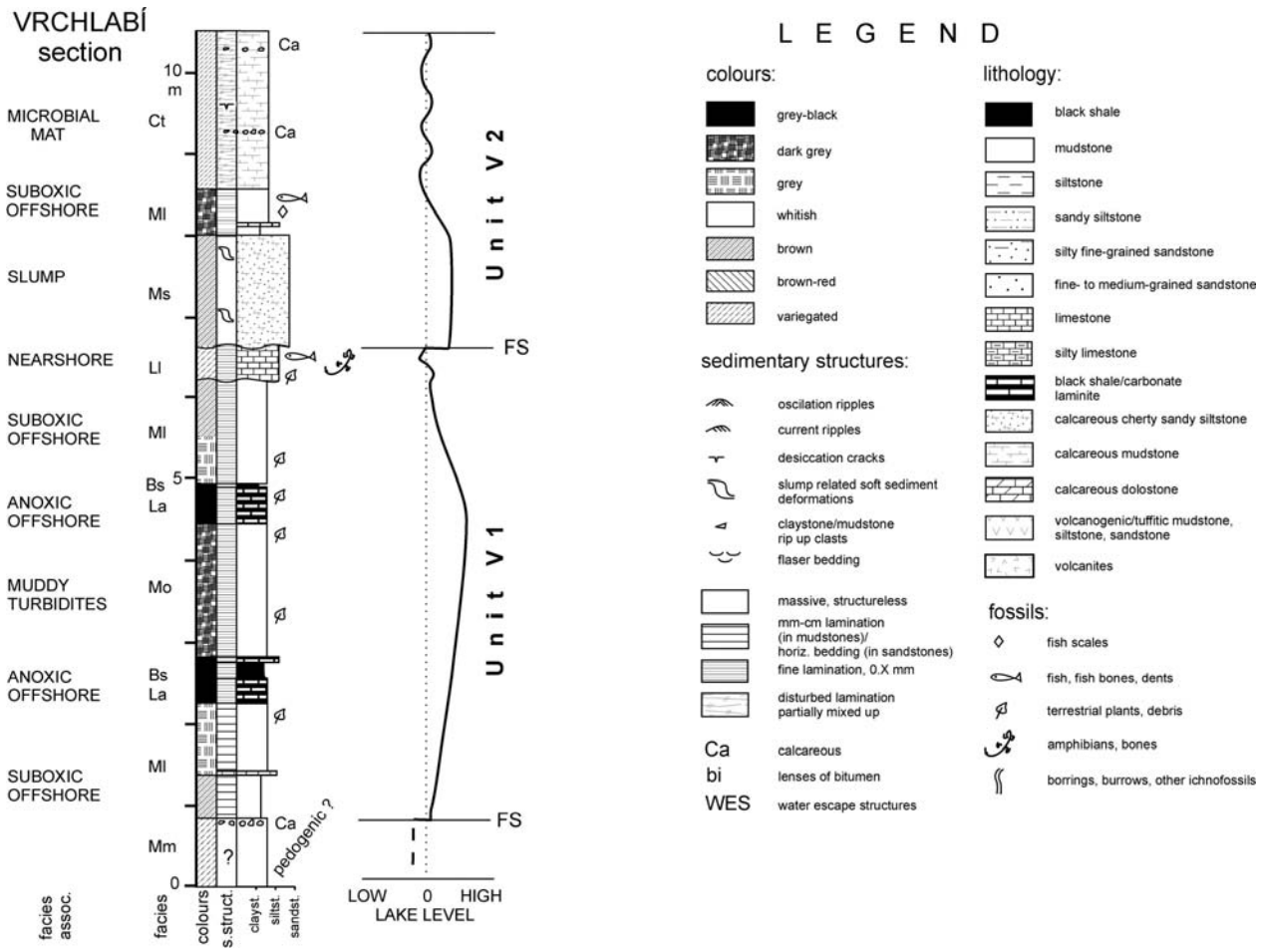

Figure 6. Sedimentological section measured at Vrchlabí, sedimentary facies (Table 1), facies subassociations and interpreted lake-level changes are shown.

3.3.2.2. Čistá 2 section: deepwater turbidite fans

The Čistá 2 section comes from a well core from the north-eastern part of the basin (Fig. 1). Lower boron values are interpreted as sedimentation in more freshwater conditions at times of high lake level, in contrast to higher boron values, which are interpreted as sedimentation in more saline conditions during low lake level (Blecha et al., 1999). The lower part of the well core mainly represents lacustrine deposits of the Rudník member (Fig. 5). The overlying succession is mainly formed of red-brown mudstones of alluvial/ephemeral lake origin. It contains millimetre – centimetre thick intercalations of early diagenetic displacive gypsum, indicating hydrologically closed basin conditions and high water output/input ratio.

Based on flooding surfaces, located at the base of laminated offshore lacustrine facies (e.g. black shale) intervals, the section can be divided into five units (Fig. 5). The lower 3 units, unit C1, C2 and C3 show a distinctive shallowing-up pattern. The lower part of these units is usually formed by offshore mudstone facies Mm and Bs; the Mm facies is interpreted here as offshore, because of low boron values (Fig. 5). Massive or graded sandstones of Sg facies are also present. Alternation of millimetre – centimetre laminae of black shales and turbidite sandstones is a very common feature (Fig. 8e). Nearshore Mss and Dm facies, or Mm facies with higher boron values overlie these beds. Mudflat Mc facies can be present on the top of units. The recognition of a flooding surface between units C3 and C4 is problematic, because the massive mudstone facies Mm of the lower part of unit C4 can be interpreted as deposited on an alluvial plain as well as in a lacustrine environment. In addition, no sharp surface or lithological boundary was observed. The overlying succession of the Mm and Sg facies probably records occasional turbiditic sedimentation during a rise in lake level. Unit C5 is also a shallowing-up unit, but is distinguished from units C1-3 by a thick offshore succession dominated by turbidite sandstones with minor black shales in the lower part. Nearshore Mss facies and mudflat Mc mudstones form the upper part of the unit. The presence of a relatively thick sandstone turbidite succession can provide evidence of a nearby high gradient basin margin and can be interpreted as part of a deep-water turbidite fan. Alternatively the turbidites could have been generated from a large delta built by a river entering the lake from an axial or flexural margin direction (cf. L. Tanganyika, Tiercelin and Mondeguer, 1991; Huc et al., 1990).

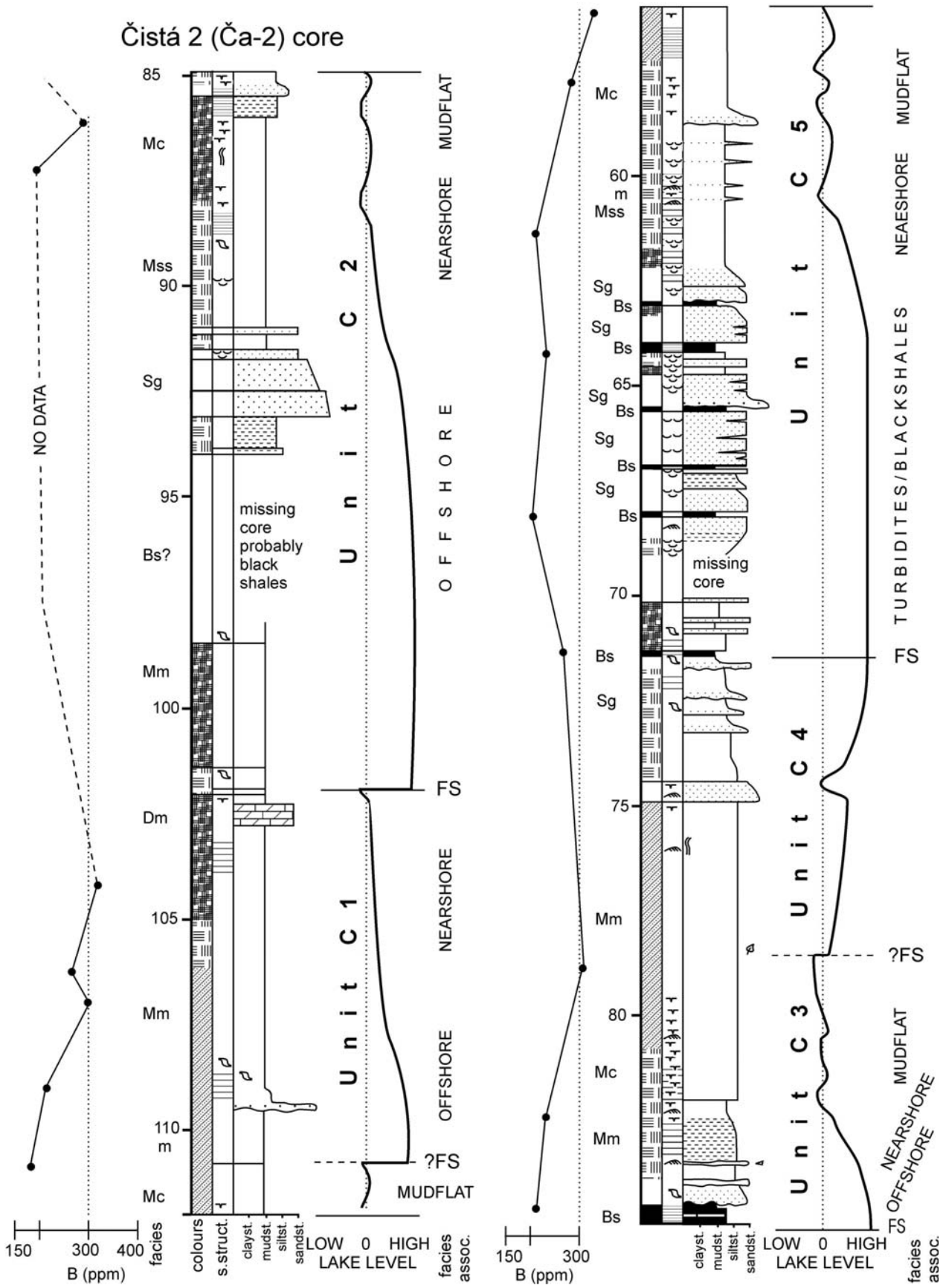

Figure 7. Sedimentological section measured in well core Čistá 2 (Ča-2), sedimentary facies (Table 1), facies subassociations and interpreted lake-level changes are shown. For legend see Fig. 4.

3.3.2.3. Prostřední Lánov section: fan-delta system

The Prostřední Lánov section is situated near the present northern basin margin (Fig. 1).The section can be divided in two distinctive shallowing-up units, which are separated by a flooding surface (FS, Fig. 6). Unit PL1 is characterised by a transition from offshore anoxic facies Mo and Bs at the base towards nearshore siltstone and sandstone facies Sr and Mss (Table 1). Current ripples show climbing, and oscillation ripples, load casts, ball and pillow and water escape structures are also present. The latter facies indicate rapid sedimentation from traction and oscillation currents, which is typical for nearshore sand bodies. They probably represent nearshore bars and sand bodies and their progradation was most likely due to a drop of lake level. The top of unit PL1 is overlain by anoxic offshore facies Bs and La, which form the base of unit PL2 and is interpreted as the result of a significant rise of lake level. The upper part of unit PL2 is interpreted as progradation of the sandstone and conglomerate bodies. The lower part of the succession is characterised by progradation of Mss, Sg and Sr facies, which are characterised by sharp bases and graded bedding. They are traction and turbidity current products. This contrasts to the upper part of section, where, in addition to the Sg and Sr facies, Gm conglomerates form a significant portion. Both matrix-supported and clast-supported conglomerates are present and are interpreted as deposits of cohesive and non-cohesive debris flows, respectively. The evidence for rapid sedimentation and vertical facies succession supports the interpretation of a fan-delta system. The lower part of the fine-grained sandy turbiditic unit PL2 probably represents distal fan-delta deposits, conglomeratic debris flows are interpreted as having been deposited on the proximal part of a fan-delta. There are no indicators of water depth in this part of the section, so it is not clear whether sedimentation took place in a subaquaous or a subaerial part of the fan-delta (Sneh, 1979).

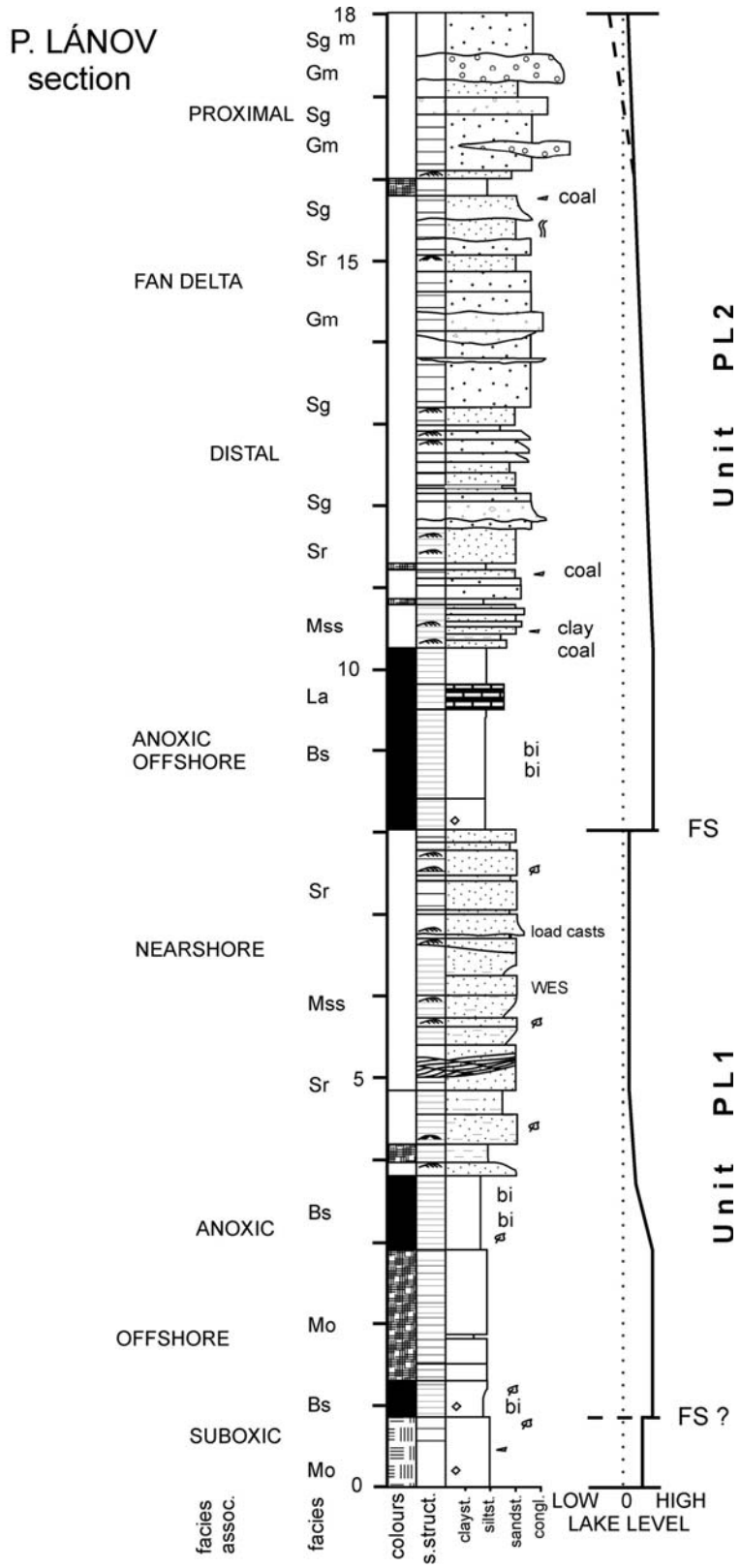

Figure 8. Sedimentological section measured at Prostřední Lánov, sedimentary facies (Table 1), facies subassociations and interpreted lake-level changes are shown. For legend see Fig. 4.

3.3.2.4. Honkův Potok section: sandy nearshore

The section of Honkův Potok records a relatively short period of lacustrine sedimentation in the northwestern part of the basin (Fig. 7a). The section is located in the small valley of Honkův Potok Creek, where several small and scattered (usually 1 – 2 metres thick) sections of mainly lacustrine black shales containing lacustrine fauna of the Rudník member occur (Fig. 1).

The lower part of the section is dominated by sandstones of the Sr and Shcs facies (Fig. 7a), interpreted as sedimentation products from traction and oscillatory stream wave currents, storm waves and currents, respectively. Alternation of these facies probably indicate changing water depth with conditions of sedimentation alternating between a near fair-weather wave base and a near storm-weather wave base, which can be interpreted in terms of lake-level fluctuations. Facies Sr, with its small oscillation ripples (5 – 20 cm wavelength), were probably deposited in much shallower water depths than the overlying Shcs facies with antiforms and synforms (hummocks and swales) with a wavelength of a few metres (Dam and Surlyk, 1993). But alternation of these facies may also be attributed to changes in storm intensity and magnitude.

The upper part of the section is poorly preserved; sedimentary structures and sandstone body geometries have been altered by weathering. Grey laminated and bioturbated siltstones are overlain by flat and trough beds of mostly massive coarse-grained clayey sandstones with a pebble admixture. This part of the section may represent 1) progradation of sand bodies or migration of channels on a delta plain, 2), deposits of a subaqueous delta front setting, and 3) alluvial/fluvial channels and overbank deposits.

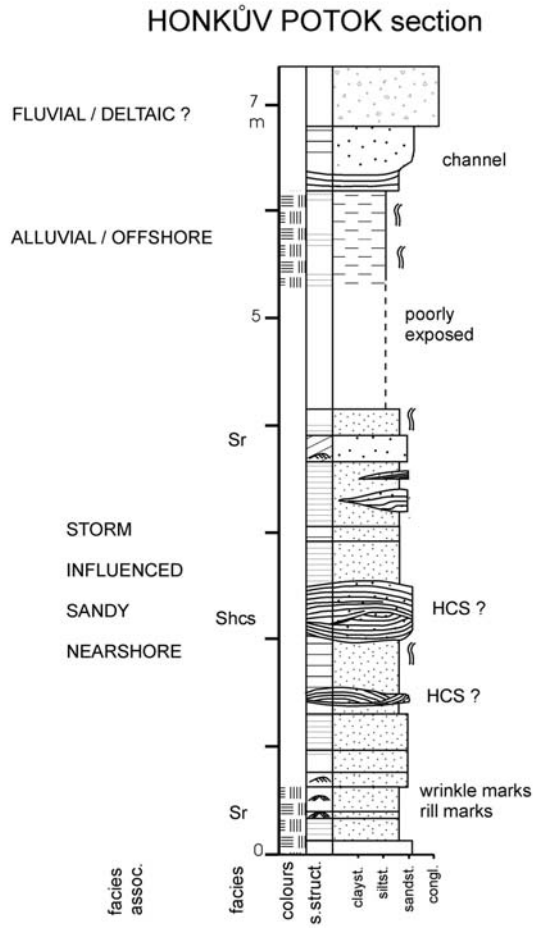

Figure 9a. Sedimentological sections measured at Honkův Potok locality, sedimentary facies (Table 1), facies subassociations and interpreted lake-level changes are shown. For legend see Fig. 4, for detailed description see text.

3.3.2.5. Kundratice section: mudstone-dominated, low-gradient lake margin

In the Kundratice section, three shallowing-up units were recognised (Figs. 1, 7b). Unit K1 consists of basal anoxic offshore black shales of the Bs facies overlain by an offshore, finely laminated dark grey carbonate bed, which passes up into nearly massive grey mud-cracked nearshore carbonate of the Cm facies. The top of unit K1 is formed by mudcracked mudstones of the mudflat facies, Mc. Unit K1 records lake regression accompanied by carbonate precipitation. Offshore black shales at the base of the unit K2 sharply overlies the mudflat mudstones of unit K1. The base of black shales is interpreted as a flooding surface. Black shales of the Bs facies, representing anoxic offshore sedimentation, are relatively thin and pass gradually into grey laminated mudstones interpreted as having been deposited in more oxygenated offshore sediments. The top of unit K2 is formed by nearshore Mss facies. Unit K3 shows similar features as the underlying units. The basal black shale bed is overlain by a succession of nearshore/mudflat mudstones with interbeds of lenticular, nodular, muddy micritic dolostone beds of the Dm facies. These dolostone facies are interpreted as being precipitated from shallow saline water with the possible influence of fresh groundwater (cf. Muir et al., 1980; Rosen et al., 1989). The dolomites show evidence of subaerial exposure and vadose environments such as mudcracks, secondary porosity, and drusy calcite cement (Table 1, Fig. 9a), and are interpreted as modified or partly formed in a palustrine environment (Freyet and Plaziat, 1982; Platt and Wright, 1992). Unit K4 is incomplete, but consists of rapidly deposited and slumped beds (Ms), possibly of volcanogenic origin, and offshore black shales (Bs).

The absence of coarser clastic material within this section, and the presence of a succession of nearshore/mudflat facies, up to several metres thick, indicate a low sediment input and low-gradient lacustrine environment. Such environments would be very sensitive to lake-level fluctuations, which were probably the main driving mechanisms producing the facies patterns. Lake-level fluctuations of several orders can be documented. Large lake level rises are marked by four flooding surfaces, minor fluctuations are marked by abundant mudcracks

within the nearshore and mudflat facies. The interbedded offshore black shales and mudcracked mudflat facies provide strong support for the changes in relative lake level interpretation discussed below.

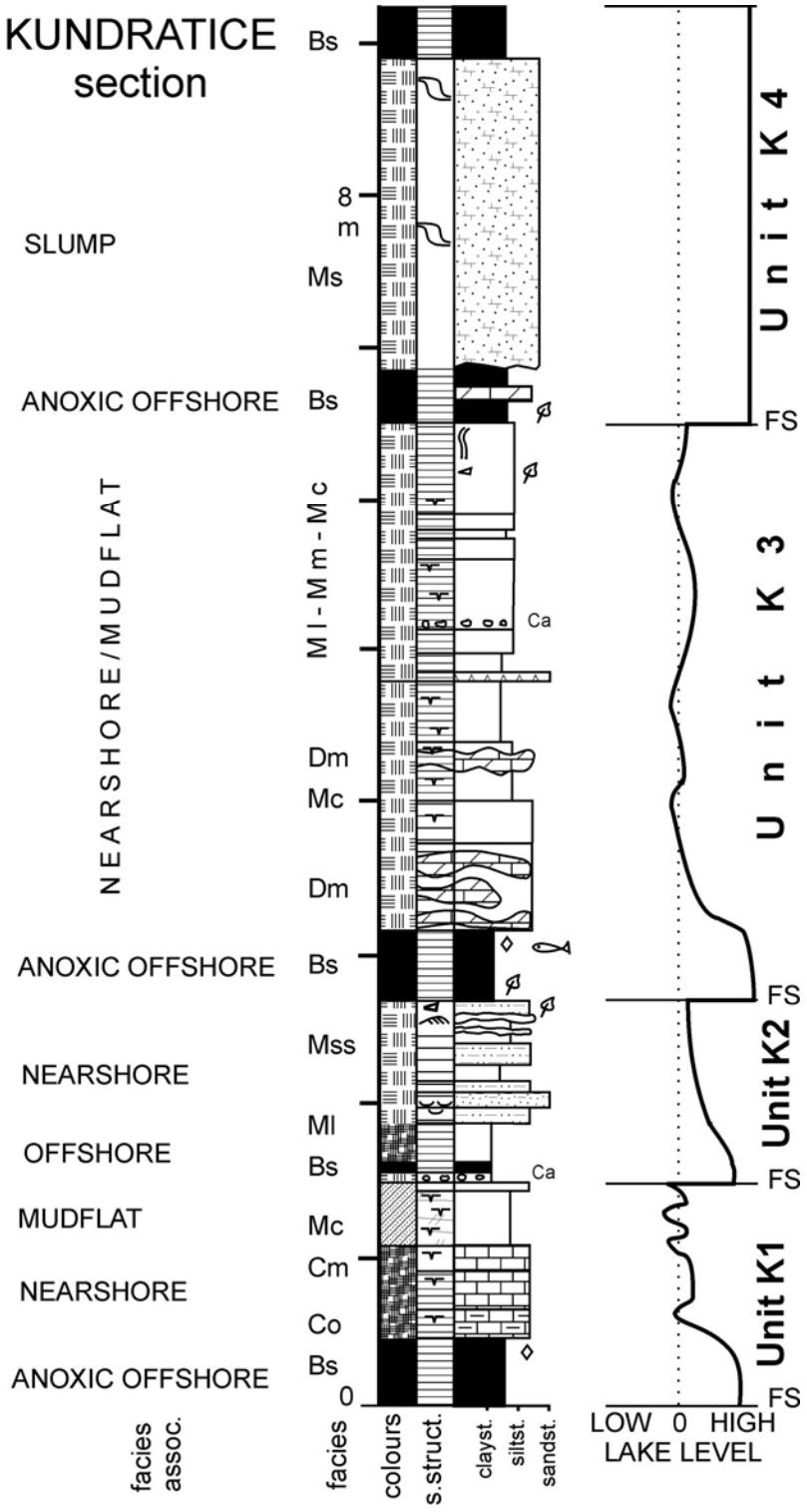

Figure 7b. Sedimentological sections measured at Kundratice localities, sedimentary facies (Table 1), facies subassociations and interpreted lake-level changes are shown. For legend see Fig. 4, for detailed description see text.

3.3.3. Lacustrine calcite and dolomite

Most of the mudstone and carbonate facies contain different proportions of calcite and dolomite. Calcite is present in the form of: 1) micrite or microspar, finely dispersed in mudstone or forming discrete laminae; 2) microspar forming

early diagenetic lenses in laminated Bs and La facies; and 3) calcite spar cementing secondary porosity, which is found only in Dm facies. Dolomite is present in the form of dolomicrite and dolomicrospar occurring in the same setting as calcite micrite and microspar. No displacive/replacive textures are found. Grains of detrital dolomite were found within the silty turbiditic laminae of Mo facies. Facies Bs, La, Ml and Dm show changes in dolomite/calcite ratios (Table 1). Black shales of Bs facies are calcite dominated with minor dolomite, while in the muddy dolomites of Dm facies dolomite dominates and the calcite content is very low. Facies La and Ml usually contain significant amounts of calcite as well as dolomite.

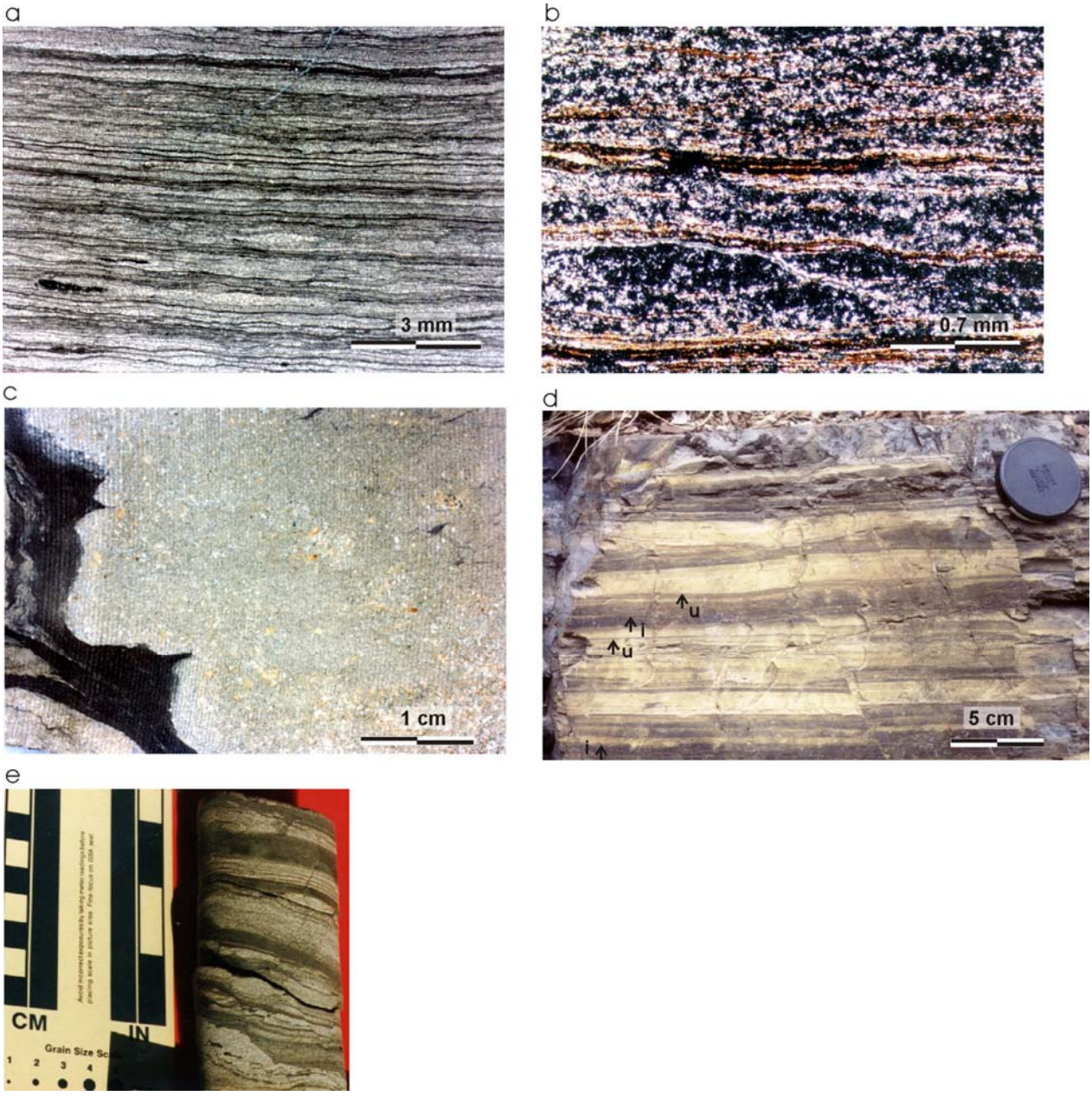

Figure 10. a) Even lamination of black shale facies (Bs). Most of the rock is composed of clay minerals, black laminae are rich in organic matter, which is interpreted as having been deposited during annual/seasonal algal blooms. Whitish lenses and lensy laminae are composed mainly of clay minerals and microspar crystals of early diagenetic origin; black lenses (lower left) are later diagenetic bitumen lenses. Kundratice section, 0.2 m, rock slab, reflected light. b) Close-up view showing even algal laminae (brown) and mixture of kaolinite, illite and analcite (grey to black) and microspar crystals (bright) scattered in a clay mineral matrix. Transmitted light, crossed nicols. c) Base of the slump bed (facies Ms) showing large plastically deformed laminated black shale rip up clast (black), smaller grey mudstone rip up clast and pale yellow intraclasts of probable volcanogenic origin. Kundratice section, 6.9 m, rock slab, reflected light. d) Outcrop showing facies Mo in Vrchlabí section 3.5 m. Sharp- to erosional-based normally graded silty laminae of distal turbidity underflows and sharp- to diffuse-based silty laminae of interflows can be seen. Lens cap is 5 cm in diameter. e) Čistá 2 well core showing alternation of mm – cm laminae of black shales (Bs) and turbidite sandstones (Sg). Small-scale faults can also be seen in the lower part. Ča-2, 67.30 m.

Because of the lack of displacive/replacive textures most calcite micrite, microspar, dolomicrite and dolomicrospar was probably precipitated primarily from the lake water or early diagenetically from pore water. Almost all recent lacustrine dolomite is precipitated from saline lake waters with a high Mg/Ca ratio (Last; 1990). Precipitation from pore waters with high Mg/Ca ratio in relatively freshwater lakes is rare. The black shale facies (Bs) with low dolomite content is interpreted as a product of sedimentation/precipitation from the least saline water during high lake levels, in contrast to muddy dolomites of the Dm facies, which needs much more saline water with a higher Mg/Ca ratio to precipitate. These conditions suggest a low lake level. Facies La and Ml, with both dolomite and calcite content, are interpreted as products of sedimentation/precipitation products from moderately saline water during intermediate lake-level. This requires a hydrologically closed lacustrine system with higher salinities during low lake levels and lower salinities during high lake levels. The possibility of early diagenetic dolomitization mediated by organic matter (Slaughter and Hill, 1991) cannot be excluded. Calcite and dolomite of the Bs, La, Mo, Cm, Co and Dm facies are mostly ferroan calcite and ferroan dolomite, which indicates precipitation in reducing conditions.

Figure 11. a) Secondary porosity developed in muddy dolomite facies (Dm) showing drusy calcite cement fringe (bright) and later analcite infill (black). Kundratice section, 3.6 m, transmitted light, crossed nicols. b) Gradual transition between organic-rich laminated mudstone (facies Ml, at the base) and muddy dolomite (Dm, at the top). Transitional unit (Tr, in the middle), originally facies Ml, is modified by early dolomitization, euhedral to subhedral small dolomite crystals (bright) are abundant. Kundratice section, 3.6 m, transmitted light, crossed nicols. c) Microbial mat with well-preserved undulose laminated grey lower part and oxidised, probably pedogenically disturbed red-brown upper part. Vrchlabí section, 10.1 m, polished rock slab.

3.4. Palaeogeography and tectonosedimentary model of the Rudník Lake

Palaeontological evidence suggests that the faunal and floral assemblages of all sections of Rudník Lake deposits belong to one lacustrine period (Blecha et al., 1997; Drábková et al., 1990; Zajíc, 1997; Šimůnek, 1997; Drábková, 1997). Correlation of particular beds between most outcrop sections is not possible because of the large distances between sections (Fig. 1), the high degree of lateral facies variability and postsedimentary deformation of the basin. Only sections situated close to each other can be correlated bed-by-bed. Several black shale dominated outcrops in the Kundratice-Košťálov area, not more than a few kilometres apart, contain almost the same sedimentary succession with small variability in the thickness of particular beds. The anoxic offshore facies found in almost all sections of Rudník Lake deposits represent highstand sedimentation in one large lake, which covered an area of at least 400 km^2. During lowstands the lacustrine basin could have been divided into several partly or completely isolated lake sub-basins.

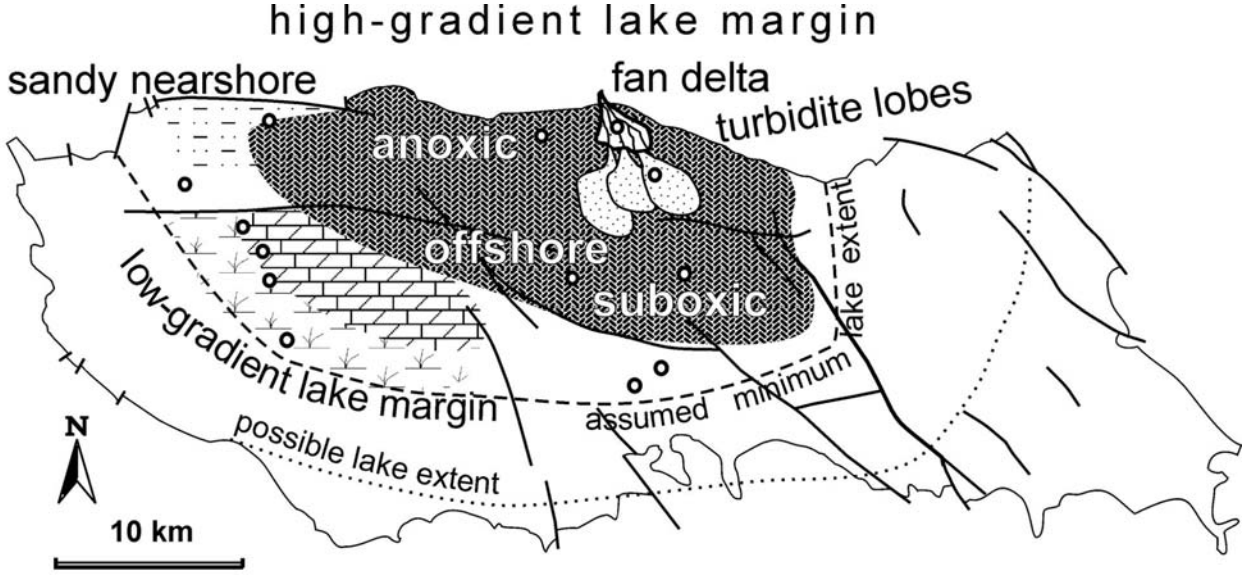

Figure 12. Simplified palaeogeographical sketch of the Krkonoše Piedmont Basin during the sedimentation of Rudník Lake showing distribution of sedimentary environments. Three palaeogeographic elements are recognised: the anoxic offshore axial basin, a low-gradient mudstone/carbonate dominated southwest margin, and a high-gradient northern margin with gravity driven deposits. Sedimentary environments are placed in the context of the present-day outcropping basin. Circles refer to the studied localities and boreholes (Fig. 1).

Three areas of distinctive facies development were found (Fig. 10): 1) a central-axial part of the basin dominated by anoxic to suboxic offshore mudstones; 2) the northern basin margin dominated by anoxic black shales and sandy to gravelly gravity currents or nearshore deposits indicating a high gradient basin margin; and 3) the west-central part of the basin dominated by black shales and nearshore facies and mudflats of a low-gradient basin setting.
The presumed lateral distribution of sedimentary environments during deposition of the Rudník member in the Krkonoše Piedmont Basin is shown in Fig. 10. The central-northern part of the basin, probably representing the deepest, axial part of the basin (Vrchlabí section, borehole HK-1, Fig. 1), contains the thickest succession of anoxic to suboxic offshore facies (Bs, La, Ml). Along the northern basin margin, coarser clastic facies are distributed. Nearshore sandstone facies of the Honkův Potok section probably originated by the redistribution of nearby alluvial fan or fan-delta or fluvial clastic material. These facies could have also been deposited in an accommodation zone between two half-grabens (cf. Gawthorpe and Leeder, 2000) or a hinge zone (sensu Soreghan and Cohen, 1996). The fan-delta system of the Prostřední Lánov section probably supplied the Čistá 2 section's sandstone turbidite bodies. These facies indicate a steep gradient along the northern basin margin. In contrast to this steep-gradient sedimentary system, mainly mudstone/carbonate facies occur in the southwest part of the Rudník Lake. These facies are stacked in several relatively thin, shallowing-up, offshore – nearshore units (section Kundratice in Fig. 7b) and indicate a low-gradient sedimentary system, which was sensitive to lake-level fluctuations. The lateral distribution of sedimentary facies (Fig. 10) and the asymmetry of the basin fill (Fig. 3) allow us to interpret the tectonic setting of the basin during the Asselian as a half-graben. Subsidence along the northern basin margin fault (Fig. 11) was the main driving mechanism determining the sedimentary architecture of the basin fill. Unfortunately, we do not have kinematic indicators to interpret whether the fault was dip-, oblique- or strike-slip. The basin could have developed as a simple half-graben in an extensional regime or as series of transtensional sub-basins along a strike- or oblique-slip fault (Crowell and Link, 1982; Coward, 1986; Scholz, 1995). Because of the limited preservation of nearshore

facies along the present-day northern basin margin, we suggest that the main boundary fault was situated northwards of the present-day boundary fault during the Early Permian.

Although no reliable bathymetrical indicators are available, the minimum depth of the Rudník Lake during highstand is interpreted to have been about several tens of metres. This interpretation is based on the presence of lake water stratification indicated by black shales found over an area of 300 km^2 and the thickness of the siliciclastic progradational successions, which need accommodation space to develop. Unit C5 of the Čistá 2 section is thus more than 15 m thick and its original thickness before compaction could have been ca 25 m. The minimal areal extent of a highstand offshore facies of 400 km^2 needs a minimum water depth of several tens of metres to cover topographic highs. Faunal assemblage is relatively diversified. Vertebrates are represented by acanthodians (1 species; Acanthodes), xenacanthid sharks (1 species; Bohemiacanthus), actinopterygians (7 species; Paramblypterus, Amblypterus, Igornichthys), dipnoans (1 species; Sagenodus), amphibians (4 to 5 species; Archegosaurus, Melanerpeton, ?Cheliderpeton, "Ptyonius"), and reptiles (unidentified remains). Invertebrates are represented by pelecypods (?Anthraconaia), conchostracans (Limnestheria, Pseudestheria), ostracods (Carbonita), malacostracans (Uronectes, Monicaris), and unidentified insects (Schneider and Zajíc, 1994; Zajíc, 1997). The diversified lake ecosystem including large predators such as 0.5 – 1 m long sharks needed sufficient time and water volume to develop.

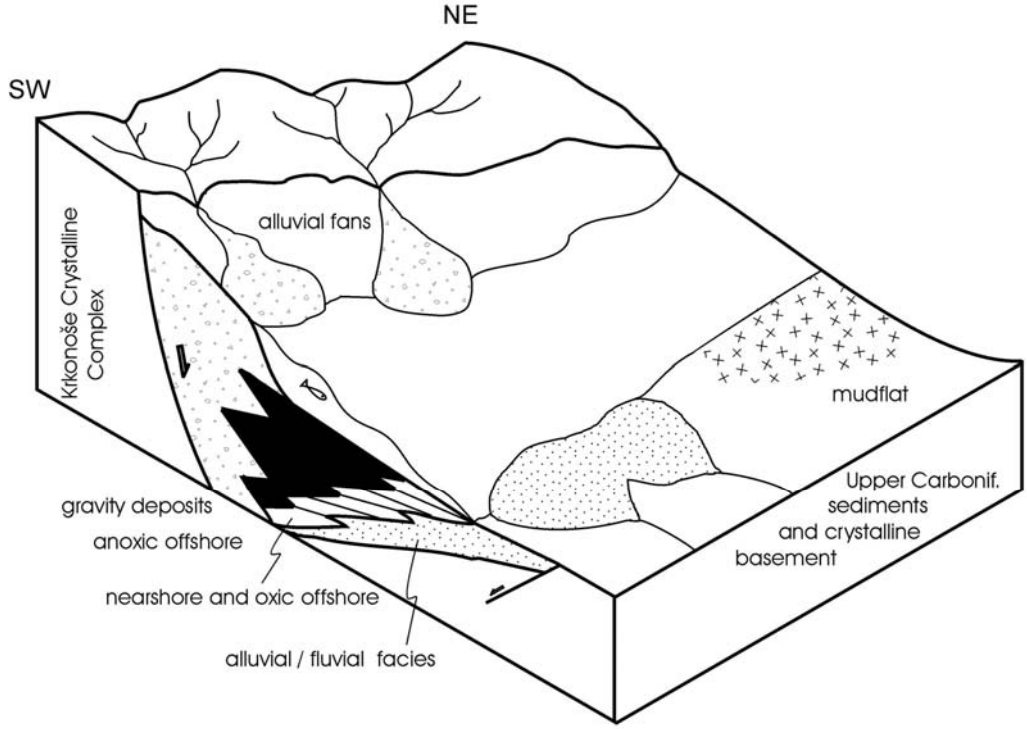

Figure 13. Depositional model of the Rudník Lake during a lake-level highstand. Facies architecture was controlled mainly by subsidence along the northern marginal fault. The reconstruction incorporates postsedimentary northwestern dextral strike slip deformation of the basin. For explanation see text.

4. Geochemical record

4.1. Approach

Several geochemical methods were applied in order to understand the response of the Rudník Lake to different climatic conditions reflected in changes of hydrological regime, water chemistry and bioproductivity. Stable isotopes of calcite have indicated the hydrological conditions in different basins (Talbot, 1990), boron content in clay is often closely associated with relative changes in palaeosalinity (Bohor and Gluskoter, 1973; Stewart and Parker, 1979; Goodarzi and Swaine, 1994), and organic geochemistry provides evidence about the biological source of organic matter, bioproductivity associated with nutrient supply and lake-level changes, redox conditions during transport and deposition, microbial degradation and diagenesis (Tissot and Welte, 1984).

4.2. Methods and samples

4.2.1. Stable isotopes of calcite

Most of the sampled rocks are well-laminated mudstones to limestones with low to very high organic matter content (up to 23% TOC) and with varying proportions of calcite and dolomite. Organic rich carbonate mudstones and carbonate laminites (facies Bs, La, Ml, Mc, Dm and Mo) were analysed to determine the stable isotopic composition of carbon and oxygen of calcite. Offshore facies in the Vrchlabí section and offshore as well as nearshore facies in the Kundratice section were sampled. A petrological study of thin sections allows five calcite phases to be recognised, which were analysed separately (Figs. 8a, 8b, 9a, 9b; Figs. 18a, 18c). (1) Micrite of the black-grey, organic matter rich, clayey laminae of the carbonate mudstones (Bs, La and Mo facies). (2) Micrite to microspar of the grey clayey laminae of the carbonate mudstones with a lower organic matter content (Bs and Mo facies). (3) Whitish coarse pure microspar to fine-grained sparite lenticular laminae and lenses of assumed early diagenetic origin, containing very small admixtures of organic matter and clay minerals (Bs, La and Mo facies). (4) Microspar from laminae of carbonate mudstones with a dominant proportion of clay (Mc and Ml facies). (5) Microspar from nodular beds of muddy calcareous dolomite (Dm).
Types 1, 2 and 3 are referred to as primary, because they are believed to have been formed by the primary precipitation of micrite and microspar from lake water. No displacive/replacive structures were found in these samples.
Samples of laminated rocks, where different mineral phases occur in individual laminae, were taken using a dentist's microdrill. Calcium carbonate samples were decomposed under a vacuum in 100% H_3PO_4 at 25°C (McCrea, 1950). Even though some samples contain a higher proportion of dolomite, more than 50% in a few samples, only calcium carbonate was decomposed at 25°C, and higher temperatures for dolomite decomposition were not applied. All obtained values represent the samples' calcium carbonate phase. Released CO_2 was analysed on the Finnigan MAT 251 mass-spectrometer. The results are reported in per mil deviation from the V-PDB standard using the δ notation. The precision of both carbon and oxygen isotope analyses is better than ±0.1‰. A total of 64 samples were analysed.

4.2.2. Organic petrology

Organic macerals were examined on polished surface samples of whole rocks using a UMSP 30 Petro microscope-photometer (Zeiss-Opton) at total magnification of 450x and 650x, under reflected non-polarized light and oil immersion (n = 1.518). Random reflectance was measured in monochromatic light of λ (wavelength) 546 nm. For fluorescence analyses a halogen discharge lamp and an F 109 filter set with blue light irradiation were used.

4.2.3. Elemental analysis, pyrolysis, gas chromatography and stable isotopes of organic matter

The total organic and total inorganic carbon contents (TOC and TIC, %) were measured using an ELTRA elemental analyser. Selected samples were analysed using a Rock-Eval 5 pyrolyser (Bordenave et al., 1993) in nitrogen flow with a temperature programme from 300 to 650 °C. A flame ionisation detector measured three parameters: 1) S1 – free (volatile) hydrocarbons (mg HC/g rock); 2) S2 – bound hydrocarbons and non-hydrocarbon compounds released by pyrolysis, S2 represents residual source potential (mg HC/g rock or kg HC/ tonne rock); 3) Tmax – maximum temperature of the pyrolytic peak S2 (°C) that indicates the thermal maturity of kerogen.
The hydrogen index is calculated using the equation: HI = 100 * S2/ TOC (mg/g TOC) and represents the relative amount of hydrogen in kerogen molecules. This parameter is especially sensitive to organic facies.
Three samples were extracted by organic solvent (CH_2Cl_2) and the saturated hydrocarbon fraction analysed using capillary HP gas chromatography.
For mass-spectrometric analyses of the stable isotopic composition of organic carbon, carbonates were first removed by hot, diluted hydrochloric acid. The residue, after washing and drying, was combusted in a FISONS 1108 elemental analyser, which is coupled online with a Finnigan MAT 251 mass-spectrometer in continuous flow mode. The δ values were defined as the per mil deviation from the V-PDB standard. The reproducibility was ± 0.25‰.
A total of 13 samples of organic-rich rocks, mostly black shales and laminites of the Bs and La facies, were analysed. Samples with very high TOC content and samples with significant changes of $\delta^{18}O$ and $\delta^{13}C$ of calcite in vertical sections were selected for analysing the $\delta^{13}C$ of organic matter.

4.2.4. Distribution of boron in mudstones

A total of 65 samples of mudstones were crushed and then leached with 4% monochloracetic acid to remove carbonates from the suspension. The solid phase was decanted and washed by resuspension in distilled water. The clay fraction (<2 μm) was decanted from non-settled matter in suspension. The mineralogy of the separated clay fraction of all samples was checked by the X-ray diffraction technique. The separated clay was digested with HNO_3 and HF in microwave dissociation equipment. The concentration of boron in the solution was determined by the ICP MS technique using Varian UltraMass equipment. Stable isotopic, Rock-Eval pyrolysis and gas chromatography analyses were carried out by the laboratories of the Czech Geological Survey, boron determinations were done by the Geological Laboratories of Charles University.

4.3. Results

4.3.1. Stable isotopes of calcite

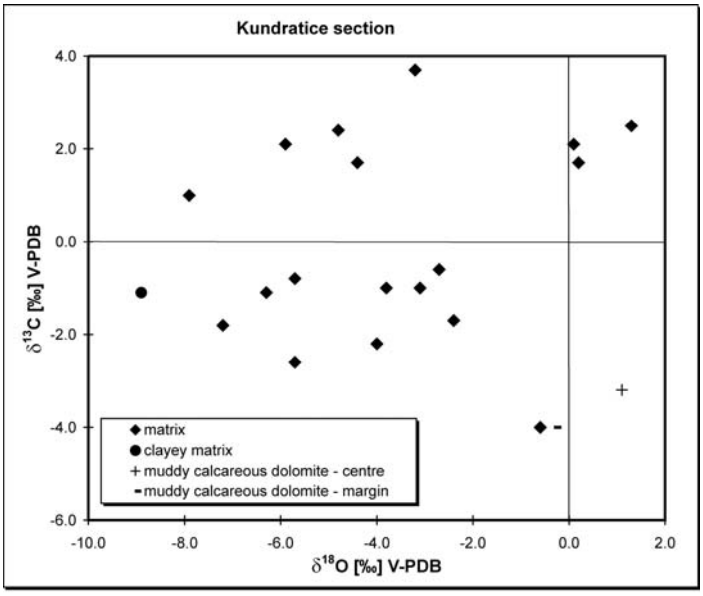

The values obtained are within the range of -11.0 to +1.3‰ $\delta^{18}O$ and -5.1 to +3.7‰ $\delta^{13}C$ (Figs 12,13). Calcite from shallow water muddy calcareous dolostones of the Dm facies shows higher $\delta^{18}O$ and lower $\delta^{13}C$ values in comparison to the rest of the data set (Fig. 12). The higher $\delta^{18}O$ and $\delta^{13}C$ values of pure microspar – sparite laminae, in comparison to the dark clayey organic-rich matrix laminae in most samples from the Vrchlabí section, can also be seen; analyses of different calcite phases from the same hand specimen are linked by arrows (Fig. 13). There is a covariant trend of grey matrix values with a high correlation coefficient R = 0.896. Samples of primary calcite from Kundratice are richer in ^{13}C in comparison to the Vrchlabí section (Fig. 14).

Figure 14. The $\delta^{18}O$ / $\delta^{13}C$ plot of calcite from samples of the Kundratice section.

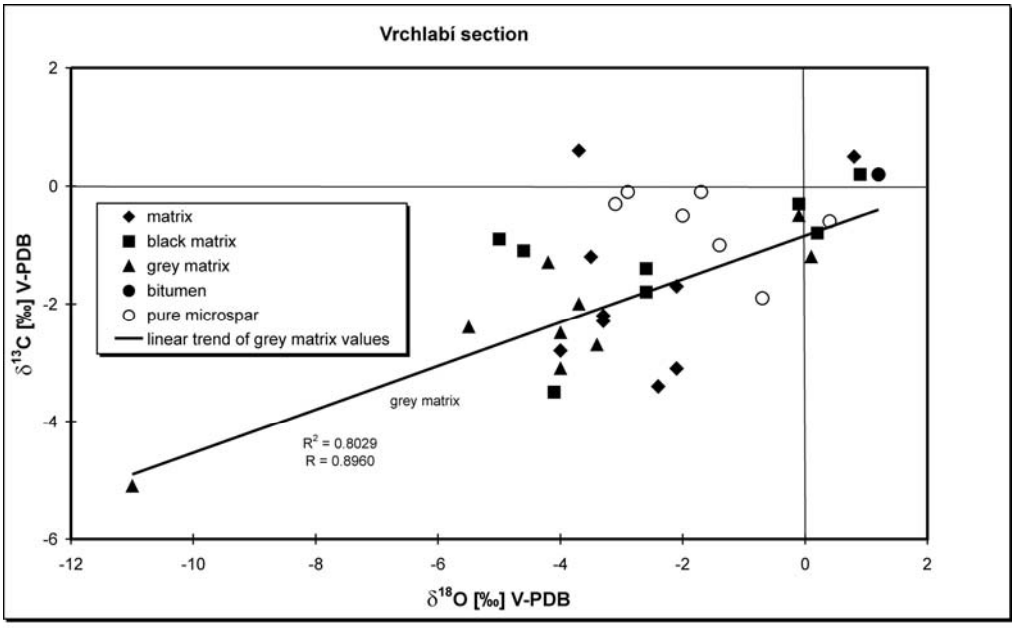

Figure 15. The $\delta^{18}O$ / $\delta^{13}C$ plot of calcite from samples of the Vrchlabí section. The covariant trend of clay matrix values is discussed in the text.

In vertical sections, values of $\delta^{18}O$ and $\delta^{13}C$ show several distinctive features, the most striking of which is that $\delta^{18}O$ values follow the same trends as $\delta^{13}C$ values as noticed in many different lacustrine carbonates (e.g. Talbot, 1990; Talbot and Kelts, 1990), but this remains unsatisfactorily understood. At the base of the Kundratice section, a significant decrease in both $\delta^{18}O$ and $\delta^{13}C$ values can be seen at the transition from a black shale bed of Bs facies to the organic-rich carbonate bed of Co facies (Fig. 15, 0.5 m, trend no. 2). Within the upper black shale bed (facies Bs, 2.7 – 3.3 m, trend no. 1) a gradual upwards increase in $\delta^{18}O$ and $\delta^{13}C$ values can be observed. Within the overlying nearshore facies both values decrease (3.3 – 4.8 m, trend no. 3). In the Vrchlabí section $\delta^{18}O$ and $\delta^{13}C$ values within the lower laminite bed (Fig. 16, La, 2.3 – 2.75 m, trend no. 1) show similar increasing upwards trends to $\delta^{18}O$ and $\delta^{13}C$ in the Kundratice upper black shale bed. Fluctuations in the $\delta^{18}O$ and $\delta^{13}C$ values are visible at the top of black shale (Bs) and at the bottom of the mudstone turbiditic unit (Mo, 2.7 – 3.3 m, trend no. 4).

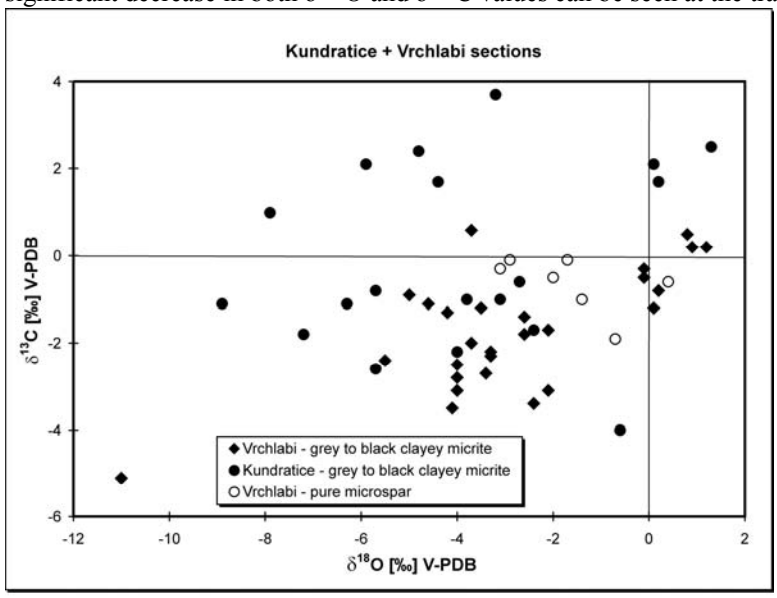

Figure 16. Summary $\delta^{18}O$ / $\delta^{13}C$ plot of calcite from samples of the Vrchlabí and Kundratice sections showing higher $\delta^{13}C$ of samples from Kundratice.

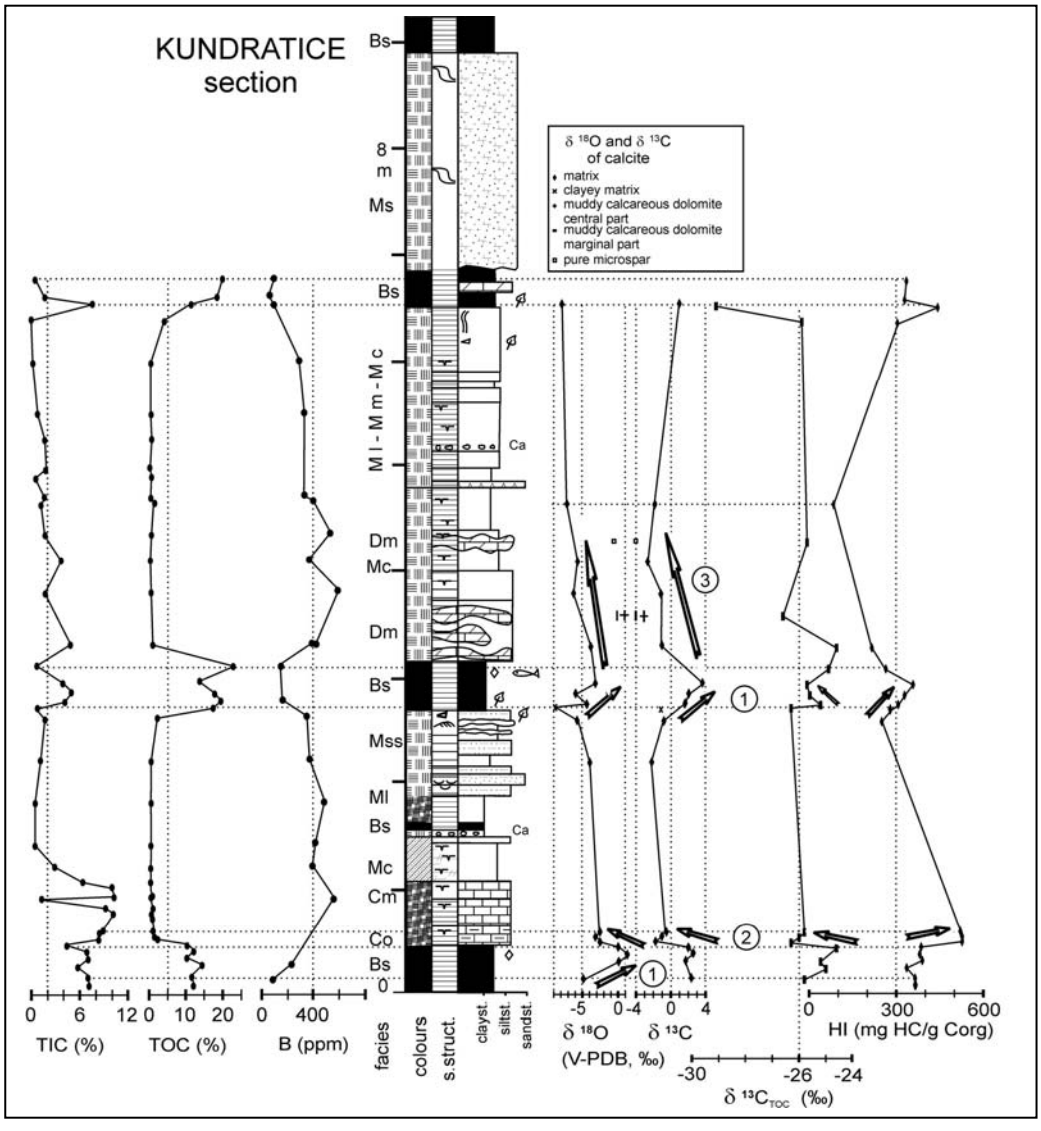

Figure 17. Log of the Kundratice section showing distribution of total organic carbon (C_{TOC}), total carbonate carbon (Cmin), boron, $\delta^{18}O$ and $\delta^{13}C$ of calcite, $\delta^{13}C$ of organic matter, and hydrogen index. Circled numbers refer to different vertical trends discussed in the text.

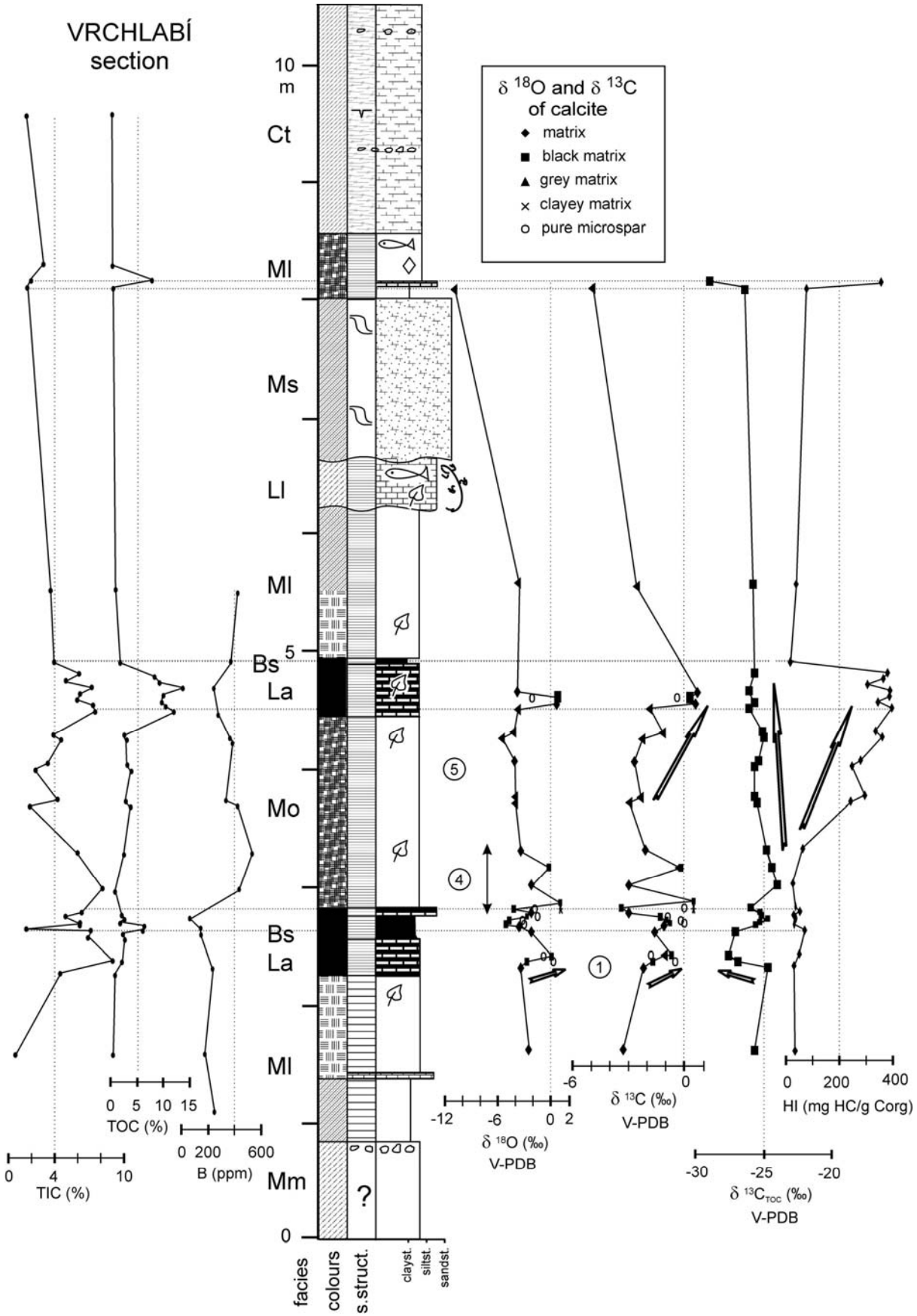

Figure 18. Log of the Vrchlabí section showing distribution of total organic carbon (C_{TOC}), total carbonate carbon (Cmin), boron, $\delta^{18}O$ and $\delta^{13}C$ of calcite, $\delta^{13}C$ of organic matter, and hydrogen index. Circled numbers refer to different vertical trends discussed in the text.

4.3.2. Petrology and geochemistry of organic matter

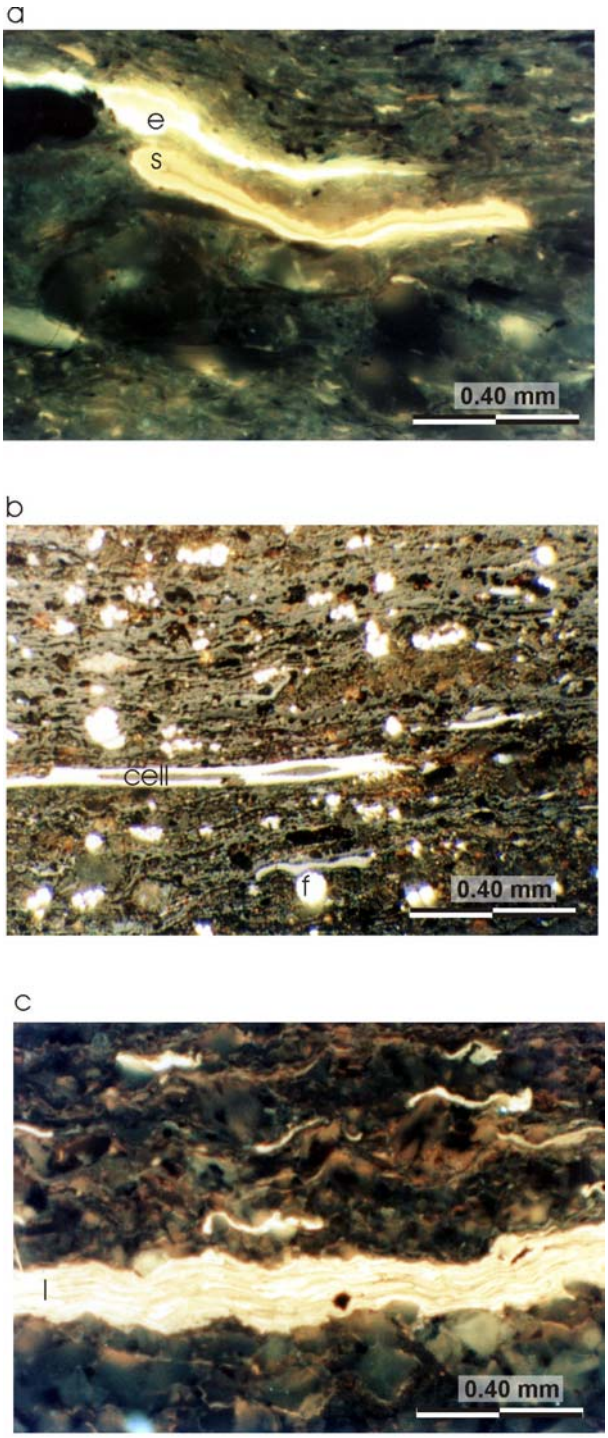

The organic maceral composition was closely examined in eight samples of the anoxic facies Bs, La and the pelagic unit of Mo. The main petrographic features in most samples include a few micrometres to millimetres thick laminae, abundant occurrences of algal and amorphous organic matter commonly associated with terrestrial plant debris and framboidal pyrite (Figs. 17 and 18).
The major organic macerals identified following Taylor et al. (1998) comprise of: 1) Liptinite with benthic colonial algae, e.g. *Botryococcus braunnii*, or lamalginite (kerogen type I), sporinite and resinite (kerogen type II). 2) Amorphous organic matter formed by microbial decomposition of organic matter. 3) Dispersed mineral-bituminous groundmass (common) and exsudatinite filling fissures and voids (less common) visible in fluorescent light. 4) Fusinite and semifusinite with well-preserved cell walls and higher reflectance, which represents partly oxidized or charred terrestrial plant debris. 5) Vitrinite, the gelified humic substance (kerogen type III), which is present in many but not all samples as structureless collinite and telinite with partly visible plant tissues.
The proportions of the macerals vary in different lithologies and intervals. The maceral composition is closely associated with the geochemical parameters, e.g., hydrogen index or stable isotopes, and influences the apparent thermal maturity. Vitrinite reflectance (R_r) is commonly suppressed by 0.1 – 0.2% in samples rich in alginite. In many mudstone samples only fusinite, semifusinite and liptinites are identified (e.g. Table 2) and the thermal maturity was determined only from the T_{max} of the Rock-Eval pyrolysis. In both profiles the vitrinite reflectance varies from 0.6 to 0.8% and the T_{max} from 425 to 447°C, corresponding to the beginning of the oil generative window (Bordenave et al. 1993; Tissot and Welte, 1984). The observed maceral composition and measured thermal maturity is in agreement with earlier studies of Permian rocks in this basin (Müller, 1987; Malán, 1989; Kříbek, 1990) aimed at oil shale prospecting and potential evaluation.

Figure 19. a) Black shale (Bs facies). Matrix (grey) rich in carbonate with a small amount of dispersed liptodetrinite; high intensity hydrocarbon (e – exsudatinite) originated from deformed spore (s) in the centre (lower intensity). Čistá 2 section, 85.80 m, polished section, UV light. b) Black shale (Bs facies). Detail of lamina rich in organic matter. Large fusinite particle showing some faint cell structure (in the centre, high intensity reflectance). Highest intensity framboidal (circular) particles of pyrite are abundant (f). Matrix is formed by amorphous organic matter with clay minerals (upper part of section, light grey). Lamalginite forms dark elongated grains. Kundratice section, 0.2 m, polished section, reflected light. c) Kundratice 0.2 m in UV light. Lamalginite (high intensity) forms dispersed elongated particles and discrete lamina (in the centre) (l). Matrix is rich in carbonate grains with exsudatinite coatings. Compare also to Fig. 8. b).

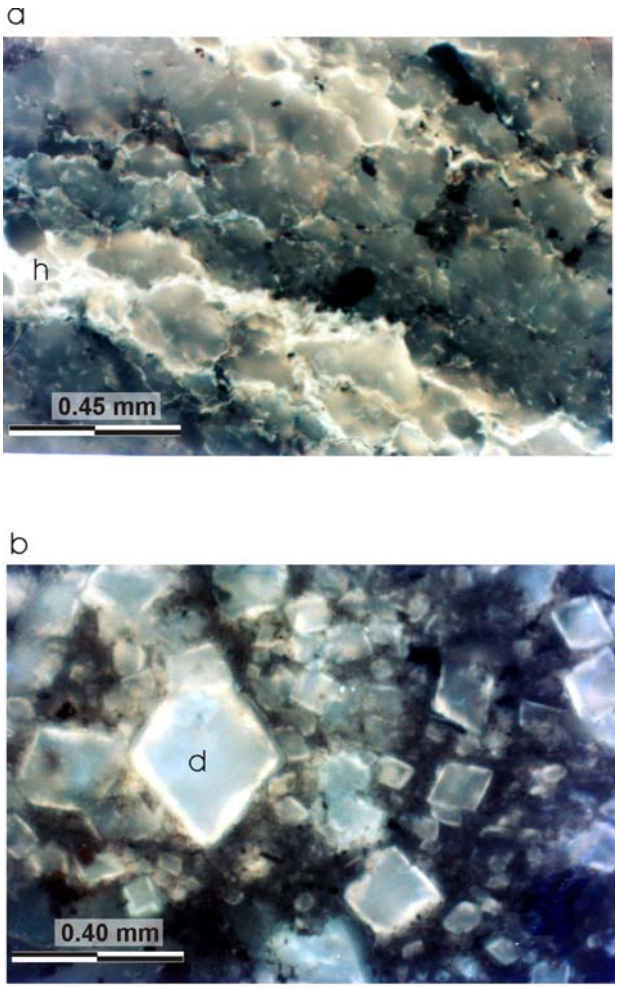

A total of 77 samples of organic-rich laminated mudstones, black shales and carbonates of facies Bs, La, Co and Mo from the Kundratice and Vrchlabí sections were analysed for total inorganic and organic carbon content (TIC and TOC, $\%_{wt}$) and 50 samples were analysed using Rock-Eval pyrolysis. The TOC values range from 0.10 to 13.73$\%_{wt}$ in the Vrchlabí section and from 0.14 to 23.13$\%_{wt}$ in the Kundratice section with an average value of 4.67$\%_{wt}$ (Figs. 15,16,19 and 20). The gas chromatograms of n- and isoprenoid alkanes of three characteristic samples in the Vrchlabí section are shown in Fig. 21.

The $\delta^{13}C$ values of total organic matter ($\delta^{13}C_{TOC}$) from the Vrchlabí and Kundratice sections are from -24.0 to -29.0‰, most of them are between -25 and -27‰. Covariance between carbon isotopic composition and organic matter content was not found. The differences in $\delta^{13}C_{calcite}$ and $\delta^{13}C_{TOC}$ are not homogeneous through the sections, but vary from 20.9 to 29.4‰.

Figure 20. a) Organic-rich dolomite bed enclosed in black shales (facies Bs). Hydrocarbon (exsudatinite, bright) coatings on carbonate grains. Laminae rich in hydrocarbons (high intensity) (h) alternate with laminae of pure carbonate (dark). Kundratice section, 6.7 m, polished section, UV light. b) Organic-rich mudstone (facies Mo). Detail of silty carbonate lamina showing zoned dolomite rhombs (d) in clay matrix. Vrchlabí section, 3.2 m, polished section, UV light. c) Vrchlabí section, 3.2 m in reflected light. White heterogeneous migrabitumen coatings in detrital carbonate grains (larger grey crystals). Sharp contact between fine-grained black shale laminae (Bs), lower left and silty carbonate lamina (C), upper right is also seen. Polished section, reflected light.

4.3.3. Distribution of boron in mudstones

The average boron content in recent marine sediments is higher than in freshwater sediments (Goldschmidt and Peters, 1932; Reynolds, 1972). Water of some saline lakes can contain considerable amounts of boron; e.g. 360 ppm at Little Borax Lake in California (Livingstone, 1963). Because the boron content is almost unaffected by later diagenesis (Degens and Keith, 1959; Goldberg and Arrhenius, 1958) it has been used as a palaeosalinity indicator to discriminate ancient marine, brackish and freshwater sedimentary environments (e.g. Bohor and Gluskoter, 1973; Stewart and Parker, 1979; Goodarzi and Swaine, 1994). The boron content in mudstones can be covariant with Fe

oxides/hydroxides due to preferential sorption to these minerals (Kraska, 1981b). In some Upper Cretaceous mudstone samples boron content covaries with organic matter content, reflecting preferential sorption of boron on organic matter (Uličný, 1989).
The boron content has already been used as a palaeosalinity indicator in the Upper Palaeozoic non-marine mudstones of the Bohemian Massif. Boron content has been interpreted as representing increasing aridity from the Late Carboniferous to the Late Permian (e.g. Bouška and Pešek, 1985, 1983, and 1976). These authors did not consider the particular sedimentary environment of sampled mudstones, therefore the interpretation has a limited ability as evidence.
In this study we tested the hypothesis that boron can be used as a palaeoenvironmental indicator in the Upper Palaeozoic lacustrine deposits. The boron content in mudstones has been successfully used as a palaeosalinity indicator in different lacustrine strata of the Early Permian age in the same basin (Blecha et al., 1999).

Results

Values of boron in the separated clay fraction (<2 μm) are in the range from 73 ppm to 603 ppm, the average value being 350 ppm. In the Kundratice section values are from 82 to 603 ppm (Fig. 15), in the Vrchlabí section (Fig. 16) from 73 to 535 ppm and in the Čistá 2 borehole (Fig. 5) from 194 to 437 ppm.
The main mineral components detected by X-ray diffraction are quartz, analcite, 10 Å fraction (illite, hydrated muscovite), 7 Å fraction (chlorite, kaolinite), feldspars (orthoclase as well as plagioclases) and a small amount of hematite.
The covariance between boron content and mineral composition was investigated by statistical methods. Spearman's rank correlation coefficient was calculated for each mineral phase (Johnová, 1996). No correlation between boron values and analcite was found (r = 0.088); there was a very low correlation between boron and illite and/or muscovite (r = 0.262), quartz (r = 0.355), kaolinite and/or chlorite (r = 0.564) and hematite (r = -0.326). The portion of samples which could covary is less than 10 % for all calculated relationships.
The covariance between boron and organic matter (OM) content was also tested. Boron analyses were carried out in the same 30 samples as before and after removal of OM by heating to 450^{o}C, respectively. The values of boron content after removing OM are slightly higher, which approximately correspond to a loss of the samples' total weight (samples with higher TOC content show a proportionally higher shift in boron values, Johnová, 1996).

4.4. Interpretation of geochemical results

4.4.1. Stable isotopes of calcite

Longinelli (1996 and references therein) emphasized experimental work, which proved that carbon-oxygen bonds in carbonates are not stable and the isotopic composition can be substantially modified during diagenesis. We believe that our data reflect the primary and early diagenetic composition of calcite. The first reason is the lack of displacive and/or replacive structures and the preservation of primary and early diagenetic structures. Additionally diagenetic overprint would probably cause homogenisation of values, but our data show substantial changes of δ values in vertical sections, within individual beds, even between individual adjoining laminae. Finally a diagenetic overprint may cause a shift of all samples in sections towards more rich or depleted values. Therefore our interpretations are based mainly on vertical sections' relative changes of values.
The $\delta^{18}O$ and $\delta^{13}C$ values from both sections fall in the range of freshwater limestones (Hoefs, 1997). Samples of primary calcite from Kundratice are richer in ^{13}C in comparison to the Vrchlabí section (Fig. 14), which can be ascribed to higher bioproductivity in a more restricted environment.
Higher $\delta^{18}O$ and lower $\delta^{13}C$ values of calcite from shallow water muddy calcareous dolostones of the Dm facies (Fig. 12) can be interpreted in terms of enrichment by ^{12}C from partly decaying organic matter, which is present in the surrounding mudstones as well as the dolostone itself. The higher $\delta^{13}C$ values of pure microspar – sparite laminae, in comparison to the dark clayey organic-rich matrix laminae in most samples from the Vrchlabí section, can be explained by hypertrophic conditions during summer (Fig. 13). Kelts and Hsü (1978) described seasonal lacustrine lamination with pure microspar summer laminae precipitated during algal blooms. Shifts of calcite stable isotopic values from the calculated equilibrium reflects eutrophication; hypertrophic conditions led to precipitation of much larger calcite crystals - up to 50 μm (Teranes et al.,1999). Most of the pure microspar – fine spar laminae of the Rudník Lake anoxic offshore deposits show these features, therefore we interpret them as a seasonally bioinduced precipitation. Enrichment in ^{18}O can be caused by higher evaporation/salinity during hypertrophic conditions.
Fig. 13 also shows a covariant trend of the grey matrix values with a high correlation coefficient R = 0.896. Primary calcite precipitated from hydrologically closed lakes show covariance of ^{13}C and ^{18}O values (Talbot, 1990), and lakes with R= 0.7 and higher are considered as hydrologically closed. We suppose, that the Rudník Lake was

hydrologically closed at least during the precipitation of grey matrix samples (Vrchlabí section, Fig. 16). Samples of grey, clay-rich matrix are scattered along the section from the bottom to the top (2.4 – 8.12 m), and are mostly from rocks with no distinctive fine lamination or from rocks, where three types of laminae, black, grey and whitish, were present.

4.4.2. Hydrogen index (HI)

The TOC data are plotted against S2 (bound hydrocarbons) and cluster into four major groups (Fig. 20). The slopes of the trend lines are proportional to the hydrogen indexes (HI) and are characteristic for specific kerogen types (Talbot et al., 2004). The first group of rocks with a very high TOC of 8 – 23%$_{wt}$ and S2 30 – 60 mg/g comprises black shales and laminites from the later stage of lake development and eutrophication. These are excellent source rocks with very good hydrocarbon generative potential. The second group consists of mudstones and calcareous dolomite with a similar kerogen type as the first group (both have an HI of 322 mg/g TOC) but are more diluted by the mineral matrix and hence have a lower organic matter concentration. The organic rich carbonates have a relatively low TOC, 1 – 2%, but the quality of kerogen is very high (average HI = 552 mg/g TOC) due to the high amount of algae and scarcity of fusinite or other terrestrial plant debris. The last group, with the lowest hydrogen index (HI = 33 mg/g TOC), comprises of laminites and black shales from the initial stage of lake development. The kerogen is rich in fusinite, semifusinite and other humic substances derived from land plants. Only minor differences are observed between the two sections. The Vrchlabí section does not reach as high a concentration and quality of organic matter as the rocks in the Kundratice section, probably due to its position in a deeper part of the basin closer to the northern, steeper slopes of the rising Krkonoše Mountains, which provided higher detrital influx into the basin.

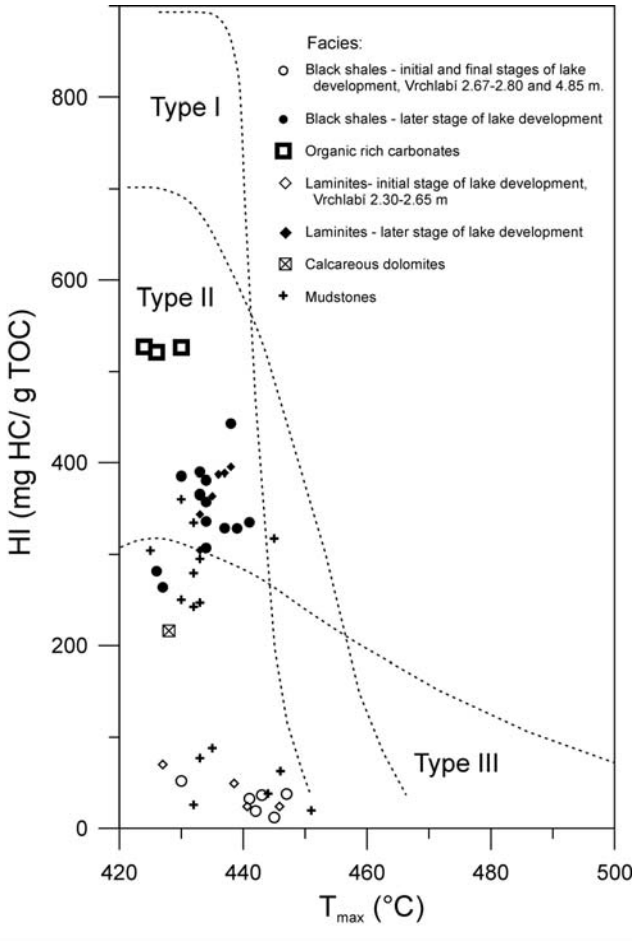

Figure 21. Plot of hydrogen index (HI) versus Tmax values with main types of kerogen. Most of the samples are mixtures of algal and terrestrial organic matter (type II) formed during the later stages of lake development, but some samples are enriched in kerogen type III and are dominated by terrestrial plant debris transported to the lake during its initial stage of development.

The plot of the hydrogen index in relation to thermal maturity expressed by T_{max} show the envelopes of major kerogen types and their thermal degradation during diagenesis (Fig. 19). At the time of deposition, the original HI values were probably higher and the organic-rich carbonates would have plotted as typical type I kerogen. Yet, the thermal diagenetic overprint is not very high and the organic matter parameters still indicate many aspects of the evolving palaeo-environment.
Several trends are apparent in vertical sections (Figs. 15 and 16). In the Vrchlabí section between 1.6 and 4.8 m a striking upward increasing trend of HI values is shown (Fig. 16). In the Kundratice section a similar trend can be seen within the upper black shale bed (2.7 – 3.1 m) and a large shift of HI to higher values at the transition from the basal black shale bed to the organic-rich carbonate (0.5 m). These trends are interpreted as a record of algal blooms and lake eutrophication.

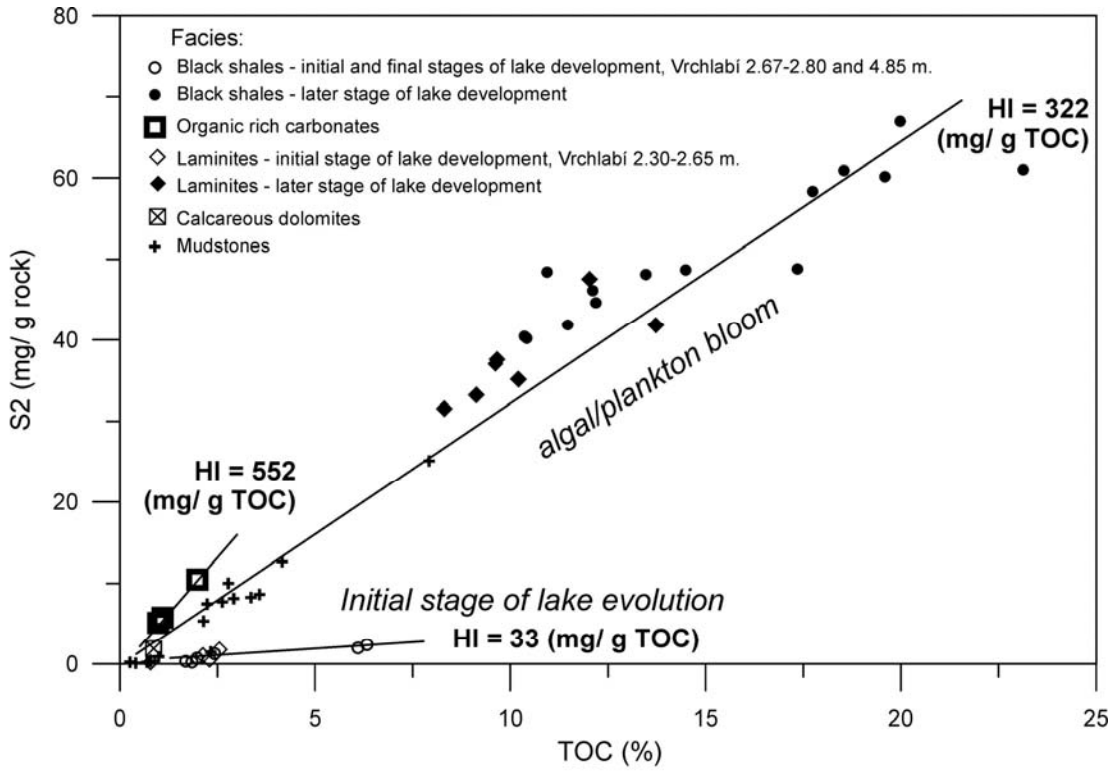

Figure 22. Characterisation of organic matter by pyrolytic hydrocarbons (S2) and total organic carbon (TOC). The slope of the trendlines is proportional to the Hydrogen Index (HI). Symbols depict different lithologies and form clusters related to palaeoenvironmental settings. The highest HI is observed in organic-rich carbonates with almost pure indigenous planktonic algae kerogen, the lowest HI occurs in sediments with redeposited terrestrial plant detritus rich in inertinite.

4.4.3. Saturated hydrocarbons in rock extracts

The distribution of the saturated hydrocarbons with n-alkanes (n-C10 .. n-C38) and isoprenoid hydrocarbons (ip-C13 .. ip-C20) in the rock extracts shows several organic matter characteristics and a depositional environment in three selected lithologies and lake development stages (Fig. 21). The black shale (Fig. 21, Vrchlabí section VB 2.7 m, Bs) has a distinct predominance of n-alkanes over the isoprenoids, pristane/phytane (ip-C19/ip-C20) ratio close to 1.1 and odd/even predominance in the n-C13 to n-C18 range. These characteristics are typical of dysoxic conditions in the water column and predominantly plankton-derived organic matter (Tissot and Welte, 1984). The organic matter rich mudstone (Fig. 21, Vrchlabí section VB 4.5 m, Mo) is strikingly different with pristane/phytane < 1 typical for reducing conditions in the water column. Abundant higher alkanes with notable odd/even predominance in the n-C25..n-C33 range and isoprenoids > n-alkanes in the lower molecular range suggest early thermal maturity and significant contribution of terrestrial plant debris to the kerogen composition. High hopane content (next to n-C31) indicates possible microbial reworking of the deposited organic matter. The laminite sample (Fig. 21, Vrchlabí section VB 4.6 m, La) shows maximum abundant n-alkanes around n-C15..n-C17 with odd/even predominance in this range and a high n-alkanes/isoprenoids ratio, a pristane/phytane ratio close to 1 and low amounts of n-alkanes in the n-C25-32 range. This pattern is characteristic for dysoxic carbonate depositional environments with high algae and low terrestrial input.

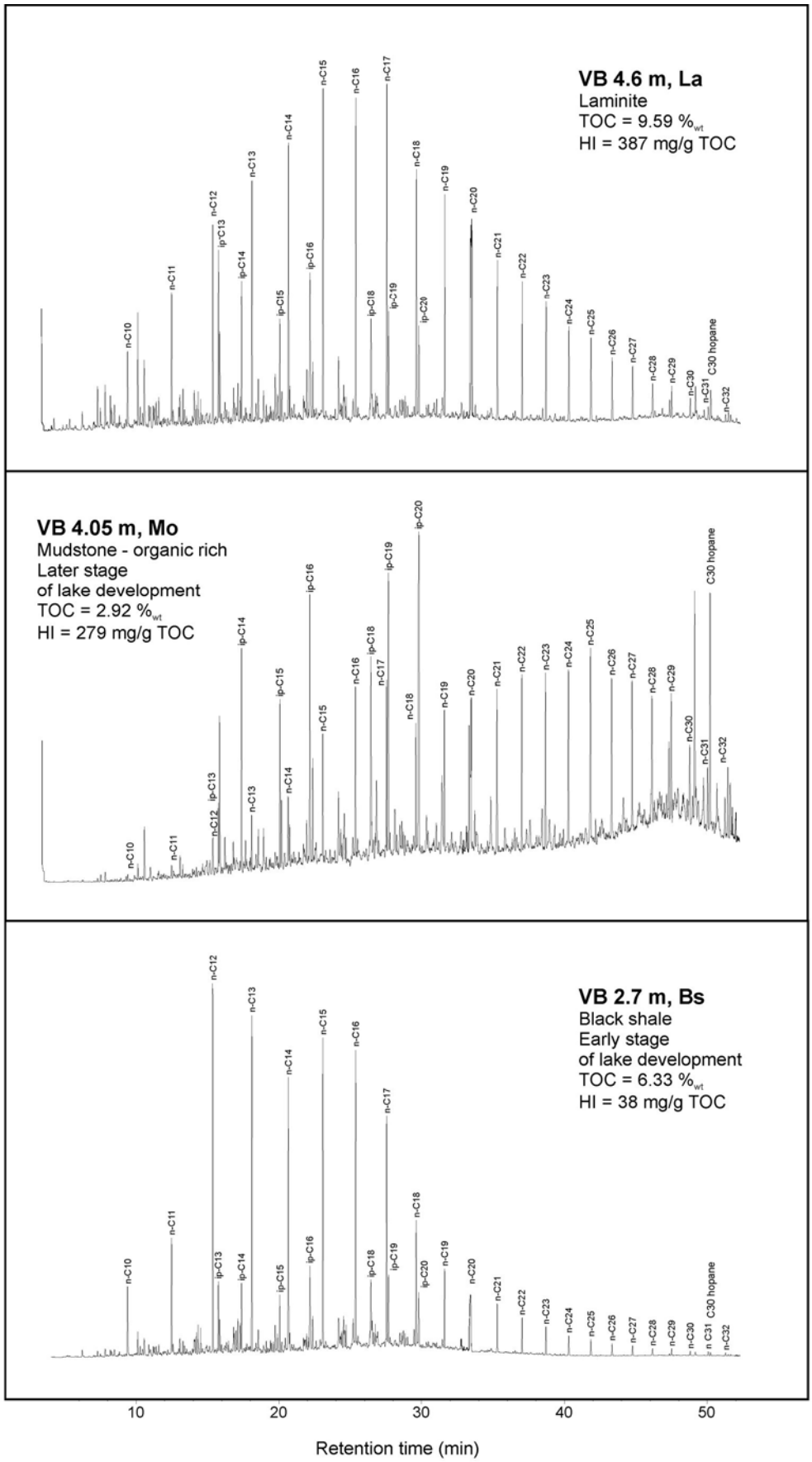

Figure 23. Distribution of the saturated hydrocarbons in rock extracts of three characteristic lithologies and lake evolution stages in the Vrchlabí section.

4.4.4. Stable isotopes of organic carbon

The $\delta^{13}C$ values of biological material are determined by the isotopic composition of the carbon source and by isotopic fractionation of carbon during photosynthesis and metabolic reactions. Diagenetic alteration commonly leads to a small shift towards a ^{13}C depletion of 1 – 2‰ (Galimov, 1980). This shift is common to all kerogens which have experienced similar diagenetic alteration. The high range in $\delta^{13}C$ values (at least several ‰) of sedimentary organic matter should reflect primary isotope heterogeneities in the biological precursor material (Arneth, 1984).

Hemicellulose, proteins and pectins are enriched in ^{12}C relative to bicarbonate by about 17‰, cellulose and lignin by 23‰ and lipids by 30‰ (Degens et al., 1968). It follows that organic material rich in lipids, such as algae, shows lower $\delta^{13}C$ values than organic matter formed from terrestrial plants rich in lignin, such as coal. The respective average $\delta^{13}C$ values of Carboniferous coals from the Polish Silesian Basin are about -23.5‰, the Saar coals -24.4‰ and the Aachen coals -23.9‰ $\delta^{13}C$ (Rice and Kotarba, 1993). Modern plants with C3 metabolism have $\delta^{13}C$ values from -23.1 to -27.9‰ (Meyers, 1990). It is possible to assume that samples from the Rudník member contained organic matter rich in lignin and cellulose (kerogen type III, with low HI) with $\delta^{13}C$ values close to -24‰, organic matter rich in lipids with lower $\delta^{13}C$ values and high HI, and a mixture of both types.

The differences in $\delta^{13}C$ values of calcite and organic matter, which were calculated for all samples, vary from 20.9 to 29.4‰. The wide range of $\Delta\delta^{13}C$ values could be explained by different carbon sources for calcite and organic matter; diagenetic alteration of calcite is probably of minor importance. Organic matter redeposited from the coast and rivers was brought into the lake as sedimentary organic matter, which was not necessarily oxidised and calcite precipitated from lake water with a different $\delta^{13}C$ composition of total dissolved carbon (TDC). Carbonate and organic matter was not necessarily formed in the same water column depth. Concentrations and carbon isotopic compositions of CO_2 in lakes from New England (USA) show CO_2 $\delta^{13}C$ values of about -8.6‰ for water from shallow water layers (epilimnion), whereas $\delta^{13}C$ values of CO_2 from deeper in the water column are from -10 to -22.6‰ (Oana and Deevey, 1960). Lower $\delta^{13}C$ values in deeper water are explained by the higher portion of CO_2 originating from organic matter decomposition.

4.4.5. Vertical trends of geochemical parameters

The onset of low $\delta^{18}O$ values at the base of several black shale and laminite beds and gradually increasing upwards trend of $\delta^{18}O$ values in the upper parts of these beds probably records the onset of the highest lake level (trend no. 1, Fig. 15, Vrchlabí section 2.3 – 2.5 m, Fig. 16, Kundratice section 0.1 – 0.4 m and 2.7 – 3.0 m). The maximum proportion of meteoric water was during a humid period and the importance of evaporation increased gradually during a later, more arid, period (see Talbot, 1990). A consequent gradual drop in lake level can be supposed. In some places (Kundratice 2.7 – 3.1 m, Vrchlabí 2.2 – 2.6 m) oxygen isotopic trends are accompanied by upwards increasing $\delta^{13}C_{calcite}$ and HI values and decreasing $\delta^{13}C_{TOC}$, indicating increasing bioproductivity in the lake, which can be interpreted in terms of a shift towards a warmer climate. The abundance of mostly juvenile fish fossils at 3.0 m in Kundratice can most easily be explained by eutrophication (Zajíc, 1997), which fits very well with the geochemical data. The highest TOC values (23%) suggest intensified anoxic conditions during this stage of basin evolution.

The large shift of HI to higher values, the highest in the dataset, in the Kundratice section at the transition from the basal black shale bed to the organic-rich carbonate (Fig. 16, 0.5 m, trend no. 2) can be explained by a reflection of transgressive or highstand conditions with low siliciclastic and low degraded OM input and high primary productivity. Also rapid carbonate precipitation, which enables better preservation of aquatic OM can explain high HI values. Large shifts of $\delta^{18}O$ and $\delta^{13}C_{calcite}$ values in this part of the section can be interpreted as a result of different sources of calcium carbonate during precipitation of carbonate bed. This can be caused by changes in source area or bloom of plankton or necton with calcareous tests (e.g. Ostracods reported by Zajíc, 1997); the increase in bioproductivity is indicated by a shift of $\delta^{13}C_{TOC}$ towards more negative values.

The gradual upwards decreasing trends of $\delta^{18}O$ and $\delta^{13}C_{calcite}$ values in the Kundratice section within the muddy nearshore succession (Fig. 16, 3.3 – 4.8 m, trend no. 3) can be ascribed to lake water gradually mixing with, for example, river water rich in pedogenic ^{12}C.

Several types of offshore facies occur in the Vrchlabí section. The transition from basal laminites to the muddy turbidites (Fig. 15, 2.9 – 3.3 m, trend no. 4) is characterized by a high variation in $\delta^{18}O$ and $\delta^{13}C$ values which can be interpreted as a record of the different proportions of primary and redeposited material in particular samples. It could also be a record of lake level fluctuations in a hydrologically closed regime and significant changes in the isotopic composition of TDC in lake water caused by changes in bioproductivity and different proportions of pedogenic CO_2 transported from the land. A general upwards increasing trend in $\delta^{13}C_{TOC}$ values in this part of the section can be explained in terms of an increasing portion of land-derived organic matter and a decrease in phytoplankton organic matter during the onset of turbidite sedimentation.

The upper part of the Vrchlabí section (Fig. 15, 3.3 – 4.8 m, trend no. 5) has generally low and homogeneous $\delta^{18}O$ values accompanied by upward increasing trends in $\delta^{13}C_{calcite}$ and HI values and upwards decreasing $\delta^{13}C_{TOC}$ trend. Stable and low oxygen isotope values can be ascribed to lake-level highstand and hydrologically open conditions during most of this period (cf. Talbot, 1990). The significant upward trend of increasing HI and $\delta^{13}C_{calcite}$ and decreasing $\delta^{13}C_{TOC}$ provide evidence of increasing bioproductivity during this time (Talbot and Livingstone, 1989; Neumann et al., 2002).

The Kundratice section is characterized by higher HI and higher total organic matter contents compared to the Vrchlabí section. It is interpreted as reflecting a generally higher bioproductivity and lower input of redeposited terrestrial material due to the position of the Vrchlabí section close to the palaeo-shoreline of the steep northern basin margin.

Boron

Mudstone mineralogy, the presence of volcanogenic or organic material, and mineralogy within the source area are the main factors assumed to influence the palaeosalinity record (e.g. Curtis, 1964; Spears, 1965; Kraska, 1981a). Covariance between boron content and mineral composition or TOC content were not found. The studied sections represent a relatively short period of time and so we do not interpret any substantial changes in sediment provenance. Finally volcanogenic material was found in only one bed (facies Ms) in the Vrchlabí and Kundratice sections. These observations led us to interpret changes in boron content of mudstones of the Rudník Lake deposits as reflecting changes in palaeosalinity.

In the Kundratice section, the offshore facies show the lowest boron values (from 82 to 241 ppm), which are interpreted as a record of low lake water salinity during lake-level highstands. The nearshore mudstones and siltstones of facies Mss, Mo and Ml show higher values (294 – 496 ppm), and mudflat facies Mc exhibit the highest values (542 – 603 ppm). This is interpreted as a record of higher lake water salinity during lower lake levels. In the Vrchlabí section the lowest values are also concentrated in the anoxic offshore facies (Bs and La, 73 – 246 ppm) representing highest lake level. The highest values occur in the muddy turbidites (Mo, 337 – 535 ppm). An increase of values in the lower part of Mo succession is probably related to a large fall in lake level and muddy turbidite sedimentation could have been triggered by such lake level fluctuations. In the Čistá 2 section anoxic offshore facies (Bs) show the lowest values (205 – 268 ppm) as well. The highest values (293 – 437 ppm) were recorded within mudcracked mudstones of mudflat (Mc) facies. Absolute values of boron content in different sections are not compared, because they probably represent more or less different lacustrine subsystems of different palaeohydrochemistry history and different clay mineralogy.

Higher salinity during the lake-level lowstand indicates hydrologically closed conditions; on the contrary, lower salinity during the lake highstand, which was stable for a relatively long time, can indicate hydrological opening of the lake during highstand. The distribution of boron in the studied sections indicates substantial changes in lake water salinity, which was related to lake level changes recorded by sedimentary facies. Lake level was driven mainly by a precipitation/evaporation ratio, so lake level changes must have been induced by climatic changes.

5. Summary and discussion

Highstand periods of the Rudník Lake are recorded in most sections by the deposition of organic-rich finely laminated mudstones and carbonates. High organic content (up to 10 – 23% of TOC), common presence of autochthonous organic matter, abundant pyrite and lack of bioturbation indicate high bioproductivity and anoxic bottom conditions. The lake must have been eutrophic to oligotrophic with well-developed stratification for most of the year. Two types of seasonal lamination within the anoxic organic-rich offshore facies are present. The first consist of clayey organic-rich dark laminae alternating with whitish pure microspar laminae in La facies (cf. Kelts and Hsü, 1978). The pure microspar laminae are considered to represent late summer bioinduced calcite precipitation during algal blooms. The second type of lamination, found in several Bs facies beds, comprises almost pure algal laminae alternating with clay-dominated laminae (Figs. 8a, b). These probably also reflect seasonal algal blooms but

under different conditions. The lack of carbonate within these deposits can be explained by low carbonate input and the resulting low carbonate content in lake water or by acid conditions in the hypolimnion, which prevent accumulation of carbonate minerals due to their dissolution near the lake bottom. Low carbonate input seems improbable, because these black shales are usually overlain by carbonates. Dissolution of carbonates in the hypolimnion can be due to the high concentrations of CO_2 released from decaying OM (Dean and Fouch, 1983; Pilskaln, 2004). Eutrophic lake deposits may thus contain less carbonates in comparison to the lower productivity lake deposits situated in a similar source area and climatic setting (Dean 1981). High aridity, high temperature and a rainfall regime in the seasonal Pangean interior during the Early Permian are the principal common conclusions of most climatic models (Barron and Fawcett, 1995). Therefore the Bohemian Massif could have been in the zone of influence of seasonal monsoons occurring in the peri-Tethys region.

The widespread presence of dolomite in most carbonate and mudstone facies of the Rudník Lake deposits is interpreted as mostly the product of primary precipitation, because of a lack of displacive structures. Primary precipitation of dolomite in lacustrine settings is widely accepted (Hardie, 1987; Tucker and Wright, 1990), but requires waters highly supersaturated with carbonate ions and a high Mg/Ca ratio, which are restricted to evaporitic conditions. Most of the non-detrital dolomite found in recent and Quaternary lakes come from saline lakes (Last, 1990). We propose a model of primary precipitation of high Mg calcite and protodolomite for the Rudník Lake deposits, which could soon have been early diagenetically modified to dolomite, a process which does not require extensive neomorphism. Degradation of organic matter could raise pH, ionic strength and carbonate alkalinity, which are, in addition to Mg supply, substantial factors controlling dolomite precipitation (Slaughter and Hill, 1991). The source of Mg could have been intrabasinal basic volcanic rocks and low-grade Lower Palaeozoic metasediments surrounding the basin, which contain abundant chlorite and basic metavolcanics.

The study of vertical changes in boron content in the clay fraction of the lacustrine mudstones shows that high lake level stages were periods of lower salinity, and periods of falling lake level were followed by significant increases in salinity. This could reflect climatic variability with humid periods reflected by a relatively hydrologically more open state (recorded by low boron values of offshore deposits) and more arid periods by a hydrologically closed state (indicated by increase of boron values in nearshore/mudflat deposits).

A vertical trends of upward increasing $\delta^{18}O$, $\delta^{13}C_{calcite}$ and HI and decreasing $\delta^{13}C_{TOC}$ (Figs. 15 and 16) are interpreted as reflecting an increase in bioproductivity and lake-level lowering. They probably represent change from a relatively humid to a warmer and more arid climate. An increase in $\delta^{18}O$ could reflect an increase in the evaporation/precipitation ratio, which can be most likely explained in terms of lake level lowering during the onset of a more arid and warmer period.

Another vertical trend characterized by the increase of $\delta^{13}C_{calcite}$ and HI, and by a decrease of $\delta^{13}C_{TOC}$ followed by stable and relatively low $\delta^{18}O$ values (Figs. 15 and 16) probably reflects an increase in bioproductivity during the periods of high lake level and probably hydrologically open regime, indicated by low and stable oxygen values. An increase of hydrogen index and TOC can indicate a rise of lake level, due to the better OM preservation of an oxygen-depleted lake bottom during high lake level stages (Talbot and Livingstone, 1989). The low and stable $\delta^{18}O$ values in calcite of the Rudník Lake deposits, however, do not reflect any substantial change in the $^{18}O/^{16}O$ ratio in the lake water, which would have followed rise in lake level. The increase in bioproductivity during the stable high lake level can be caused by higher nutrient supply and/or a change of climate to warmer and more humid conditions. The highest lake-level was controlled by topography, discharge, and could not have been further increased by more humid conditions.

The basin was in a hydrologically closed state during the low lake levels. Millimetre – centimetre thick intercalations of early diagenetic displacive gypsum, found in the red mudstone-dominated succession overlying the Rudník Lake deposits, indicate continuing hydrologically closed basin conditions and the high water output/input ratio in the Rudník Lake.

During the Permian most of the Pangean interior was arid, and a positive water budget is proposed only in some peri-Tethys areas influenced by monsoons (Barron and Fawcett, 1995). Average July temperatures of the area where the Bohemian Massif was situated during the Early Permian, were around 20 – 25°C and January average temperatures between 25 – 30°C (Crowley et al., 1989). According to these climatic models the Pangean interior was characterised by high climate continentality and seasonality with large differences between day/night and summer/winter temperatures. Which corresponds to our interpretation of the carbonate/black shale laminites of the Rudník Lake deposits as products of seasonal lamination (see chapter 3). The Bohemian Massif was situated between 2^{o} and 4^{o} N Early Permian latitude (Krs and Pruner, 1995), and a hot semiarid climate is expected, which can most easily explain the well-established stratification, periods of high bioproductivity, and high rate of evaporation leading to substantial drops of lake level and increasing salinity, $^{18}O/^{16}O$ ratio and carbonate ion concentrations in the lake water.

Several orders of climatic cyclicity are recorded in the Rudník Lake deposits. Lake-level fluctuations recorded by transgressive/regressive facies units several metres to tens of metres thick, probably represent periods of tens to possibly hundreds of kyr (section Čistá 2, Fig. 5). Higher salinity during lowstands and lower salinity during

highstands can most easily be explained by more arid and humid climatic conditions, respectively. Lake-level and bioproductivity fluctuations in the order of kyr or possibly hundreds of years, recorded by stable isotopes and OM geochemistry, are very probably climatically driven. The seasonal lamination represents the highest-frequency climatic record of the Rudník Lake.

Quaternary analogues can help the understanding of such climatic oscillations. Tropical African lakes were subject to a major dry period and low lake-levels during the last glacial maximum (~18 kyr BP) (Talbot and Johannessen, 1992; Gasse et al., 1989; Johnson et al., 2000; Stager et al., 2002; Trauth et al., 2001), which are ascribed to a weakening of the Afro-Asian monsoon (Stager et al., 2002). A similar pattern was found by Benson et al. (1998) in mid-latitude Mono Lake (California). In Lake Tanganyika the water-level fluctuations are in phase with glacioeustatic sea-level changes (Gasse et al., 1989).

The two main maxima of the Late Palaeozoic glaciation are suggested as being in the Westphalian and Sakmarian; based on the extent of ice-rafted deposits (Frakes et al., 1992). The Asselian, when the Rudník Lake was formed, was a period when the Sakmarian glacial period initiate. Lake level changes of the Rudník Lake may reflect climatic oscillations of the order of tens of thousands years, comparable to lower orders of glacial/interglacial cycles. Evidence of glacial/interglacial climatic oscillations in the equatorial environments has only been rarely documented. Milankovitch-type climatic cyclicity was found by Olsen and Kent (1996) in lacustrine cycles of the Upper Triassic Newark Supergroup and by Fredriksen et al. (1998) in lacustrine/aeolian/fluvial cycles of the Permian Brodrick Beds, Scotland. Triassic playa deposits in Germany with a cyclicity driven by a Pangean monsoon-like system were changing intensity within the Milankovitch frequency band (Reinhardt and Ricken, 2000).

6. Conclusions

1. Four facies associations recognized within the Rudník Lake deposits are interpreted as: a) anoxic offshore deposits (pelagic, finely laminated black shales, carbonate/black shale laminites and carbonates), b) suboxic to oxic offshore deposits (pelagic to hemipelagic laminated grey, variegated to red mudstones and carbonates), c) nearshore and mudflat deposits (nearshore sandstones, sandstone/mudstone heterolithics, carbonates, mudflat mudstones) , and d) gravity driven deposits (turbidite sandstones, distal turbidite silty mudstones, debrite conglomerates).
2. The lateral distribution of sedimentary facies with high gradient facies (turbidites, debris flows) and the thickest offshore facies succession distributed along the present-day northern basin margin, and much thinner offshore facies successions and low-gradient facies (mudstone and carbonate dominated), found in the south and south-west of the basin, point to the asymmetry of Rudník Lake deposits.
3. The apparent asymmetry of the basin fill and the distribution of sedimentary facies reveal an original half-graben basin geometry. Subsidence along the northern basin margin fault was the main factor controlling large-scale facies architecture of the Vrchlabí Formation (Asselian) within the basin. A substantial increase in subsidence rate was probably responsible for the formation of the large (300 – 500 km^2), relatively deep and long-lived lacustrine system of the Rudník Lake.
4. The observed seasonal lamination is in agreement with climate models for the Early Permian.
5. The Rudník Lake was a complex lacustrine system with well-developed offshore and nearshore zones, a stratified water column, periods of high and mainly algal bioproductivity and eutrophication which favoured the accumulation of large amounts of hydrogen-rich kerogen in the sediments: TOC is up to 23% and HI > 500 mg/g.
6. Major lake level fluctuations of the Rudník lacustrine system, recorded by shallowing-up facies units in most sections throughout the basin, were followed by significant changes in lake water salinity, reflected by changes in boron content in the clay fraction of mudstones. The highstands were periods of hydrologically more open conditions and lower salinity, indicated by the low boron values. The lowstands, on the other hand, were characterized by higher salinity and higher boron values. This is interpreted as a response to an increase in the evaporation/precipitation ratio in a hydrologically closed lake.
7. Lake level fluctuations of the Rudník Lake can also be traced in the monotonous offshore facies-dominated section, where no sedimentological evidence of lake-level changes exists. Evidence of such changes is documented by variations in $\delta^{18}O$ and $\delta^{13}C$ values of primary calcite, $\delta^{13}C$ and Hydrogen Index (HI) of organic matter. In the first case, an upward-increase of $\delta^{18}O$, $\delta^{13}C_{calcite}$ and HI and a decrease of $\delta^{13}C_{TOC}$ in vertical sections are interpreted as a result of increased bioproductivity and lake-level lowering. It probably represents a change in climate from relatively humid to a warmer and more arid period. In the second case, the increase in $\delta^{13}C_{calcite}$ and HI, and decrease in $\delta^{13}C_{TOC}$ followed by stable and relatively low $\delta^{18}O$ values reflect an increase in bioproductivity during a period of high lake level and probably a hydrologically more open regime. This can be interpreted as the transition to warmer conditions during a stable, humid climate period.

Acknowledgements

The research was performed with the support of the Grant Agency of the Czech Republic project No. 205/94/0692, Ministry of Education project No. MSM 113100006 and by kind permission of the Aquatest Co. We wish to thank V. Prouza and R. Tásler for their suggestions, discussions and help with selecting suitable outcrops and to Harry Shaw and Karel Žák for discussions and thorough reviews of the first versions of the manuscript. We gratefully acknowledge the anonymous editor and three reviewers for improving the manuscript and for additional references. K.M. also wish to thank to J. Zajíc, Z. Šimůnek and J. Drábková for help with understanding palaeoecological and biostratigraphical aspects. Many thanks to Richard Withers for English review. Most of the work was done by K. Martínek as part of his PhD thesis.

References

Alexander, J., Leeder, M.R., 1987. Active tectonic control on alluvial architecture. In: Ethridge, F.G., Flores, R.M., Harvey, M.D. (Eds.), Recent Developments in Fluvial Sedimentology, Spec. Publ. SEPM 39, pp. 143 – 252.

Allen, P.A., Allen, J.R., 1990. Subsidence history. In: Allen, P.A., Allen, J.R.: Basin Analysis, Principles and Applications. Blackwell Science, pp. 263 – 281.

Arneth, J.D., 1984. Stable isotope and organo-geochemical studies on Phanerozoic sediments of the Williston basin, North America. Isotope Geoscience 2, 113 – 140.

Barron, E.J., Fawcett, P.J., 1995. The Climate of Pangea: A Review of Climate Model Simulations of the Permian. In: Scholle, P.A, Peryt, T.M., Ulmer-Scholle, D.S. (Eds.), The Permian of Northern Pangea. Vol.1 , Springer-Verlag, pp. 37 – 52.

Benson, L.V., Lund, S.P., Burdett, J.W., Kashgarian, M., Rose, T.P., Smoot, J.P.,Schwartz, M., 1998. Correlation of late-Pleistocene lake-level oscillations in Mono Lake, California, with North Atlantic climate events. Quaternary Res. 49, 1 – 10.

Blair, T.C., Bilodeau, W.L., 1988. Development of tectonic cyclothems in rift, pull-apart, and foreland basins: Sedimentary response to episodic tectonism. Geology 16, 517 – 520.

Blecha, M., Martínek, K., Drábková, J., Šimůnek, Z., Zajíc, J., 1997. Environmental changes at the Carboniferous/Permian boundary and their impact on the floral and faunal assemblages of the fossiliferous lacustrine horizons of the Krkonoše Piedmont Basin.. Final report, project GAČR 205/94/0692, Czech Geological Survey, Prague, Czech Republic. (in Czech)

Blecha, M., Martínek K., Mihaljevič M., 1999. Sedimentary and geochemical record of the ancient Kalná Lake, Lower Permian, Krkonoše Piedmont Basin, Czech Republic. Acta Universitatis Carolinae 43(4), 657 – 665.

Bohor, B.F., Gluskoter, H.J., 1973. Boron in illite as an indicator of paleosalinity of Illinois Coals. J. Sed. Petrol. 43, 945 – 956.

Bordenave, M.L., Espitalie, J., Leplat, J., Oudin, J.L., Vandenbroucke M., 1993. Screening techniques for source rock evaluation. In: Bordenave, M.L., (Ed.), Applied petroleum geochemistry. Paris, Editions Technip, pp. 217 – 278.

Bouška, V., Pešek, J., 1976. The geochemical role of boron in the Carboniferous sediments of Czechoslovakia. Proceedings of the 7th Conference on Clay Mineralogy and Petrology, Karlovy Vary, 1976, 203 – 209.

Bouška, V., Pešek , J., 1983. Boron in the Permo-Carboniferous aleuropelites of the Bohemian Massif, Czechoslovakia. Proceedings of the 9th Conference on Clay Mineralogy and Petrology, Zvolen, 1982, 209 – 216.

Bouška, V., Pešek, J., 1985. Boron in the aleuropelites of the Bohemian Massif. 5th Meeting of the European Clay Groups, Prague, 1983, Charles University, Prague, pp. 147 – 155.

Bush, M.B., Miller, M.C., De Oliveira, P.E., Colinvaux, P.A, 2002. Orbital forcing signal in sediments of two Amazonian lakes. Journal of Paleolimnology 27, 341 – 352.

Coward, M.P., 1986. Heterogeneous stretching, simple shear and basin development. Earth Planet Sc Lett 80, 325 – 336.

Crowell, J.C., Link, M.H., (Eds.), 1982. Geologic History of the Ridge Basin, southern California. – Los Angeles, Pacific Section, Society of Economic Paleontologists and Mineralogists, pp. 1 – 304.

Crowley,T.J., Hyde,W.T., Short, D.A.,1989. Seasonal cycle variations on the supercontinent of Pangea: implications for Early Permian vertebrate extinctions. Geology 17, 457 – 460.

Csato, I., Kendall C.G.S.C., Nairn, A.E.M., Baum, G.R., 1997. Sequence stratigraphic interpretations in the southern Dead Sea basin, Israel. GSA Bulletin 108, 1485 – 1501.

Curtis, C.D., 1964. Studies on the use of boron as a paleoenvironmental indicator. Geochim. Cosmochim. Acta 28, 1125 – 1137.

Dam, G., Surlyk, F.,1993. Cyclic sedimentation in a large wave- and storm-dominated anoxic lake; Kap Stewart Formation (Rhaetian-Sinemurian), Jameson Land, East Greenland. In: Posamentier, H.W., Summerhayes, C.P., Haq, B.U., Allen, G.P. (Eds), Sequence Stratigraphy and Facies Associations. IAS Spec. Publ., 18, pp. 419 – 448.

Dean, W.E., 1981. Carbonate minerals and organic matter in sediments of modern north temperate hardwater lakes. In: Ethridge, F.G., Flores R.M., Recent and Ancient Non-marine Environments: Models for Exploration., Spec. Publ. SEPM, 31, Tulsa, 213 – 231.

Dean, W.E., Fouch, T.D., 1983. Lacustrine Environment. In: Scholle, P.A., Bebout, D.G., Moore,C.H. (Eds), Carbonate depositional environments. AAPG Memoir 33 , Tulsa, pp. 97 – 130.

Degens, E.T., Keith, M.F., 1959. Geochemical indicators of marine and freshwater sediments. Res. Geochim., 38 – 61.

Degens, E.T., Behrendt, M., Gotthardt, G., Reppmann, E., 1968. Metabolic fractionation of carbon isotopes in marine plankton. II. Data on samples collected off the coasts of Peru and Ecuador. Deep Sea Res. 15, 1, 11 – 20.

Drábková, J., 1997. Palynology of Rudník Horizon. In: Blecha, M., Martínek, K., Drábková, J., Šimůnek, Z., Zajíc, J. (Eds.), Environmental changes at the Carboniferous/Permian boundary and their impact on the floral and faunal assemblages of the fossiliferous lacustrine horizons of the Krkonoše Piedmont Basin. (in Czech). Final report, project GAČR 205/94/0692, Czech Geological Survey, Prague, Czech Republic, pp. 104 – 111. (in Czech)

Drábková, J., Šimůnek, Z., Zajíc, J. 1990. Paleontologické zpracování sběrů z lokality Vrchlabí - zářez silnice na jz. okraji města. Report, Czech Geological Survey, 1-83, Praha. (in Czech)

Frakes, L.A., Francis, J.E., Syktus, J.I. 1992. Climate modes of the Phanerozoic. Cambridge University Press, UK.

Fredriksen, K.S., Clemmensen,L.B., Lawætz H.S., 1998. Sequential architecture and cyclicity in Permian desert deposits, Brodrick Beds, Arran, Scotland. J. Geol. Soc. London 155, 677 – 683.

Freyet, P., Plaziat, J.C. 1982. Continental Carbonate Sedimentation and Pedogenesis, Late Cretaceous and Tertiary of Southern France. E. Schweizerbartsche Verlagsbuchhandlung, Contribution to Sedimentology 12, Stuttgart,1 – 273.

Galimov, E.M., 1980. 13C/12C in kerogen. In: Durand, B. (Ed.), Kerogen, Ch. 9. Technip, Paris, pp. 271 – 291.

Gasse, F., Ledee, V., Massaul, M., Fontes, J.C., 1989. Water-level Fluctuations of lake Tanganyika in phase with oceanic changes during the last glaciation and deglaciation. Nature 342, 57 – 59.

Gastaldo, R.A., DiMichele, W.A., and Pfefferkorn, H.W., 1996. Out of the Icehouse into the Greenhouse: A Late Paleozoic Analog for Modern Global Vegetational Change. GSA Today 6, 1 – 7.

Gawthorpe, R.L., Leeder, M.R., 2000. Tectono-sedimentary evolution of active extensional basins. Basin Research 12, 195 – 218.

Gawthorpe, R. L., Fraser, A. J., Collier, R. E. L., 1994. Sequence stratigraphy in active extensional basins: implications for the interpretation of ancient basin-fills. Mar. Petrol. Geol., 11, 642 – 658.

Goldberg, E.D, Arrhenius, G.O.S., 1958. Chemistry of Pacific pelagic sediments. Geochim. Cosmochim. Acta. 13, 153 – 212.

Goldschmidt, V.M., Peters, C., 1932. The geochemistry of boron: I, II. - Nachr. Ges. Wiss. Gottingen, Math.-Physik. K1., 402 – 407, 528 – 545.

Goodarzi, F., Swaine, D.J., 1994. Paleoenviromental implications of the boron content of coals. Geological Survey of Canada Bulletin 471, 1-76.

Hardie, L.A., 1987. Dolomitization a critical view of some current views. J. Sedim. Petrol. 57, 166 – 183.

Hoefs, J., 1997. Stable Isotope Geochemistry. 4th ed. Springer-Verlag, Berlin.

Huc, A.Y., Le Fournier, J., Vandenbroucke, M. and Bessereau, G., 1990. Northern Lake Tanganyika - an example of organic sedimentation in an anoxic rift lake. In: Katz, B.J., (Ed.), Lacustrine Basin Exploration - Case Studies and Modern Analogs, AAPG Memoir 50, Tulsa, pp. 169-185.

Janaway, T.M., Parnell, J. 1989. Carbonate production within the Orcadian basin, northen Scotland - a petrographic and geochemical study. Palaeogr. Palaeocl. Palaeoecol. 70, 89 – 105.

Johnová, R., 1996. Boron as an paleosalinity indicator in the Czech Permo-Carboniferous. Bc. thesis, Charles University, Prague. (in Czech)

Johnson, T.C., Halfman, J.D., Showers, W.J., 1991. Paleoclimate of the past 4000 years at lake Turkana, Kenya, based on the isotopic composition of authigenic calcite. Palaeogr. Palaeocl. Palaeoecol. 85, 189 – 198.

Johnson, T.C., Kelts, K., Odada, E., 2000. The holocene history of Lake Victoria. AMBIO 29, 2 – 11.

Kelts, K., Hsü, K.J., 1978. Freshwater carbonate sedimentation. In: A.Lerman, (Ed.), Lakes, Chemistry, Geology, Physics, pp. 295 – 323, Springer Verlag, New York.

Kraska, F., 1981a. Die Bormethode. Wissenschaftliche Zeitschrift der Ernst-Moritz-Arndt Universität 30, Greifswald, 9 – 18.

Kraska, F., 1981b. Kritische Bemerkungen zur Bormethode. Wissenschaftliche Zeitschrift der Ernst-Moritz-Arndt Universität 30, 19 – 26.

Kříbek,B., 1990. Uhlíkaté formace a jejich úloha při metalogenezi Českého masívu. DrSc thesis, Karlova Universita, Praha. (in Czech)

Krs, M., Pruner, P., 1995. Paleomagnetism and Paleogeography of the Variscan Formations of the Bohemian Massif, Comparison with other European Regions. J. Czech Geol. Soc. 40/1-2, 3 – 46.

Last, W. M., 1990. Lacustrine dolomite - an overview of modern, Holocene, and Pleistocene occurences. Earth Science Reviews 27, 221 – 263.

Liro, L.M., 1993. Sequence stratigraphy of a Lacustrine System: Upper Fort Union Formation (Paleocene), Wind River Basin, Wyoming, U.S.A. AAPG Memoir 58, 317 – 333.

Livingstone, D.A., 1963. Chemical composition of rivers and lakes. U.S. Geol. Survey Prof. Paper. 440-G.

Longinelli, A., 1996. Pre-Quaternary isotope palaeoclimatological and palaeoenvironmental studies: Science or artifact ? Chem. Geol. 129, 163 – 166.

Malán, O., 1989. Organic petrology. In: Hošek (Ed.), Bituminous shales in Krkonoše Piedmont area. Final report. MS Geofond, Geoindustrie, Praha. (In Czech)

Martinsen, O.J., Ryseth, A., Helland-Hansen, W., Flesche, H., Torkildsen, G., Idil, S., 1999. Stratigraphic base level and fluvial architecture: Ericson Sandstone (Campanian), Rock Springs Uplift, SW Wyoming, USA. Sedimentology 46, 2, 235 – 259.

McCrea, J.M., 1950. The isotopic composition of carbonate and paleotemperature scale. J.Chem. Physics. 18, 849 – 857.

Meyers, P.A., 1990. Impacts of late Quarternary fluctuations in water level on the accumulation of sedimentary organic matter in Walker Lake, Nevada. Palaeogeogr. Palaeoclim. Palaeoecol. 78, 229 – 240.

Müller, P., 1987. Pyrolýza Rock-Eval a stanovení C_{TOC}, Cmin v horninách podkrkonošského permokarbonu a cyprisového souvrství (in Czech). Report, Czech Geological Survey, Brno.

Muir, M., Lock, D., von der Borch, C., 1980. The Coorong model for penecontemporaneous dolomite formation in the middle Proterozoic McArthur Group, Northern Territory, Australia. Spec.Publ. SEPM 28, 51 – 67.

Neumann, T., Stogbauer, A., Walpersdorf, E., Stuben, D., Kunzendorf, H., 2002. Stable isotopes in recent sediments of Lake Arendsee, NE Germany: response to eutrophication and remediation measures. Palaegeography Palaeclimatology Palaeoecology 178, 75 – 90.

Oana, S., Deevey, E.S., 1960. Carbon-13 in lake waters and its possible bearing on paleoclimatology. Am. J. Sci. 258A, 253 – 272.

Olsen, P.E., 1986. A 40-million-year lake record of Early Mesozoic orbital climatic forcing. Science 234, 4778, 842 – 848.

Olsen, P.E., Kent, D.V., 1996. Milankovitch climate forcing in the tropics of Pangaea during the Late Triassic. Palaegeography Palaeclimatology Palaeoecology 122, 1 – 26.

Pilskaln, C. H., 2004. Seasonal and interannual particle export in an African rift valley lake: A 5-year record from Lake Malawi, southern East Africa. Limnol. Oceanogr., 49, 964-977.

Platt, N.H., Wright, V.P., 1992. Palustrine carbonates and the Florida Everglades; towards an exposure index for the fresh-water environment ? J.Sedim. Petrol. 62, 1058 – 1071.

Posamentier, H.W., Allen G.P., 1999. Siliciclastic sequence stratigraphy: concepts and applications. SEPM Concepts in Sedimentology and paleontology 7.

Prouza, V., Tásler, R., 2001. Krkonoše Piedmont Basin. In: Pešek J. (Ed.), Geologie a ložiska svrchnopaleozoických limnických pánví České republiky. Czech Geological Survey, Praha, pp. 128 – 166. (in Czech)

Prouza V., Šimůnek Z., Zajíc J., 1997. A new locality of the Rudník Horizon (Autunian) in the Mnichovo Hradiště Basin at Proseč pod Ještědem. (in Czech) Czech Geological Survey Reports in 1996, 37 – 38, Praha.

Reinhardt, L., Ricken, W., 2000. The stratigraphic and geochemical record of Playa Cycles: monitoring a Pangaean monsoon-like system (Triassic, Middle Keuper, S. Germany). Palaegeography Palaeclimatology Palaeoecology 161, 205 – 227.

Reynolds, R.C., 1972. Boron: element and geochemistry. In: Fairbridge, R.W., (Ed.), The Encyclopedia of Geochemistry and Environmental Sciences. Van Nostrand Reyhold Co., New York, pp. 88 – 90.

Rice, D.D., Kotarba, M., 1993. Origin of Upper Carboniferous coalbed gases, Lower and Upper Silesian coal beds, Poland. Proceedings of the 1993 international Coalbed methane symposium, pp. 649 – 658.

Ricketts, R.D., Johnson, T.C., 1996. Climate change in the Turkana basin as deduced from a 4000 year long delta O-18 record. Earth Planet Sc Lett 142, 7 – 17.

Rider, M.H., 1996. The geological interpetation of well logs. Blackie, Glasgow, United Kingdom.

Rosen, M.R., Miser, D.E., Starcher, M.A., Warren, J.K., 1989. Formation of dolomite in the Coorong Region, South Australia. Geochimica et Cosmochimica Acta 53, 661 – 669.

Sánchez-Moya, Y., Sopeña, A., Ramos, A., 1996. Infill architecture of a nonmarine half-graben Triassic basin (central Spain). J. Sedim. Res. 66, 1122 – 1136.

Schlische, R.W., 1992. Structural and stratigraphic development of the Newark extensional basin, eastern North-America – evidence for the growth of the basin and its bounding structures. Geol Soc Am Bull 104 (10), 1246 – 1263.

Schlische, R.W., 1993. Anatomy and evolution of the Triassic-Jurassic continental rift system, eastern North-America. Tectonics 12 , (4), 1026 – 1042.

Schneider, J., Zajíc, J., 1994. Xenacanthiden (Pisces, Chondrichthyes) des mitteleuropäischen Oberkarbon und Perm - Revision der Originale zu Goldfuss 1847, Beyrich 1848, Kner 1867 und Fritsch 1879 – 1890. Freiberg. Forsch.-H., R. C, 452, 101 – 151.

Scholz, C.A., 1995. Deltas of the Lake Malawi Rift, East Africa: Seismic Expression and Exploration Implications. AAPG Bulletin 79, (11), 1679 – 1697.

Scholz,C.A., Rosendahl, B.R., 1990. Coarse-Clastic Facies and Stratigraphic Sequence Models from Lakes Malawi and Tanganyika, East Africa. AAPG Memoir 50, 151 – 168.

Sclater, J.G., Christie, P.A.F., 1980. Continental stretching: an explanation of the post Mid-Cretaceous subsidence of the central North Sea Basin. J. geophys. Res. 85, 3711 – 3739.

Shanley, K.W., McCabe, P.J. 1994. Perspectives on the sequence stratigraphy of the continental strata. AAPG Bull 78, 544 – 568.

Šimůnek, Z., 1997. Fytopaleontologie rudnického obzoru. (in Czech) In: Blecha, M., Martínek, K., Drábková, J., Šimůnek, Z., Zajíc, J. (Eds.), Environmental changes at the Carboniferous/Permian boundary and their impact on the floral and faunal assemblages of the fossiliferous lacustrine horizons of the Krkonoše Piedmont Basin. Final report, project GAČR 205/94/0692, Czech Geological Survey, Prague, Czech Republic, pp. 79 – 94. (in Czech).

Slaughter, M., Hill, R.J., 1991. The influence of organic matter in organogenic dolomitization. J.Sedim. Petrol. 61, 296 – 303.

Sneh, A., 1979. Late Pleistocene fan-deltas along the Dead Sea rift. J Sedim Petrol 49, 541 – 551.

Soreghan, M.J., Cohen, A.S., 1996. Textural and Compositional Variability Across Littoral Segments of Lake Tanganyika: The Effect of Asymmetric Basin Structure on Sedimentation in Large Rift Lakes. AAPG Bulletin 80, 382 – 409.

Soreghan, M.J., Scholz, C.A., Wells, J.T., 1999. Coarse-grained, deep-water sedimentation along a border fault margin of Lake Malawi, Africa: seismic stratigraphic analysis. Journal of Sedimentary Research 69: 832-846.

Spears, D.A., 1965. Boron in British Carboniferous sedimentary rocks. Geochim. Cosmochim. Acta 29, 315 – 328.

Stager, J.C., Mayewski, P.A., Meeker, L.D., 2002. Cooling cycles, Heinrich event 1, and the desiccation of Lake Victoria. Palaegeography Palaeclimatology Palaeoecology 183, 169 – 178.

Stewart, A.D., Parker, A., 1979. Paleosalinity and environmental interpretation of red beds from the late Precambrian ("Torridonian") of Scotland. Sedimentary Geology 22, 229 – 241.

Sweet, M.L., 1999. Interaction between aeolian, fluvial and playa environments in the Permian Upper Rotliegend Group, UK southern North Sea. Sedimentology 46, 171 – 187.

Talbot, M.R., 1990. A review of the paleohydrological interpretation of carbon and oxygen isotopic ratios in primary lacustrine carbonates. Chem. Geol. 80, 261 – 279.

Talbot, M.R., Livingstone, D.A., 1989. Hydrogen index and carbon isotopes of lacustrine organic matter as lake level indicators. Palaeogeogr Palaeoclim Palaeoecol 70, 121 – 138.

Talbot, M.R., Kelts, K., 1990. Paleolimnological Signatures from Carbon and Oxygen Isotopic Ratios in Carbonates from Organic Carbon-Rich Lacustrine sediments. AAPG Memoir 50, 99 – 112.

Talbot, M.R., Johannessen, T., 1992. A high-resolution paleoclimatic record for the last 27,500 years in tropical west Africa from the carbon and nitrogen isotopic composition of lacustrine organic-matter. Earth Planet Sc Lett 110, 23 – 37.

Talbot, M.R., Morley, C.K., Tiercelin, J.J., Le Herisse, A., Potdevin, J.L., Le Gall, B., 2004. Hydrocarbon potential of the Meso-Cenozoic Turkana Depression, northern Kenya. II. Source rocks: quality, maturation, depositional environments and structural control. Marine and Petroleum Geology, 21, 63-78.

Tásler, R., Havlena, V., Prouza, V., 1981. New lithostratigraphical division of the central and western part of the Krkonoše Piedmont Basin. Věstník Ústředního Ústavu geologického 56, 129 – 143. (in Czech with English Abstr.)

Taylor, G.H., Teichmuller, M., Davis, A., Diessel, C.F.K., Littke, R., Robert, P., 1998. Organic Petrology. Gebruder Borntraeger, Berlin & Stuttgart, 704 p.

Teranes, J.L., McKenzie, J.A., Lotter, A.F. Sturm, M., 1999. Stable isotope response to lake eutrophication: Calibration of high-resolution lacustrine sequence from Baldeggersee, Switzerland. Limnol. Oceanogr. 44 , 320 – 333.

Tiercelin, J-J., Mondeguer, A., 1991. The geology of the Tanganyika Trough. In: Coulter, G.W. (Ed.) Lake Tanganyika and its Life, , Oxford, Oxford University Press, 7-48.

Tissot, B., Welte, D.H., 1984. Petroleum Formation and Occurrence. 2nd ed., Springer-Verlag, Berlin.

Trauth, M.H., Deino, A., Strecker, M.R., 2001. Response of the East African climate to orbital forcing during the last interglacial (130 – 117 ka) and the early last glacial (117 – 60 ka). Geology 29, 499 – 502.

Tucker M E., Wright V. P. (1990). Carbonate Sedimentology. Blackwell, London.

Uličný, D., 1989. Boron and the organic carbon-to-reduced sulphur ratio in the Peruc-Korycany Formation (Cenomanian), Bohemia. Věstník Ústředního Ústavu geologického 64, 121 – 128.

Wells, J.T., Scholz, C.A., Soreghan, M.J., 1999. Processes of sedimentation on a lacustrine border-fault margin: interpretation of cores from Lake Malawi, East Africa. Journal of Sedimentary Research 69, 816 – 831.

Zajíc, J., 1997. Zoopaleontology of Rudník Horizon. (in Czech) In: Blecha M., Martínek K., Drábková J., Šimůnek Z. and Zajíc J. (Eds.), Environmental changes at the Carboniferous/Permian boundary and their impact on the floral and faunal assemblages of the fossiliferous lacustrine horizons of the Krkonoše Piedmont Basin. Final report, project GAČR 205/94/0692, Czech Geological Survey, 94 – 104, Prague, Czech Republic. (in Czech)

Appendix 1

The geographic coordinates of the localities and wells studied.

outcrop/well	*X (*WGS84)	*Y (*WGS84)	Z (metres)
Honkův Potok	15º23’20”E	50º37’10”N	415
HPK-1	15º21’54.46”E	50º35’41.93”N	332.87
Kv-1	15º24’10.62”E	50º34’23.91”N	352.53
Kundratice	15º25’40”E	50º34’35”N	385
Lt-1	15º25’11.88”E	50º33’26.37”N	368.04
Ba-2	15º26’1.83”E	50º31’52.37”N	438.24
Ro-1	15º25’24.58”E	50º31’5.57”N	411.03
Vrchlabí	15º35’50”E	50º37’25”N	510
Prostřední Lánov	15º39’35”E	50º37’35”N	380
Ča-2	15º41’26.49”E	50º37’1.06”N	506.75
HK-1	15º36’4.30”E	50º34’6.05”N	435.00
HPK-9	15º25’55.06”E	50º32’26.47”N	371.81

Appendix 2

Tables 1 – 6 presenting geochemical data (stable isotopes, TOC, Rock-Eval pyrolysis, boron) are available on CD-ROM and also via the on-line data repository at http://www.sciencedirect.com/science?_ob=MImg&_imagekey=B6V6R-4H40J5C-1-1H&_cdi=5821&_user=2788347&_orig=browse&_coverDate=01%2F17%2F2006&_sk=997699998&view=c&wchp=dGLbVlz-zSkWW&md5=ff282d2d216409623019ddaba487d6b2&ie=/sdarticle.pdf.

Chapter 2

Climatic vs. tectonic controls on the fluvial/alluvial Trutnov Formation, Upper Rotliegend, Bohemian Massif: an integrated well-log, outcrop and heavy mineral study

K. Martínek[a] and D. Uličný[b]

[a] Institute of Geology and Palaeontology, Charles University, Albertov 6, 128 43 Prague 2, Czech Republic, karel@natur.cuni.cz
[b] Geophysical Institute, Academy of Sciences of the Czech Republic, Boční II/1401, 14131 Praha 4, Czech Republic

submitted

Motto:
On those stepping into rivers the same, other and other waters flow. (You could not step twice into the same river.)

Heraclitus of Ephesus, B 91

Abstract

This study interprets the characteristics of a depositional system of the Trutnov Formation in the Krkonoše Piedmont Basin (KPB) and the controls on its deposition. The KPB formed in the northern part of the Bohemian Massif as a post-orogenic basin of inferred extensional/transtensional regime and records a history of continental sedimentation between the Late Carboniferous and Early Triassic. The Trutnov Náchod subbasin (TNSB), which contains the Trutnov Formation, is probably a pull-apart structure superimposed on the eastern part of the KPB during the Permian – Triassic period. The identification of basin-wide tectonic events and the climatic record in continental deposits and changes in fluvial style in basin and meso-scale was enabled by integration of several methods, despite of unsatisfactory outcrop and borehole coverage. This study integrates recognition of smaller-scale sedimentary features observed in outcrops with basin-scale features, which can be identified by correlation of individual outcrops to well-logs using heavy mineral data and outcrop gamma-ray logging.

Based mainly on well-log data, the Trutnov Formation is divided into three main genetic stratigraphic units. Well-log data also give an insight to the relationships between the southern and northern parts of the basin. Unit 1 is represented by alluvial conglomerates in the south, passing to alluvial mudstones and siltstones in the central and playa lake calcareous mudstones with gypsum in the northern parts of the basin. Overlying Units 2 and 3 record the onset of fluvial conglomerates' deposition in the north, fluvial sandstones in the centre and a continuous alluvial fan – fluvial conglomerate sedimentation in the south of the TNSB. The unconformity at the base of Unit 2 is a basin-wide correlative erosional surface, which marks an important palaeogeographic change.

The detailed outcrop study focused on the conglomerates and sandstones of Units 2 and 3, which are exposed. Most of the conglomerates are situated along the northern and southern basin margins and are interpreted as fluvial-dominated, distal alluvial fan deposits. Sandstones occur mainly in the central part of the basin. Channel-fill sandstones, crevasse splay deposits, and calcretes/dolocretes are interpreted in the sandstone facies. The strata are interpreted to have been deposited by a low-sinuosity river system with the dominant paleocurrent direction being to the SE. The high variation in discharge, observed in individual measured sections 10-15 m thick and indicated by the variations in bedform type and grain size, preservation of highly unstable rock fragments, as well as the abundance of calcretes/dolocretes, suggest seasonal to ephemeral flow and arid/semiarid climatic conditions.

Distinct heavy mineral assemblages were used to correlate up to 15 km distant outcrops scattered across the basin, and allowed a larger-scale vertical trend within Units 2 and 3 to be seen. The lower part is characterized by thicker stratal units, finer-grained moderately sorted material, a low proportion of calcretes/dolocretes and bioturbation and low carbonate cementation of most of the sandstones. The upper part is characterized by generally thinner stratal units, poor sorting, a higher proportion of rip-up clasts, abundant calcretes and bioturbation, and pronounced erosional features. This vertical trend is probably a record of transition to generally lower and ephemeral discharge caused by more arid climatic conditions.

The main changes in basin fill architecture are interpreted as major tectonic events. The onset of the Trutnov Formation deposition is interpreted as a major tectonic reactivation at the Autunian/Saxonian (Lower/Upper Rotliegend) boundary, when the extensional regime changed to a strike-slip regime accompanied by a transpressional uplift of the central part of the KPB. The unconformity between Units 1 and 2 and the onset of high sandy sedimentation at the central part of the basin is interpreted as a later progradation of the coarse-grained material during the period of mostly inactive faults. The deposition of low-sinuosity sandstone dominated fluvial sediments over the mudstone dominated playa deposits must have been caused by a steepening of the depositional gradient and was probably accompanied by a change of climate to more humid conditions, which can most easily explain the increase in sediment supply to the basin. This interpretation is supported by the arid/semiarid conditions of Unit 1, the perennial character (more humid) of the lower part of Unit 2 and an ephemeral fluvial system (back to arid/semiarid) of the top of Unit 2. The TNSB is interpreted as a pull-apart basin in which deposition was governed by two major dextral strike-slip faults, Hronov-Poříčí FZ and Pilníkov FZ, which formed releasing stepover pull-apart basin.

Keywords: fluvial deposits, Lower Permian, facies, architectures, well-logs, heavy minerals, tectonic and climatic controls.

1. Introduction

In alluvial/fluvial deposits, understanding the factors controlling changes in stratigraphic architecture is not straightforward. The response of fluvial systems to changes in base-level, climate, sediment supply or the accommodation/sediment supply ratio has been widely discussed (e.g., Shanley and McCabe, 1994; Leeder et al., 1998; Martinsen et al., 1999; Blum and Törnquist, 2000). Climatically-driven changes in discharge regime can be a major mechanism forcing fluvial stratigraphy (Blum et al., 1994). Climatically-driven water table changes producing

significant erosional surfaces in fluvial, aeolian and lacustrine deposits were interpreted in Upper Rotliegend in the North Sea (Sweet, 1999). Fluvial systems are sensitive to climatically controlled changes in discharge and sediment load, but fluvial response to global climate change may vary spatially such that different regions may be out of phase (Leeder et al., 1998), and the frequency of adjustments to global climate change may vary between river systems due to the different thresholds for change, i.e. differential sensitivity (Blum and Törnquist, 2000). In addition to climate and sea/lake level changes, extensional and strike-slip basin architecture commonly depends upon a complex interaction between the three-dimensional evolution of basin linkage through fault propagation, the evolution of drainage and drainage catchments (Alexander and Leeder, 1987; Gawthorpe and Leeder, 2000). The sediment supply to the basin can be driven by the rate of uplift of source rock, which is a major control on regional denudation rates (Hovius, 1998; Allen and Hovius, 1998; Burbank and Pinter, 1999). Tectonic changes could be the main factor influencing palaeotopography, fluvial style and palaeocurrents, resulting in the structurally controlled drainage pathways (Jones et al., 2001). Tectonic rearrangement of the basin could form regional unconformities bounding fluvial sequences (e.g. Scherer et al., 2007).

For the Rotliegend non-marine sedimentary basins of Central Europe (Elbe Zone, Saxony, Sudetes) general climatic framework exists (Roscher and Schneider, 2006), but it is based mainly on palaeoecology, and in Upper Rotliegend, where fossils are very rare, data are missing. There are problems with correlation of particular events between the basins (Kozur 1988, Schneider et al. 1994, Schneider 2001, Roscher and Schneider 2005, Lucas et al. 2006) and current tectonic framework is very general (Katzung, 1991). More detailed structural studies dealing with kinematics exists, but timing of late to post-Variscan tectonics remain poorly understood (Aleksandrowski et al. 1997, Voigt 1997). There are several sedimentological studies illustrating regional and stratigraphic aspects and discussing tectonic and climatic controlling mechanisms, but they are relatively rare (Wojewoda and Mastalerz 1989, Mastalerz 1990, Gebhardt et al. 1991, Schneider et al. 1998).

The main aim of this study is to interpret the temporal and spatial variations in depositional processes and the geomorphic nature of the fluvial depositional systems of the Trutnov Formation in the Krkonoše Piedmont Basin (KPB), based on outcrop and borehole data. The Trutnov Formation was deposited as one of the red-bed units in a Late Palaeozoic, post-orogenic, "intermontane" basin, following a major tectonic rearrangement of the basin, probably from an extensional to a strike-slip regime, which occurred between the Lower and Upper Rotliegend (Uličný et al., 2002; cf. Stemmerik et al., 2000; McCann T., 1998).

Interpreting the evolution of the Trutnov Formation, including the temporal and spatial changes in the lithofacies, sediment body geometries and petrological characteristics, provides an opportunity to better understand the relative roles of climate changes and tectonic forcing in shaping a fluvial depositional system in an intermontane, strike-slip basin.

Correlation of red-bed successions, both in subsurface and outcrop, is a common problem in non-marine basins. The absence of biostratigraphic markers within the Trutnov Formation and limited and discontinuous outcrops complicate the effort to understand these strata. In order to identify and correlate significant surfaces and facies the main approaches used were a combination of well-log data with outcrop analysis of facies and the depositional architectures of the alluvial/fluvial deposits. Heavy mineral data and outcrop gamma-ray logging were supplementary methods used to help correlate distant outcrops scattered across the basin. Thus, this study also serves as an example of a combination of methods that can be used to extract significant geological information, at a range of temporal and spatial scales, from what would otherwise be an unsatisfactory database.

Geological background and lithostratigraphy

The Late Palaeozoic Krkonoše Piedmont Basin (KPB) formed in the northern part of the Bohemian Massif (Fig. 1) as a part of a system of early post-orogenic basins which originated as extensional-transtensional structures during the Westphalian times, following the climax of the Hercynian orogeny in Central Europe (cf. Ziegler 1990). The infill of the KPB, represented largely by lacustrine and alluvial units, spans the Asturian through the Early to ?Middle Triassic interval (Fig. 2), but a major change in the tectonic regime occurred between the Autunian and Saxonian (Lower/Upper Rotliegend) when the Trutnov Náchod Basin formed in the eastern part of the KPB (e.g. Prouza and Tásler 2001). The Trutnov Náchod Basin is interpreted as a pull-apart basin superimposed on the older, dominantly extensional structure of the Krkonoše Piedmont Basin (Uličný et al., 2002). The older parts of the basin fill underwent partial deformation during the formation of the Trutnov Náchod Basin. This is indicated by an angular unconformity at the base of the Trutnov Formation, the main unit of the basin infill. The Trutnov Formation, up to 600 m thick, has been divided by Prouza and Tásler 2001 into 4 distinct units in the north-central Trutnov-Úpice area: the Horní Město Conglomerates at the base of the Formation are overlain by the mudstone and siltstone-dominated Vlčice Member, the upper part is characterised by fluvial sandstones of the Havlovice Member; the Suchovršice Member at the top of the succession consists of calcareous and dolomitic sandstones (Prouza and Tásler, 2001; Fig. 2). In the southern part of the basin (Náchod – Červený Kostelec area), the basal unit of the Náchod Conglomerates, with a thickness of about 600 m, is overlain by Sandstone Beds, and the succession ends with the Calcareous Sandstone Unit (Prouza & Tásler, 2001). The stratigraphic and palaeogeographic relationships between

southern and northern basin parts are not discussed by these authors. Application of well-log correlation (see section 4, below) made it possible to clarify some problems in lithostratigraphic division and correlation. Pebble composition of the Horní Město Conglomerates shows a dominant Krkonoše Crystalline source in the North, while the Náchod Conglomerates are dominated by rocks from the Orlice-Sněžník Crystalline Unit to the southeast of the basin (Fig. 1, Prouza & Tásler, 2001).

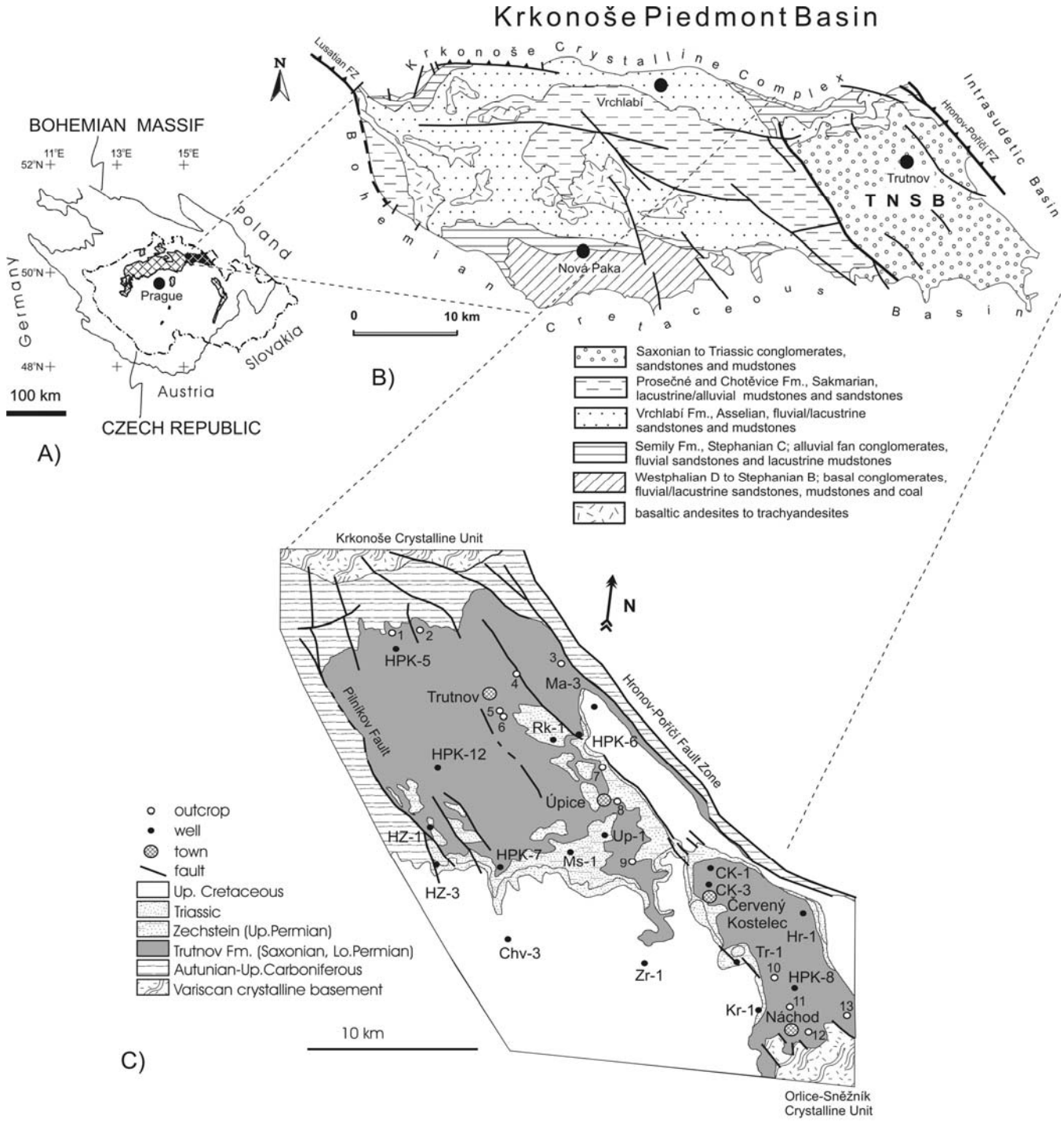

Figure 1. A) Small sketch map showing the location of the Krkonoše Piedmont Basin (KPB, dark cross-hatch) and other non-marine Carboniferous-Permian basins within the Variscan Bohemian Massif. B) A geological sketch-map of the KPB and the position of the Trutnov Náchod subbasin (TNSB). C) A map of the TNSB showing the location of boreholes and the outcrop sections studied, 1) Hrádeček, 2) Pekelský vrch, 3) Trutnov-Poříčí, 4) Trutnov-Lány, 5) Starý Rokytník quarry, 6) Starý Rokytník lodge, 7) Suchovršice, 8) Úpice, 9) Havlovice, 10) Dolní Radechová, 11) Náchod-Shell, 12) Náchod-Montace, 13) Náchod-Běloves.

Approach and methods

This study combines well-log correlation, outcrop sedimentological and gamma-ray logging and an architectural analysis, supplemented by a petrological study including heavy mineral analysis. The well-log correlation was used to derive information on the large-scale geometries and facies changes in the Trutnov Formation units. This was followed by outcrop-to-well correlations, in order to put the outcrop-scale observations into the basin-scale stratigraphic picture. The heavy mineral composition and outcrop gamma-ray logging were used to correlate individual outcrops to nearby well-logs. Although the heavy mineral record can be complicated by many hydraulic, weathering and source area factors, the integration of heavy mineral analysis with other methods was successfully used to correlate barren strata (Morton et al., 2002; Preston et al., 1998; Mange et al., 1999). Acquiring provenance information is the objective of current research and is not discussed in this paper (see Martínek and Štolfová, in press, for discussion of provenance aspects).

For the evaluation of well-log data, 15 lithological logs, and five resistivity and gamma-ray wireline logs were used. Standard measured sections obtained by logging outcrops of the Trutnov Formation were combined with an interpretation of sedimentary body geometries from the photomosaics of several laterally extensive outcrops. The approach to interpreting the geometric features of facies assemblages (architectural elements) essentially follows that of Miall (1985), but the nomenclature used does not strictly follow that of Miall (cf. also Bridge, 1993). Main facies types were also studied in thin sections by standard microscopic techniques.

Heavy mineral samples were processed by the laboratories of the Czech Geological Survey, Prague. Heavy minerals were separated from the sand fraction below 0.5 mm using heavy liquids (tetrabromethane $C_2H_2Br_4$, 2.95 g/cm^3) from disintegrated, washed and dried sandstone samples. Individual minerals were determined using a standard petrologic optical microscope.

For outcrop gamma-ray logging, the portable gamma-ray spectrometer GS-256 (NaI-Tl detector, Geofyzika a.s. Brno) was used, following the approach described by Meyers and Bristow (1989). Outcrop to well-log correlation is necessary for distinguishing local to regional-scale features in sedimentary and stratigraphic analysis. Therefore, some generalized interpretations of overall depositional systems are included in the comments to the well-log correlations, prior to the actual description and interpretation of facies observed in outcrops.

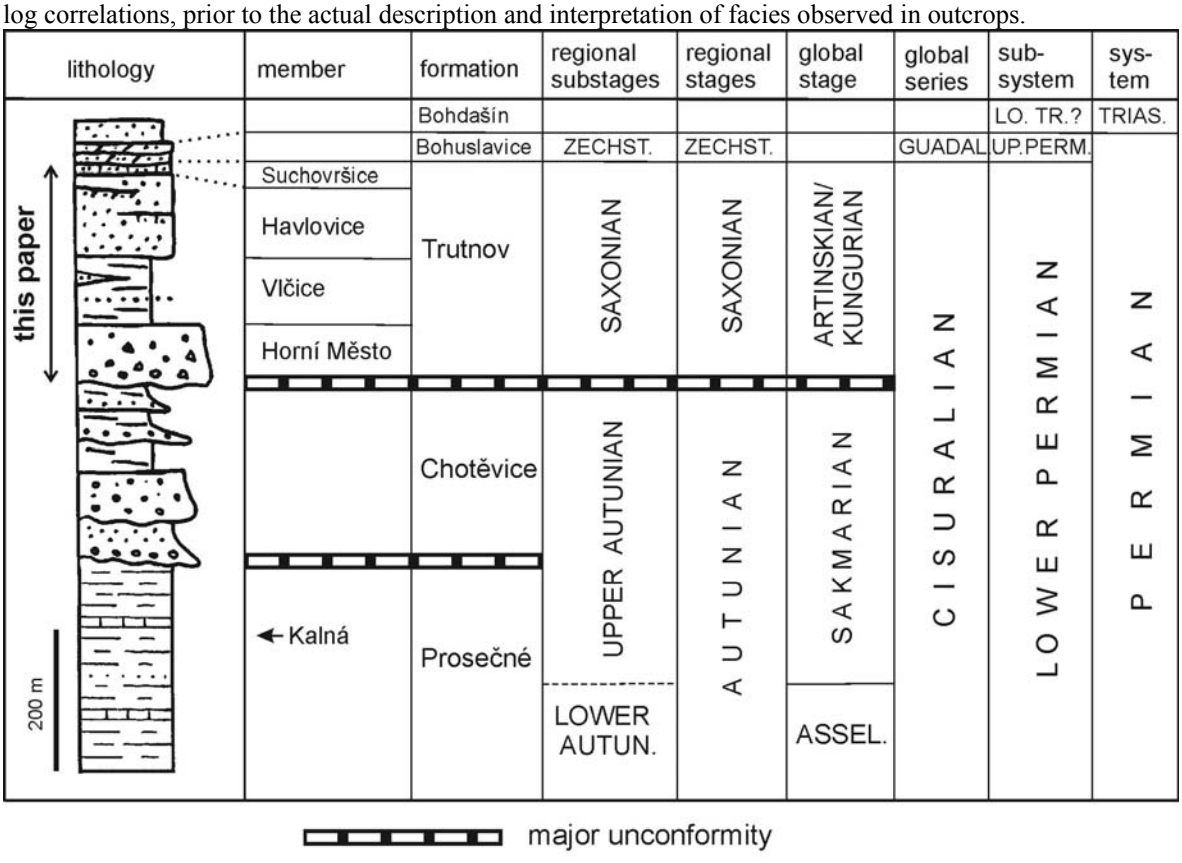

Figure 2. The Permian lithostratigraphic units of the Krkonoše Piedmont Basin, from Prouza and Tásler (2001, Carboniferous deposits not shown). This scheme is based on geological mapping and lithological well logs. In this study a different stratigraphic scheme is proposed, which also integrates wireline log information (see Figs. 3, 4 and discussion in the text).

Well-log data

Wireline log data, although available only for 5 boreholes, proved very useful for determining the regional sub-units of the Trutnov Formation. The units are defined by bounding discontinuities, i.e., surfaces of pronounced facies change that can be correlated across the basin (Units 1 - 3, see Figs. 3 and 4). This stratigraphic scheme is allostratigraphic (sensu North American Commission on Stratigraphic Nomenclature, 1983) and differs from the lithostratigraphic division of Prouza and Tásler (2001; see also Fig. 2).

In most cases the unit boundaries are marked by increased gamma-ray (GR) and decreased resistivity (RES) values, interpreted as having formed due to an increase in the mudstone/sandstone ratio, and vice versa for the surfaces marked by a sharp decrease in GR and increase in RES values. Following the inspection of the data and initial, broad-scale interpretation of the depositional systems, the surfaces are interpreted as a consequence of, respectively, either an increase or decrease in the accommodation/supply (A/S) ratio in the fluvial system (cf. Martinsen et al., 1999, see discussion below).

Importantly, the critical surfaces are traceable even from conglomeratic facies at the basin margin to alluvial/fluvial siltstones and sandstones in the centre of the basin. The following section, which precedes a detailed description and interpretation of outcrop features of the Trutnov Formation, contains interpretative aspects, but only those generalized interpretations are included that are necessary for clarifying the background of the correlations in Figs. 3 and 4.

A common feature of Unit 1, and subunits 1A, 1B and 1C, is generally a high mudstone/sandstone ratio compared to units 2 and 3, with the exception of HPK8, where Unit 1B has the highest sandstone/mudstone ratio (Fig. 3). Subunits 1A, 1B and 1C also have very similar facies content: mudstones with gypsum and carbonate interpreted as playa deposits on the north (HPK5) pass to the alluvial mudstones and siltstones in the central part of the basin (HPK6) and to alluvial/fluvial conglomerates in the south (HPK8).

The base of **Unit 1A** is marked by high GR and low RES in HPK 5, 6, in HPK 8 the RES response is less clear (Fig. 3). Unit 1A is characterized by generally higher mud content (higher GR, lower RES) compared to Units 1B and 1C, which can be seen in HPK 6 and 8, in HPK 5 it is probably suppressed by the carbonate and gypsum content.

Unit 1B is defined by an increase of the proportion of sandstone in comparison to the underlying Unit 1A, which can be seen in HPK 6 and 8. The lower part of Unit 1B shows several sand/mud ratio fluctuations in conglomerates (HPK 8) characterized by increasing-upward gamma values, indicating a decrease in sorting (higher abundance of clay, mica, and feldspars) or grain-size in the same direction (Fig. 3). Similar patterns can be seen in this interval in the well logs of siltstones in HPK 6. The HPK 5 well shows a more complicated response in mudstones interpreted as playa lake facies, which is probably caused by less organized distribution of carbonate and gypsum. However, general fining-up (muddying-up) trends can be observed.

Unit 1C is characterized by a, generally, higher mud content (HPK 8) and a fining up trend in HPK 8 and HPK 6, but an upward decrease trend in GR values in HPK 5. The boundary between units 1B and 1C is manifested with significant decrease in RES and increase in GR in all well logs.

The base of **Unit 2** is marked by an unconformity that can be observed across the basin. It is characterized by a significant increase in the sandstone/mudstone ratio in all well logs. The Horní Město Conglomerates sharply overlay the interpreted playa mudstones in the northern part of the basin (HPK5). Fluvial sandstones of the Havlovice Member rest sharply on interpreted alluvial siltstones in the central part of the basin (HPK 6). In the southern part of the basin, this boundary is manifested by the increase of the sandstone/mudstone ratio in the (sandstone) matrix of the Náchod Conglomerates. Correlation of HPK 6 and HPK 7 shows a transition from more proximal conglomeratic sandstone facies of Unit 2 in the SW (HPK 7) to distal fluvial sandstones of the Havlovice Member in the central part of the basin (see Fig.4). Unit 2 can be divided into three superimposed subunits 2A, 2B and 2C with a distinct muddying-up trend and sharp sand-rich base. These subunits are clearly seen in HPK 7 (Fig.4), in HPK6 and HPK8, there is local variability and two muddying up cycles can be distinguished within subunit 2B. In HPK5 the unit 2C does not show a muddying up trend. The sedimentological characteristics and heavy mineral content of the three subunits are further presented in chapters 5 – 7.

The boundary between Units 2 and 3 is characterized by the most prominent positive gamma-ray peak accompanied by a negative resistivity peak in all well logs. This is ascribed to an abrupt increase of the mud/sand ratio with possible higher U and/or K and/or Th input from source areas. In spite of **Unit 3** being of finer grain size, compared to underlying units, it has lower GR values, which is ascribed to its higher carbonate content. In uppermost part of the well logs, where RES data are missing, GR values may be influenced by borehole casing.

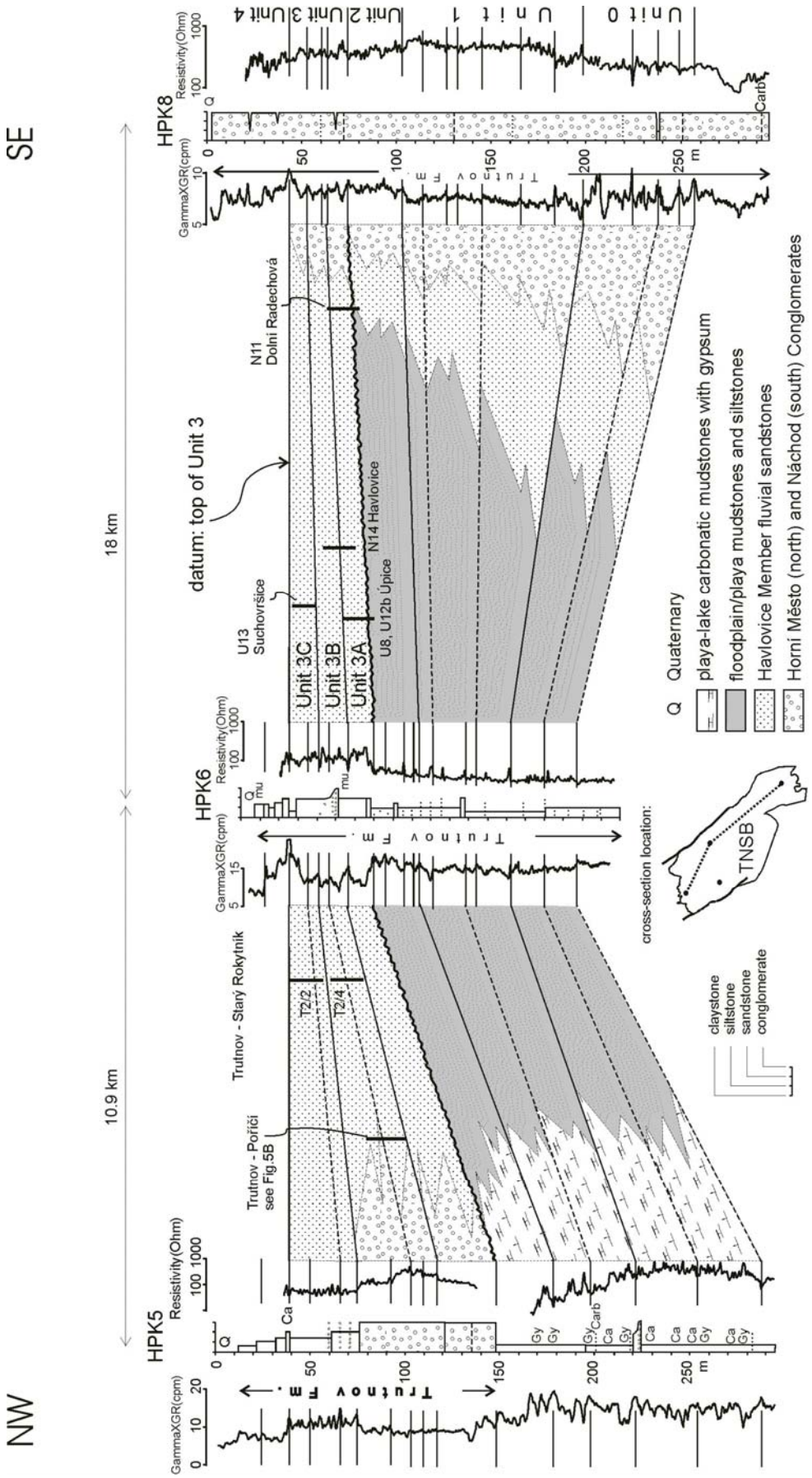

Figure 3. NW-SE cross-section of the Trutnov Formation. The small inset map shows the location of boreholes. The main genetic stratigraphic units (Units 1 - 4), based on a correlation of lithological and wireline logs, showing the relationships between lithofacies and lithostratigraphical units. Fluvial sandstones of Unit 2 are equivalent to the Havlovice Member. For the location of outcrop sections see also Fig. 12.

According to Prouza (pers. commun.) and Prouza and Tásler (2001), mudstones, siltstones and sandstones of HPK6 are younger than the succession of HPK5. However, this opinion, putting Horní Město Conglomerates, the mudstone dominated Vlčice Member, Havlovice Sandstones and Suchovršice Member (carbonatic sandstones) in superposition, is based on indirect evidence. This inference is based on geological mapping and the depth of the basement in various parts of the basin. Refraction seismic data show the basement in approximately 2000 m depth. The thickness of Upper Carboniferous strata near a southern basin margin (Ratibořice Valley area, 15 km northwest of Náchod) is of few hundred meters. Therefore, the thickness

least several hundred meters of the Trutnov Formation are inferred for TNSB. But these assumptions do not reflect thickess variability across the basin, which can be very high in a strike-slip basin. Unfortunately, the direct evidence is missing, there are no boreholes reaching the basement or reflection seismic data in the TNSB.

Alternatively to Prouza and Tásler (2001), very good correlation of HPK5 and HPK12, and good correlation of HPK12 and HPK6, HPK7, Ma-3, HZ-1, HZ-3 of core as well as well-log signaturelet us to opinion, that playa gypsiferous mudstones of HPK5 and HPK 12 are equivalent of alluvial/lake mudflat mudstones of HPK6, HPK7, Ma-3, HZ-1 and HZ-3. Which put Horní Město Conglomerates (HPK5) as a lateral equivalent of fluvial sandstones of Havlovice Member (HPK5, HPK7, Ma-3, HZ-1, HZ-3).

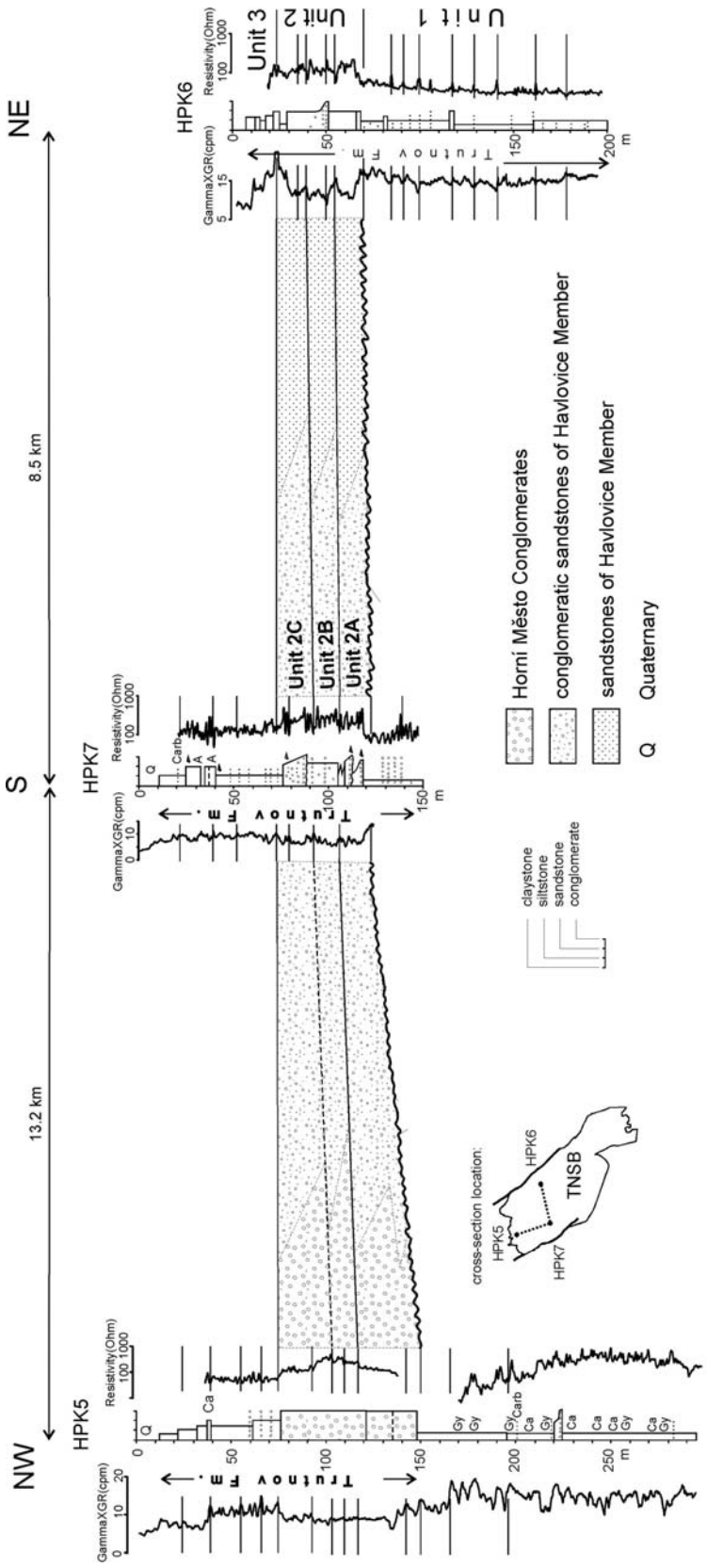

Figure 4. NW-SW-NE cross-section of the Trutnov Formation showing the relationships between conglomerate and sandstone facies of Unit 2. Fining trend from SW to NE and facies interfingering between marginal conglomerates (HPK5) and the axial part of the basin (HPK7 and 6) can be seen. The location of boreholes is shown in the small inset map.

Outcrop-scale features

The outcrop study was focused on Unit 2 that forms the only significant exposures. It comprises almost entirely of fluvial sandstones of the Havlovice and Suchovršice Members and Horní Město and Náchod Conglomerates. Finer grained units do not form larger outcrops.

Facies and depositional geometries description

The main descriptive characteristics of lithofacies present in the studied sections are summarized in Table 1. The outcrop phenomena of the main facies are illustrated in Figs 5 and 6. The text below focuses on the relationships between the facies and their geometric arrangement in architectural elements: for this reason, the description follows the grouping of facies into five main assemblages, mostly equivalent to architectural elements: (1) conglomerate sheets, (2) conglomerate bars and bedforms, (3) sandstone channel fill, ribbon-like bodies, (4) overbank tabular and wedge bodies, and, as a special category, (5) carbonate-cemented strata (cementation occurs both within the channel fills and in the overbank sedimentary bodies). Although this division is partly interpretative (cf. Bridge 1993), we decided to use it because of its simplicity and mostly because of the very obvious relationships between the channel and overbank strata in the outcrops studied.

Because the outcrops of the conglomerate facies are relatively small or show simple geometrical relationships, selected measured sections and photographs are used to illustrate the main outcrop features. For the sandstone facies, in addition to measured sections, photomosaics are used to document geometrical relationships.

Conglomerate sheet facies

Conglomerate sheets comprise facies G_L (see Tab. 1, Fig. 5D) of low-angle cross-bedded to a crudely flat-bedded conglomerate G_L. Imbrication was observed in places. Conglomerates can be chaotic to massive in some places. The proportion of angular and subangular pebbles increases close to the basin margin, where breccia conglomerates to breccias occur. Better stratified conglomerates are moderately sorted and clast supported. Crudely stratified beds are usually poorly sorted and matrix supported. Beds are tabular, 1 — 4 m thick with a sharp base and laterally persistent by more than 20 m. Carbonate cemented beds occur rarely. Conglomerate sheets occur in the most proximal setting, a few hundred meters to 2 km from the present-day basin margin.

Conglomerate bars and bedforms

Conglomerate bar and bedform facies comprise of cross-bedded conglomerate facies G_C of a planar, low-angle and trough cross-bedded conglomerate. It is poorly to medium sorted, matrix to clast supported and with imbrication in places. Rip-up sandstone clasts (1 – 10 cm, in places up to 30 cm) can occur in places. These conglomerates have sharp to erosional concave bases, lenticular or wedge shape and are up to 15 m wide in cross section. In the Trutnov area sandstone clastic dykes occur (see Fig. 5c). These facies occur several hundred metres to a few kilometres from the basin margin

Sandstone channel-fill facies assemblage

This facies assemblage is dominated by the cross-bedded sandstone facies S_c (Tab.1). But locally mudstones with poorly defined lamination fill the erosional channel forms. The channel-fill bodies are generally ribbon-shaped in cross-section (Figs. 7-8). Because most exposures strike generally parallel or oblique to the channel axis orientations, it is difficult to evaluate the flow-normal widths of the channels, with a few exceptions (Fig. 7). Individual channels show up to 1 m of erosional relief at the base, typically overlain by lag deposits containing large (up to several dm) mudstone clasts and quartz granule to pebble-sized material (Fig. 6A). Locally, large clasts of carbonate-cemented sandstones occur at the base of a channel (see below, and in Fig. 3D, F, H). High-angle cross-sets, up to 1.8 m thick, which commonly contain a high amount of gravel and rip-up mudstones in the foresets, mostly occupy the lower portions of the channels (Fig. 6C). Intraclasts of micritic carbonates also occur. Secondary Fe oxide pseudomorphs, after pyrite, were found in the sandstones, which are characterized as a lithic arkosic arenite.

Fluid-escape structures and recumbent folds are locally present in the cross-strata. Upward, the overall grain size decreases, and the cross-sets become lower-angle and thinner. Measurements of azimuths of trough cross-bed axes show a prevailing eastward palaeocurrent trend.

The main internal geometry observed in the channels is downstream accretion of the dunes, and a small degree of lateral filling (Fig. 7). Extensive channel belts of laterally accreted strata are absent, with a possible exception of a poorly exposed section in Havlovice. The maximum observed thickness of individual channel storeys is c. 4 m.

Table 1. Overview of main facies types, their descriptive characteristics and interpretations.

facies	sedimentary structures	grain size, sorting, mineralogy	dimensions, geometries	other	interpretation
low-angle cross-bedded and horizontal bedded conglomerate G_L	poorly to well developed horizontal and low-angle cross-bedding, locally high-angle cross-bedding in scour fills; chaotic to massive in places	coarse gravel (pebble) to cobble breccia conglomerate; angular to subangular clasts; maximum clast size up to 50 cm; poorly sorted; matrix supported; matrix: coarse sandstone to fine gravel conglomerate	1-4 m thick tabular beds; sharp base; laterally persistent more than 20 m (limited outcrop size)	occur in most proximal setting; carbonate cemented beds occur rarely	mostly sheet-flood deposition; massive chaotic beds with higher mudstone proportion in matrix could have been deposited as debris flow
cross-bedded conglomerate G_C	planar, low-angle and trough cross-bedding; imbrication in places	fine to coarse gravel breccia conglomerate; angular to medium rounded; poorly to medium sorted; matrix to clast supported; matrix: coarse to medium grained sandstone; rip-up sandstone clasts (cm to 30 cm)	0.2 - 3 m thick beds; tabular to lenticular; sharp to erosional base	sandstone clastic dykes occur in Trutnov area	migration of dunes and bars; channel fill
cross-bedded sandstone S_C	high-angle to low-angle, mostly trough cross-bedding; water escape structures and wave ripples can be present near the top	coarse to medium-grained sandstone; moderately to poorly sorted; cross-sets arranged in fining-up successions rip-up mudstone clasts up to 15 cm; rip-up sandstone clasts up to 80 cm; granule- to pebble-sized clasts in foresets lithic arkosic sandstone	0.3 - 1.8 m thick beds, 2 - 8 m thick bed sets erosional base: 15-90 cm erosional relief	in places appears massive due to weathering locally bioturbated	migration of dunes; channel fill; first, highest energy, flooding event ; subsequent, more confined (steady) flows
rippled sandstone S_R	ripple cross-lamination, locally supercritically climbing ripples	fine to medium grained sandstone, moderately to well sorted lithic arkosic sandstone	individual cm to 30 cm thick beds	tufitic intercalations may be present closely associated with M facies	small dunes and ripples migrating on floodplain high sediment input in places - volcanogenic material
sandstone heterolithics S_H	alternating mm-cm clayey silty and sandy laminae; current ripples or flaser bedding can occur locally	fine to medium grained high proportion of mud and silt	few cm to 80 cm thick beds	trough cross bedding can be present in thicker sandstone - dominated parts	alternation of suspension fallout and slow tractional current
bioturbated fine grained	moderately to poorly preserved horizontal	fine to medium grained poorly to medium sorted high proportion of clay	few cm-75 cm thick beds, tabular	common bioturbation; in places where	suspension fallout, migration of flat dunes; crevasse splay ?

sandstone S_{FB}	lamination or low angle cross bedding	and silt	sharp base	bioturbtion is not preserved mottling occurs	gap in sedimentation
mudstone M	poorly to well defined lamination, 1 mm – 1cm thick laminae; massive in places; desiccation cracks in places	clayey siltstone to silty claystone poorly sorted clayey silty fine-grained sandstone in some places	few cm-60 cm thick beds	interbeds of few cm-25cm thick fine to medium grained sandstone with mm-cm lamination; local bioturbation	suspension fallout; floodplain / abandoned channel fills
carbonatic sandstone C	massive appearance	calcareous to dolomitic fine to coarse grained whitish sandstone	few cm-25 cm thick beds undulose top or base in places	lateral transitions to nodular horizons; often forming interbeds in prevailing low carbonate strata	early cementation, different stages of calcrete/dolocrete formation
brecciated carbonatic sandstone C_B	no organization of particles	poorly sorted , medium to coarse-grained high proportion of calcrete/dolocrete breccia, mudstone intraclasts, redeposited pedogenic nodules, quartz pebbles, limonitized and haematitized metamorphic rocks	sharp base 30-60 cm thick beds	mottled highly mixed up material	redeposited calcrete/dolocrete

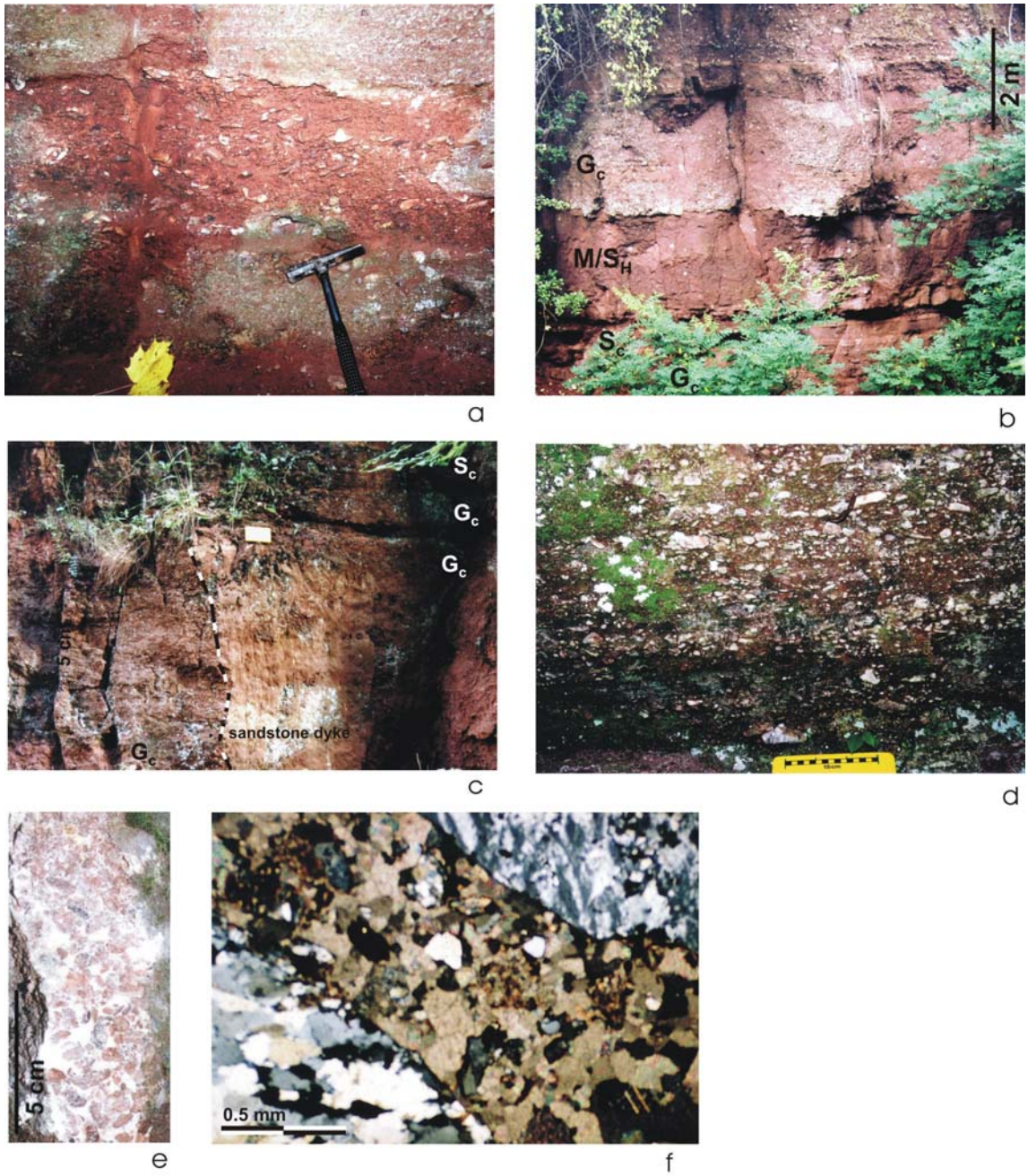

Figure 5. Photographs A-F illustrate the main features of the conglomeratic facies. (A) Imbrications in Horní Město Conglomerates ca. 20 cm above the hammer; vertical sandstone dyke in the left part (arrow), facies G_C, section T21 Pekelský vrch. (B) Alternating Horní Město Conglomerates, facies G_C, with fluvial sandstones and floodplain muddy siltstones (M/S_H), note the erosional base of the upper conglomerate bed. (C) The vertical sandstone clastic dyke below the field book, which is 18 cm long, is 5-10 cm thick, section T24 Trutnov-Poříčí, lower conglomerate bed of Fig.(B), facies G_C. (D) Low-angle cross-stratification is typical for proximal Náchod Conglomerates, facies G_L, section N313 Náchod-Běloves. (E) Carbonate cemented beds are rare in the Náchod Conglomerates. This photograph shows a calcite (white) cemented conglomerate bed, an upwards decreasing intensity of cementation can be seen. Section N314 Náchod-Běloves. (F) A microphotograph of the lower part of (E). Large polycrystalline quartz pebbles lower left and upper right, central part shows quartz and feldspar sand grains floating in calcite spar. Crossed nicols.

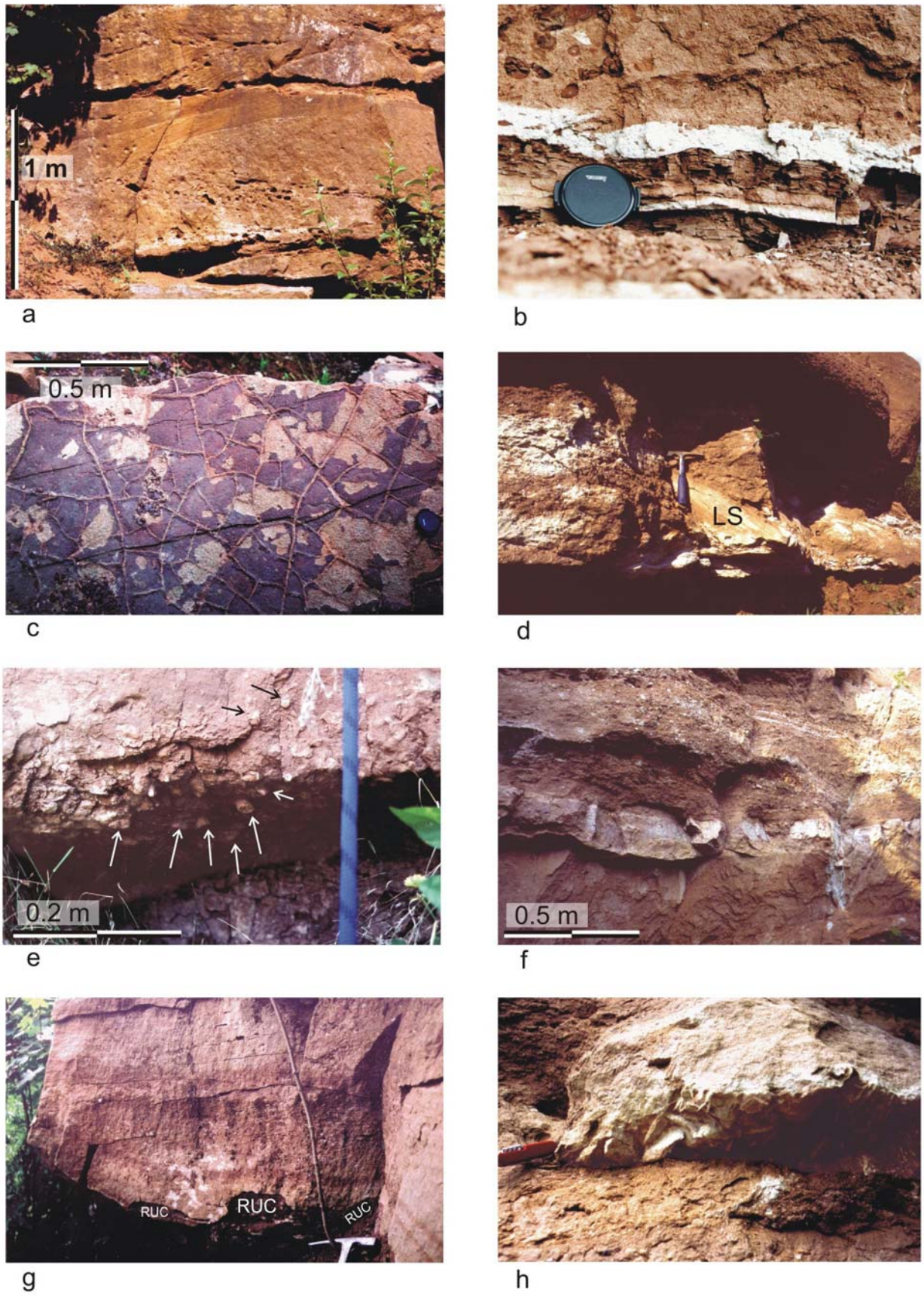

Figure 6. Photographs of selected sandstone facies; photographs A, B, D, F and H are from the exposure of the upper Trutnov Formation in an abandoned quarry along the road Trutnov – Starý Rokytník, see also Fig. 7. (A) Trough cross-bedded sandstones of varying grain size in individual sets; note the abundant mudstone intraclasts in the foreset laminae. (B) Rip-up clasts of overbank mudstone in an overlying sandstone channel (note the scoured basal surface of the sandstone). (C) Desiccation cracks in mudstones from the abandoned

channel fill. Trutnov-Lány quarry. (D) A chaotic lag deposit, interpreted as a collapsed cutbank, overlying the channel base, containing mudstone rip-up clasts, quartz pebbles, and blocks of partly lithified sandstone (LS, at the hammer bottom). (E) A highly bioturbated base of crevasse sandstone, Havlovice section N14. Field of view is 0.5 m high. (F) A calcite – cemented horizon in the upper part of a channel-fill sandstone, interpreted as a pedogenic calcrete horizon. (G) A highly irregularly scoured base of trough cross stratified sandstone, which is incised into overbank mudstones. Large muddy sandstone rip-up clasts near the base (RUC). Úpice top of section U8, units 3A/3B boundary, see also Fig. 12. (H) Close-up of a cemented block, part of a collapsed breccia at the base of the channel. Note the micro-karstification at the lower surface of the block – this was originally the calcrete surface indicating the upside-down position of the block following the bank collapse.

Overbank facies assemblage

This assemblage comprises of rippled sandstone facies S_R, heterolithic sandstone facies, bioturbated sandstone facies, and mudstone facies (Tab. 1), which all form tabular or thin wedge-like depositional geometries (Fig. 7, centre). All the above facies do not have individual bodies exceeding 1 m in thickness; for example, the rippled sandstone facies typically forms tabular beds less than 30 cm in thickness. Mudstone tufitic rip-up clasts are present in places in the rippled sandstones. The bedforms present in these facies are generally limited to ripple size, with the exception of some thicker sandstone parts of the heterolithic sandstone facies, which locally contain thin trough cross-sets. The lateral extent and preservation of the tabular bodies of overbank strata is controlled by the downcutting of intervening channels and changes in thickness of channel-fill strata.

Carbonate-cemented strata

Carbonate cementation affects sandy to silty facies regardless of their position in a channel fill or overbank facies assemblage. Carbonate cemented strata typically form thin, 1 – 25 cm thick, beds within, overall, moderately to poorly carbonate-cemented, exclusively clast-supported sandstones (Fig. 6F, 4). Thin sections show that in heavily cemented horizons, quartz and feldspar grains and rare rock fragments float in a carbonate cement (Fig. 9A). Carbonate replaces quartz and feldspar grains moderately to intensively. The carbonate cement can be present in the form of subhedral dolospar, anhedral calcite spar, and as many transitions with different proportions of dolomite vs. calcite and different proportions of a ferroan admixture. In addition to carbonate cementation, simultaneous cementation by either limonite/haematite or quartz was observed in some cases. This fabric resembles the cornstones as described by Tandon & Friend (1989). Ferroan dolomicrite was found in Havlovice section N14. Calcite spars show poikilotopic fabric in several cases.

The massively cemented horizons pass laterally into nodular zones; the upper parts of the cemented strata are locally undulating in shape and exhibit micro-karstification (Fig. 6H). Blocks of cemented sandstones were found at the bottom of a channel cut into the cemented sandstone layer (Figs. 6H, 7). A chaotic mixture of poorly sorted clasts of carbonate-cemented sandstone, mixed with mudstone intraclasts, and an admixture of pebbles of quartz and crystalline rock fragments defines the redeposited carbonatic sandstone; this facies typically forms a part of channel fills.

Interpretation of depositional and early diagenetic processes

Conglomerate sheet-flood and fluvial deposition

Tabular conglomerate sheets characterized by sandy matrix-supported fabric with imbrication of pebbles are interpreted as hyperconcentrated sheet-flood deposits (Nemec and Steel, 1984). The crudely stratified beds, which occur in the most proximal setting, can represent sheet-flood deposition on an alluvial/fluvial fan (Blair, 1987, 1999). Conglomerate bars and bedforms are interpreted to have been deposited by high-gradient, braided streams with high fluctuations in discharge. Deposition occurs mainly during high-discharge events by lateral and vertical accretion along with channel cutting and abandonment (Sánchez-Moya et al., 1996; Ramos and Sopena, 1983; Smith, 1990). These fluvial facies occur several hundred meters to a few kilometres from the basin margin and can represent the deposition of a distal fluvial fan or proximal fluvial sedimentary systems.

Cutting and filling of sandstone-filled channels

The cutting and filling of channels, predominantly by cross-bedded sandstones with a fining-up and thinning-up trend, indicates high-energy events, which led to the filling of channels by presumably channel-bar bedforms corresponding to gradually shallowing water and decreasing flow energy. Very rapid deposition of the cross-bedded facies is also suggested by common fluid-escape structures, including dish structures, which in places lead to the obliteration of the original sediment fabric. Recumbent folds formed in some cross-sets (cf. Allen &

Banks 1972) indicate shear liquification by overriding flow exerting high shear stress on the bedform (Nichols, 1995). This is also confirmed by fluid-escape structures, which occur in the same layer as recumbent folds in the Starý Rokytník quarry (Fig. 7, lower left part of the photomosaic), indicating fluidization that followed shear liquification of the dune. Other mechanisms than shear by overriding flow, which have been cited as possible causes of liquefaction, include a rapid drop of water level leading to an increase in pore pressure (common in braid bars) or a seismic shock (e.g. Fishbaugh et al. 1989). In our case, however, evidence for a wholesale liquefaction of a braid bar forming a whole channel storey is missing, we believe that the liquefaction and fluidization of individual cross-sets were due to the rapid deposition of loose, water-saturated sediment, combined with high shear stress of flows during the flood stage.

Common accumulations of large mudstone rip-up clasts at the base of channels (Fig. 6B) indicate abrupt erosional events, which led to the channel cutting and presumably caused avulsion of channels into the overbank area, with significant erosion of muddy lithologies and bank collapse, including the collapse of channel banks indurated by cementation (see below). Rare mud-filled channels are interpreted as abandoned channels, filled by suspension fallout from standing water or very low-energy flows. Single channel-fills are commonly multi-storey, sensu Bridge & Mackey (1993), that is, within a single channel-belt succession several channel-bar sequences are deposited before the channel-belt is abandoned. Unfortunately, the two-dimensional nature of most outcrops prevented a more detailed, 3-D reconstruction of bars or other architectural elements.

The small thickness of individual channel storeys, generally less than 4 m, suggests that the bankfull depth was not significantly larger than 4 m. Palaeocurrent indicators show a rather wide dispersal of the palaeoflow in a generally eastward direction. The evidence for unstable channel margins (except those indurated by cementation), lack of systematic lateral accretion in most channels, and locally consistent palaeoflow indicators, indicates a low-sinuosity (braided) channel system.

Overbank deposition

The spectrum of overbank deposits reflects a number of processes, from tractional currents to suspension fallout, in the overbank area. The tabular bodies of rippled sandstone and bioturbated sandstone facies are interpreted as splay deposits, formed during the high-energy parts of flood episodes. Heterolithic sandstone facies is interpreted as being deposited by alternating suspension fallout and tractional current, indicating a fluctuating nature of the flow. Episodes of non-deposition following the late stage of a flood resulted in the bioturbation of parts of the splay sands. The mudstone lithofacies was deposited from suspension and indicates episodes of the overbank area being flooded by standing water, which obviously alternated with episodes of prolonged exposure of floodplain strata and pedogenesis (Kraus, 1987).

Carbonate cementation

The cementation observed in many horizons of sandstone bodies was clearly syndepositional, and is attributed here to calcrete formation in a semi-arid climate. In the case of secondary carbonate precipitation, e.g. from carbonate ion-rich pore fluids, during burial diagenesis, cementation would probably affect much larger rock volumes and its distribution would probably be driven by the porosity and permeability of sandstones. However, thin carbonate-cemented horizons mostly follow the interpreted depositional palaeotopography and are thus interpreted as abiogenic calcretes, formed by evaporative pumping of ion-rich groundwater and shallow precipitation under the surface. Evaporation exceeding precipitation (negative water budget) is supposed (Talbot et al., 1994). The poikilotopic calcite spar may have formed during a later diagenetic burial overprint (Harwood, 1988), through simple recrystalization rather than secondary precipitation.

The calcrete maturity does not reach stage 4 of Wright et al. (1988), that is, the cementation typically reaches stages 2 – nodular calcrete and 3 – massive calcrete, prior to the development of a laminar horizon (which would require biogenic activity, thought to be insignificant in our case). The fact that the cementation was rapid enough to form massive, indurated horizons, is well documented by the undercutting of a massively cemented sandstone bed by a channel margin and the resulting channel-bank collapse (Figs. 6, 7). The micro-karstification of the calcrete surface is shown in the upside-down block in the channel fill in Fig. 6H. Partial or complete erosion of semi-mature calcrete horizons is indicated by the occurrence of redeposited cemented sandstone facies in some channel fills.

Interpretation of fluvial style

The evidence above suggests that the fluvial systems studied were of low-sinuosity type, characterized by a highly variable discharge. The margins of the generally broad channels are typically poorly defined, which is interpreted as a consequence of easily erodible banks and significant lateral switching of channels. One observed exception is a narrow (c. 16 m) channel, incised 2.5 m deep into a carbonate-cemented channel-belt sandstone (Fig.

7). In this case, the calcrete cementation was important in preventing lateral erosion and in focusing the erosion during a flood event into a narrow channel. Also the bottom of this channel is defined by an older calcrete surface, which presumably limited the depth of its downcutting. This situation is similar to that described by Gibling & Rust (1990) from a fluvial system with siliceous duricrusts, although in our case the impact of floodplain induration on the topography is not as dramatic as in the case described by these authors.

In general, the abundance of calcretes / dolocretes, absence of evidence for any vegetation cover (neither fossils nor roots found), high variations in discharge and preservation of feldspars and unstable rock fragments, all suggest seasonal to ephemeral flow and arid/semi-arid climatic conditions.

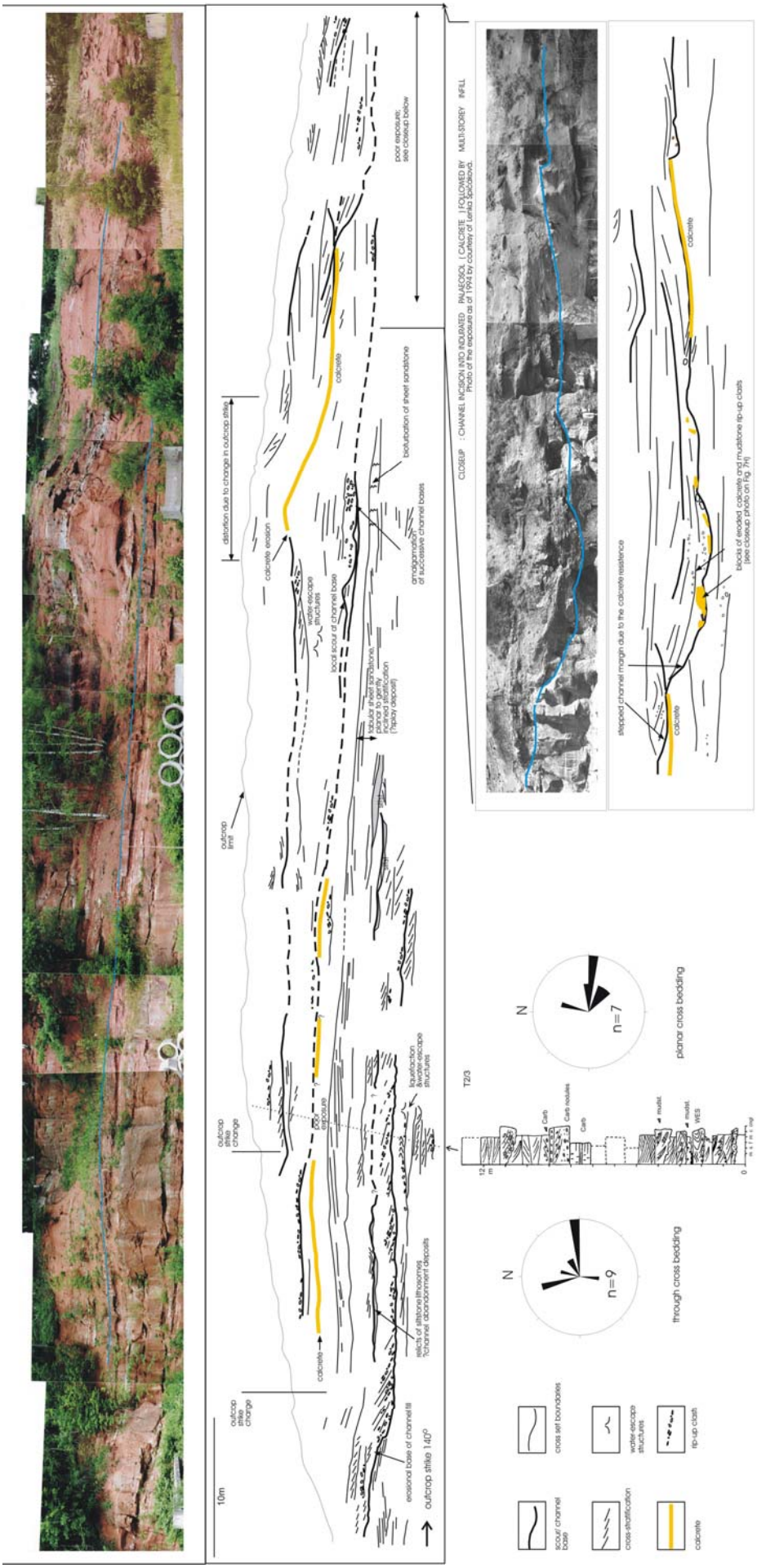

Figure 7. A photomosaic of the Trutnov - Starý Rokytník quarry. Several multi-storey channel fills and intervening mudstones. A tabular bioturbated sandstone body occurs in the middle part of the section. Calcrete horizons marked by thick yellow/grey lines. In the close-up view, note the stepped margins of the channel incised into a calcrete horizon and partly underlain by an older calcrete.

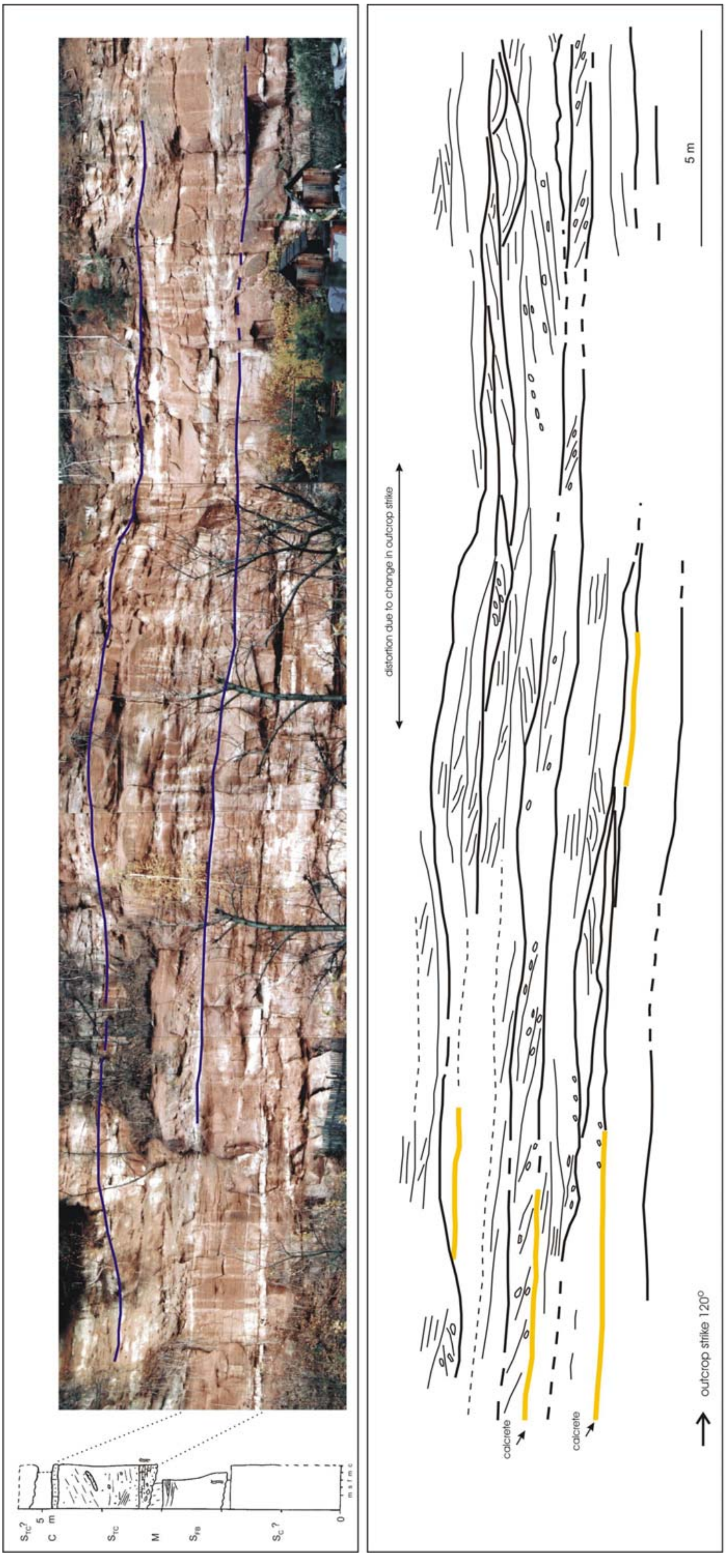
distortion due to change in outcrop strike
5 m
calcrete
calcrete
outcrop strike 120°

Figure 8. A photomosaic of Trutnov – Starý Rokytník lodge Trutnov - Starý Rokytník lodge. Amalgamated sheet-like multistorey channel fills dominate the section. Lateral migration of channels and the generally small depth of erosion is visible. Note the abundance of calcretes and the presence of relatively thin sandstone bodies. For legend see Fig. 7.

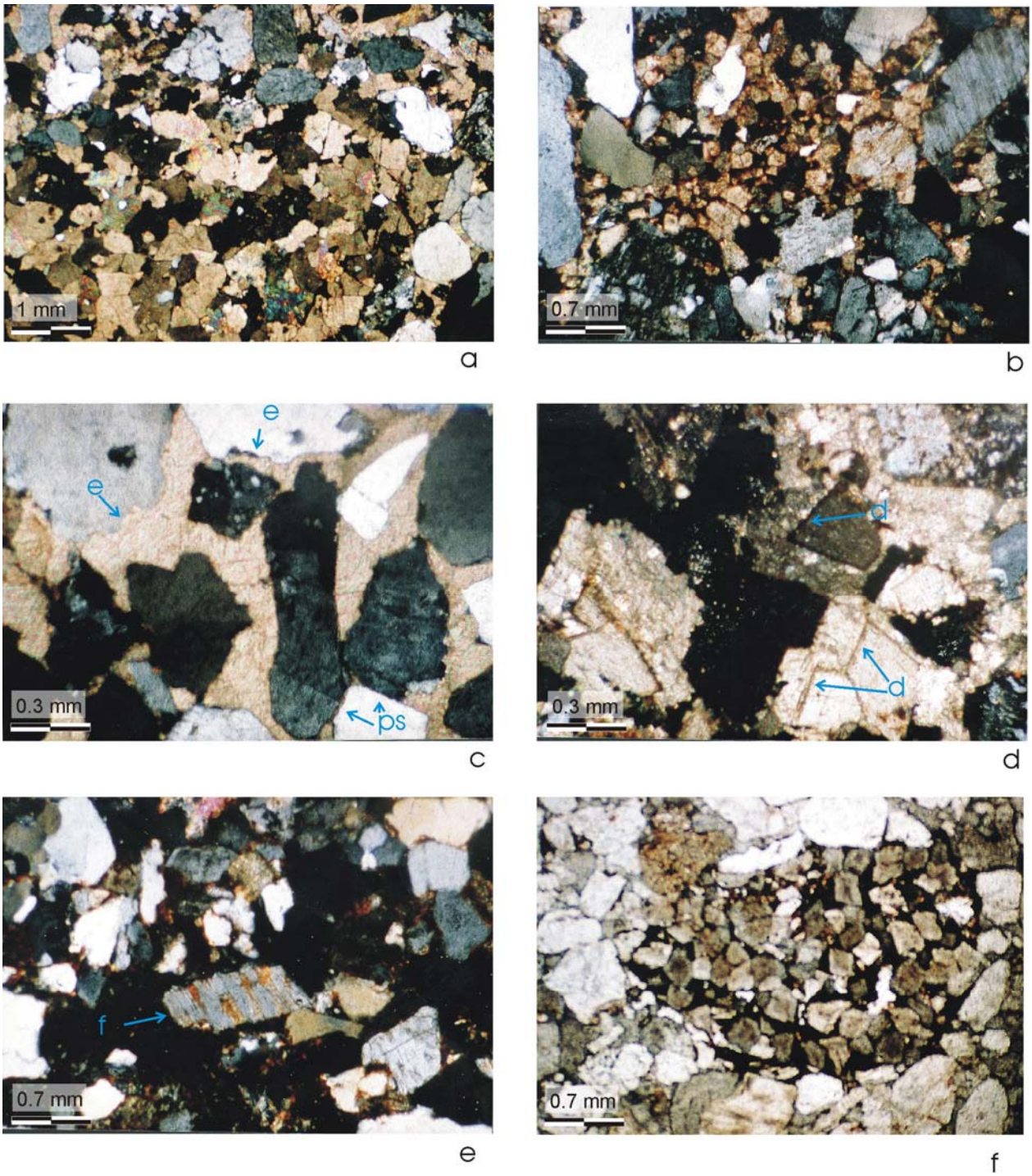

Figure 9. Microphotographs of sandstone facies. (A) Quartz and feldspar grains floating in the calcite spar. The original, probably micritic, nature of the calcrete is obliterated by recrystalization. Crossed nicols, field of view is 6 mm wide. (B) Some sandstone beds are cemented by a mixture of calcite spar (xenomorphic) and dolomite (hypidiomorphic to idiomorphic rhombs). Crossed nicols, field of view is 4 mm wide. (C) Replacement of quartz by calcite during burial cementation. Note etched (e) grain margins and grain contacts affected by pressure solution (ps). Crossed nicols, field of view is 2 mm wide. (D) Dolomitization (d) of original xenomorphic calcite cement. Crossed nicols, field of view is 2 mm wide. (E) Well preserved feldspar grains (f) and rock fragments (lower part). Crossed nicols, field of view is 4 mm wide. (F) The nodule in the centre, composed of hypidiomorphic and idiomorphic dolomite crystals cemented by Fe oxides, is surrounded by carbonate cemented quartz grains. Parallel nicols, field of view is 4 mm wide.

Basin-scale lateral and vertical trends

Outcrop correlation using heavy minerals and gamma-ray logging

The results of the heavy mineral analyses are summarized in Fig.10 and Tab. 2. The locations of individual samples are shown in Figs.1, 5 and 12. The heavy mineral composition of northern Horní Město Conglomerates and southern Náchod Conglomerates are very similar. The main source rocks are different – the Krkonoše Crystalline Complex and the Orlice-Sněžník Crystalline Complex, respectively, but both sources have similar lithologies – mostly Variscan metasediments, metavolcanics and granites (Chaloupský, 1989; Opletal, 1980). In sandstones from the central part of the basin four distinct heavy mineral associations (HMA) were recognized (Fig. 12). For these sandstones, in addition to crystalline sources, older Permo-Carboniferous sediments and volcanics from the central and western part of the basin are also considered as a possible source of detritus. HMA 1, 2 and 3 characterize Unit 2 and HMA 4 belongs to the youngest Unit 3. HMA 1 is dominated by magnetite and tourmaline, which prevails in most samples. HMA 2 is characterized by garnet, ilmenite and tourmaline, where the presence of garnet is the most prominent feature. However, the amount of garnet does not exceed 20 % (see Fig. 10). HMA 3 show a very similar composition (garnet, ilmenite and tourmaline association), but the amount of garnet is at least 50 % (see Fig. 10). HMA 1, 2 and 3 correspond to Units 2A, 2B and 2C, respectively. HMA 4 is mixed with garnet, leucoxene, rutile and tourmaline and corresponds to Unit 3. Using heavy mineral data, several outcrops were successfully correlated, and tied to well-logs using also field gamma-ray measurements. Although the spacing of GR measurements is different in outcrop survey (0.3 – 0.5 m) compared to well-logs (0.1 m), and outcrop surface unevenness has influence to GR values, the similarity in GR curve pattern enabled correlation of outcrop sections up to few km distant well logs. E.g. T21 to HPK5, T2/4 to HPK 6, U12b to U8 to HPK6, N14 to HPK6 and HPK8, and N11 to HPK8 and to HPK5. A synthesis of all this data is given in Fig. 12.

The most striking change in heavy mineral composition is the abundance of garnets in HMA 2, 3 and 4, while in HMA 1 garnets are absent. The heavy mineral information is clearer when using heavy mineral indexes (Fig. 11; Morton and Hallsworth, 1999), which emphasizes provenance information and inhibits other factors influencing heavy mineral composition (hydraulic, weathering, transport). The distinction of the sandstones into five groups can be seen in the GZi vs. ATi plot. The boundary between subunits 2A and 2B is observed in section N14 (Havlovice), where it is formed by a distinct erosional surface overlain by channel dolocrete.

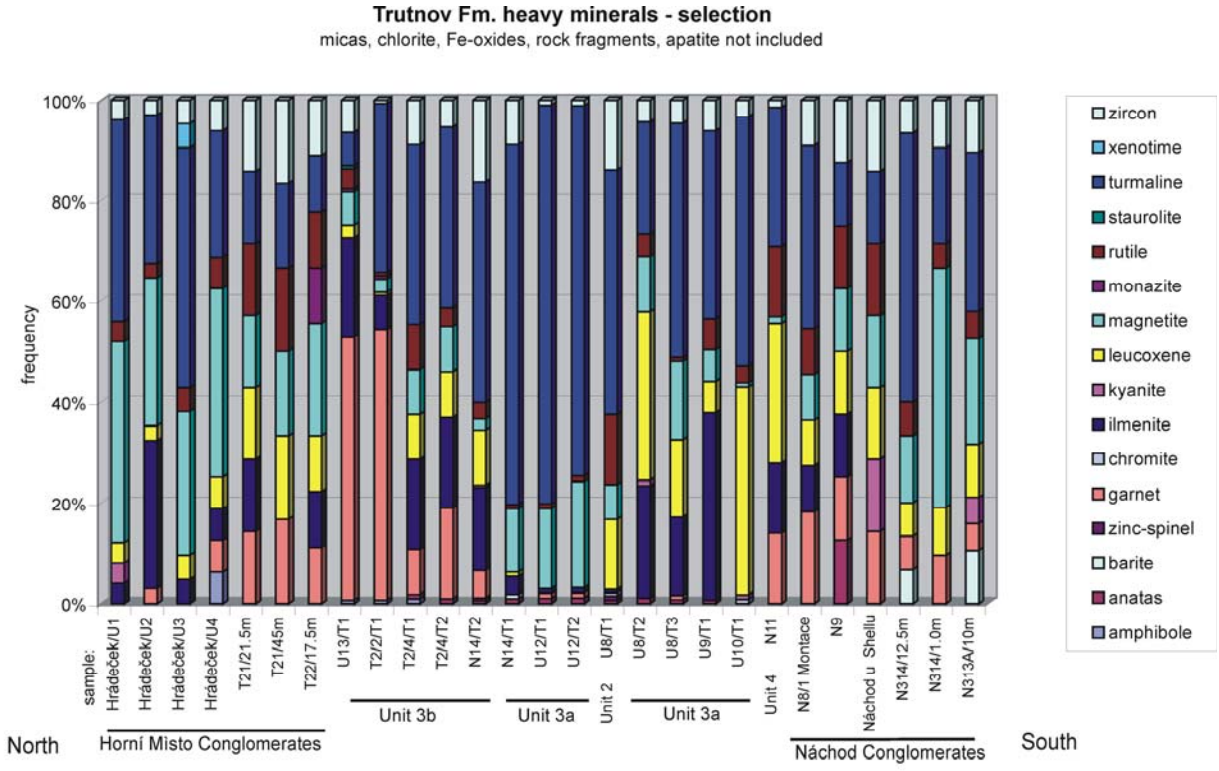

Figure 10. Heavy mineral data from Trutnov Formation. Note the garnet rich Unit 2B and garnet free Unit 2A.

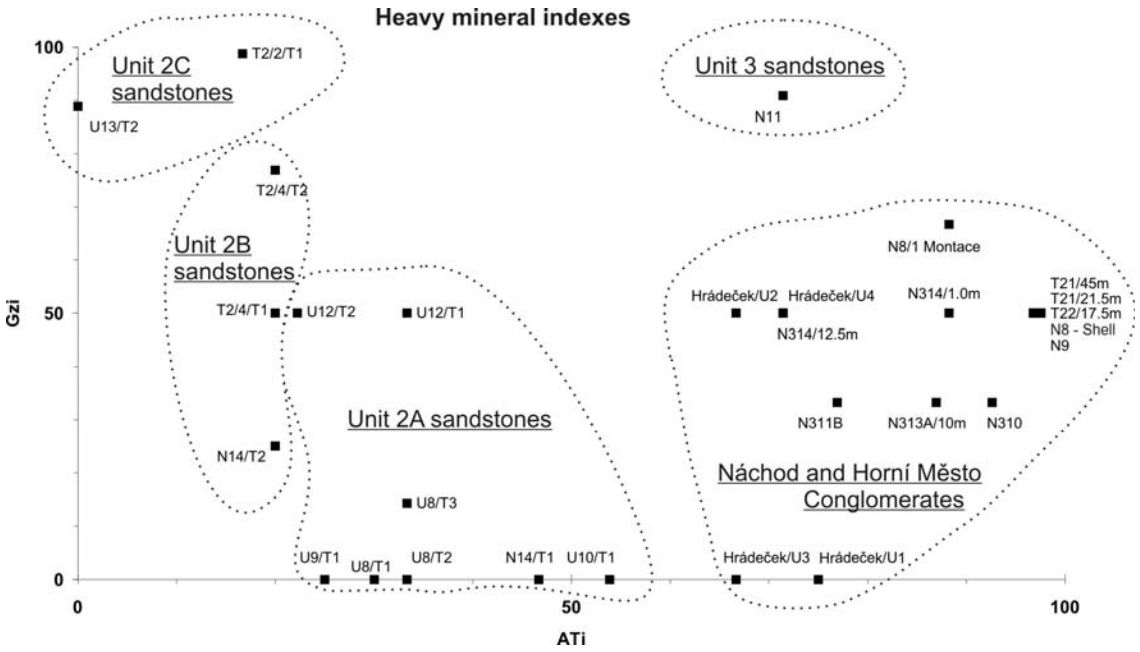

Figure 11. Heavy mineral indexes (after Morton and Hallsworth, 1999) show a very similar composition of conglomerates from north (H. Město Cgl) and south (Náchod Cgl.) and the distinct composition of different stratigraphical units (Unit 1C, 2a, 2b, 3).

Architecture variability within Unit 2 sandstones

The comparison of the lateral and vertical distribution of sedimentary facies and geometries reveals differences between Units 2B and 2C cropping out mainly in the Trutnov area, situated near the northern basin margin (sections T21, T2/2, T2/4, U13, see Fig. 1), and Unit 2A cropping out mainly in the Úpice area (sections U12b, U8 and N14), situated in the east-central part of the basin. Generally units 2B and 2C are characterized by thinner stratal units, a higher proportion of coarse-grained material, abundant calcretes and pronounced erosional features (e.g., Fig. 7). Most of the sandstones in the Trutnov area (Units 2B and 2C) are moderately cemented by calcite and dolomite. On the other hand, the deposits of the Úpice area (Unit 2A) show thicker stratal units, paucity of coarse-grained material, a low proportion of calcretes/dolocretes and low carbonate cementation for most of the sandstone bodies.

In outcrop sections, differences between the facies and architectural elements of the Havlovice and Suchovršice Members seem very small and both stratigraphic units seem to represent a single fluvial system evolving through time. It agrees with the correlation of the Suchovršice section (U13, type locality of Suchovršice Member), with the Starý Rokytník sections, representing the upper part of the Havlovice Member (Unit 2C, Fig. 12).

Palaeogeography

Pebbles of micritic carbonates, found locally in the channel sandstones, may be derived from lacustrine horizons of Stephanian and Autunian age, outcropping today in the central and western part of the Krkonoše Piedmont Basin. The same provenance is suggested by Fe-oxide pseudomorphs after pyrite in sandstones (Prouza and Tásler, 2001). Black shales containing pyrite are also typical representatives of the Stphanian and Autunian. Together with the generally east to north-east orientation of palaeocurrent measurements, this suggests a source area formed by an uplifted older part of the Krkonoše Piedmont Basin, to the west of the Trutnov Náchod Basin. Deformation and uplift of the Carboniferous – Autunian basin fill during the formation of the pull-apart Trutnov Náchod Basin is hypothesized by Uličný et al. (2002). The palaeocurrent measurements are in accordance with the suggestion of Prouza and Tásler (2001) that the depositional system of the Trutnov Formation communicated with the Intra-Sudetic Basin to the east of the Trutnov Náchod Basin.

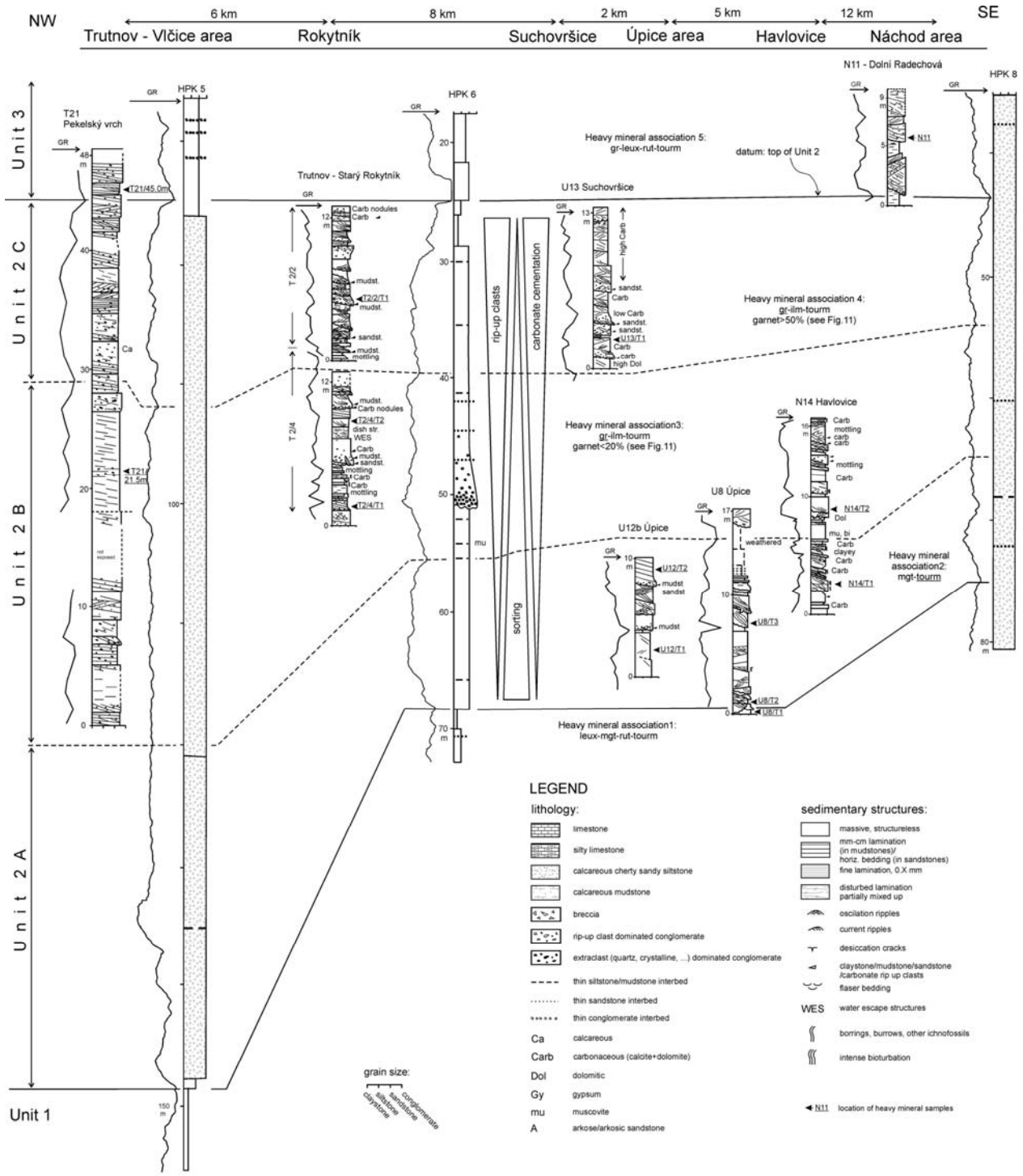

Figure 12. Stratigraphic chart integrating a correlation of outcrops and well logs based on the heavy mineral assemblages and gamma-ray logging. Arrows points to a location of heavy mineral samples (underlined, see Fig.10). For explanation see text.

Conglomerates

The Horní Město Conglomerates crops out as a narrow (ca 1 km wide) east-west oriented fringe along the northern limit of the preserved basin fill (Prouza and Tásler 2001). The syndepositional, faulted basin margin is not preserved, but it could have been a few km northward. The conglomerate thickness is 50 - 100 m and palaeocurrent indicators show prevailing south and south-east directions. The Horní Město Conglomerates are interpreted as a distal part of the alluvial fan fringe with dominance of fluvial processes. Interfingering of conglomerate/mudstone/sandstone facies occurs several km from the basin margin (Trutnov-Poříčí, Fig. 5b).

The much thicker Náchod Conglomerates probably record a high subsidence rate at the southern part of the basin. Paleocurrent data point to NNE. While outcrop and borehole data are not satisfactory, the general shape of the conglomerate body in map view is a relatively narrow fan prolonged to the north (Prouza et al., unpublished maps). The Náchod Conglomerates show the dominance of fluvial processes indicated by imbrication, cross-bedding, bar and bedform architectural elements. Conglomerate/ mudstone/ sandstone facies interfingering occurs several km from the basin margin (section N11, Figs. 5 and 12).

Inferred controls: interplay between tectonics and climate

Relatively low degree of preservation and data density (8 well logs and several outcrops on the 300 km^2 of the Trutnov Fm.) do not allow to formulate interpretations in straightforward manner. Arguments and conclusions below in this section should be considered rather as inferences and estimates based on conceptual reasoning on outcrop and well log data.

7.1. Events

The unconformity at the base of Unit 2 is a basin-wide correlative surface, which marks an important palaeogeographic change (Fig. 3). The surface is erosional, defined by the base of fluvial channels in the basin centre (HPK-6, Ma-3), base of the alluvial/fluvial conglomerates on the north (HPK-5) and increase of sandstone/mudstone ratio within Náchod Conglomerates in the south (HPK-8). This surface is a candidate for major fluvial sequence boundary sensu Martinsen et al. (1999) or Scherer et al. (2007).

Within the Unit 2 superimposed subunits 2A, 2B and 2C was recognized. They have a distinct muddying-up trend and sharp sand-rich base. These 10 – 15 m thick cycles were observed also in outcrops, they are represented by fluvial cycle: incision of medium to coarse-grained sandstone channel fill at the base which gradually pass to fine to medium-grained channel fill overlained by overbank muddy sandstones and muds (see e.g. sections U8, U13, upper part of N14 on Fig. 12). Similar depositional cycles could also be seen in well logs within Units 1B and 1C (HPK6, HPK8).

7.2. Controls

The Trutnov Formation accumulated in isolation from any marine influences within the limits of the preserved Trutnov Náchod Basin (Prouza and Tásler, 2001; cf. Ziegler, 1990), and therefore eustacy can be ruled out as an external control on accommodation and stratigraphic patterns. This leaves the discussion open for climate change versus regional and local tectonics in source areas and within the basin as possible allocyclic controls on the A/S ratio (sensu Martinsen et al., 1999) dynamics and resulting sedimentation patterns.

Presevation of the Upper Rotliegend deposits in TNSB (Trutnov Formation) and also in Intra-Sudetic and Orlice basins – east and southeast of the TNSB – could be due to reactivation of the main fault zones in the northern Bohemian Massif. High tectonic activity accompanied by basin subsidence and the rejuvenation of source areas in the late Rotliegend is reported e.g. from Elbe Zone, Saar Nahe Basin and northern Germany (Mattern, 2001, 1996; Ziegler, 1989; Henk, 1993). Major shearing on Danube and Blanice-Rödl fault zones in the southern Bohemian Massif was dated by the Ar-Ar method to 281-288 Ma (Brandmayr et al., 1995), which corresponds to the Lower/Upper Rotliegend (Sakmarian/Artinskian) boundary.

Units 1A – 1C record fine-grained playa sedimentation in the northern part of the basin (see HPK5 on Fig. 3). Abundant carbonate and gypsum interbeds point to a hydrologically closed basin with a negative annual water balance (e.g. Rosen, 1994), which is interpreted as being deposited in arid to semiarid conditions. Topographically the playa system represents the lowest part of the basin. The higher rate of accommodation (subsidence) creation in the south, inferred from the higher thicknesses of Units 1A - 1C in well-log HPK8, was probably balanced by a high rate of sediment supply from the nearby Orlice-Sneznik Crystalline Complex. In addition, Unit 1B is characterized here by lower A/S ratio compared to Units 1A and 1C. The boundary between units 1B and 1C represents an expansion surface/zone sensu Martinsen et al. (1999), which is characterized by a transition from low to high A/S ratios.

7.2.1. Unit 2

The regional basin-wide unconformity below Unit 2 records negative accommodation. To allow for subsequent accumulation the stratigraphic base level must have risen and the A/S ratio increased. The extremely sandy nature of Unit 2 suggests that the addition of new space was very slow. The nature of unconformity is unfortunately not known in detail, from a few boreholes very distant each other the amplitude of erosion can not be estimated. However it is very probable that the unconformity does not represent the base of an incised valley; a sharp surface with the abrupt onset of coarse clastic deposition is assumed, which favours an increase in sediment supply rather than a decrease in accommodation. The 1st proposed scenario explaining the unconformity emphasizes the climatic effect. It suggests that in the case of constant accommodation (i.e. no changes in subsidence, tectonics, which are more likely than uplift of the basin), the base of Unit 2 would represent a significant increase in sediment supply, interpreted here as a shift to more humid conditions (Leeder et al., 1998). The 2nd scenario stresses tectonic forces, assuming climate constant, and explains the unconformity by either an increase in sediment supply caused by an uplift of the source area or changes in the source area's drainage system (hypothesized by Bridge, 2003, Fig. 9.19).

The response of the alluvial basin to tectonism in arid/semiarid systems could be as follows: during periods of active tectonic subsidence small fans produce a narrow fringe along marginal faults and most of the basin is occupied by lake and fine-grained fluvial deposits. Drainage-basin erosion and fan sedimentation surpass the rate of tectonic subsidence during later periods of relative tectonic quiescence, resulting in fan progradation further to the basin (Blair, 1987; Blair and Bilodeau, 1998; Gawthorpe and Leeder, 2000). The main stage of tectonic subsidence is supposed at the base of Trutnov Fm. (below Unit 1A, unfortunately not captured by any subsurface or outcrop data). The absence of alluvial fan facies in Units1A – 1C of HPK5 can be explained by the location of a borehole of more than 5 km distant from the northern basin margin, where a narrow alluvial fan fringe probably occurred. The abrupt onset of Unit 2 conglomerates on the playa mudstones of Unit 1C in the north could have been amplified by a climatic change from arid to more humid conditions in the source area causing an increase in sediment supply (Blair, 1987). This interpretation is supported by the arid/semiarid conditions of Units 1A – 1C, a perennial character (more humid) of the lower part of Unit 2 and the ephemeral fluvial nature (back to arid/semiarid) of the top of Unit 2 (see discussion below).

Sandstone sorting, the occurrence of interchannel fine sediments, channel preservation and thickness all decrease upwards within Unit 2. These phenomena point to a (further) decrease of the A/S ratio. Other features, such as an upwards increase of carbonate cementation, erosional features and grain size are interpreted as probable climate change from semiarid – semihumid to more arid conditions. The lower part of Unit 2 is characterized by moderately sorted medium grained sandstones forming thick channels, with low variation in grain size and sorting, which is interpreted as the products of perennial streams with steady flow. The upper part of Unit 2, in contrast, shows a moderate to poor sorting, medium to coarse grain size, common carbonate cementation, shallow channels with abundant erosional features, large mudstone and sandstones rip-up clasts and high variation in grain size, which are interpreted as products of ephemeral streams with unsteady flow and high variation in discharge (see eg. Starý Rokytník, Figs. 7, 8). In the semiarid environment, with little or no vegetation and increasing aridity, a decrease in sediment supply is assumed. During the suggested overall decreasing A/S ratio, accommodation must have been decreasing more rapidly, resulting in practically no subsidence and most of the sediments bypassing the basin. The general thinning of Unit 2 from north to south is explained by the cessation of activity on the southern fault(s).

7.2.2. Subunits 2A, B and C

The muddying-up subunits 2A, 2B and 2C are interpreted as a drop of the A/S ratio at the base and a subsequent gradual increase upwards in the A/S ratio. Similar 10-15 metres thick depositional cycles could also be seen within Units 1B and 1C (HPK6, HPK8). These cycles show consistent fluctuations of GR and RES through different facies, which clearly point to the allocyclic character of such cyclicity. They could be caused either by climatically driven changes in sediment supply or tectonically driven changes in accommodation.

At a lower temporal and spatial scale, the Unit 2A/2B and Unit 2B/2C boundaries are also considered as basin-wide unconformities. They are also manifested (in outcrop-scale) as erosional surfaces, the recognition of different source areas characterized by a different HMA as well as the correlation in the well-log data across the basin is evidence for the basin-wide nature of these surfaces. The three subunits may represent fluvial systems with different source areas, and the boundary between them might represent a cryptic sequence boundary sensu Miall & Arush (2001). Different source areas most likely point to the tectonic reconfiguration of the surrounded source areas. The shift of climatic conditions to more arid during the deposition of Unit 2 is a continuous background process, while 3 fining-up/muddying-up subunits with different heavy mineral associations are interpreted as a record of tectonically triggered changes in the source areas. Pulses of tectonic uplift in source areas could explain the fining-up nature of the subunits.

The character of Unit 2/3 and subunits 2A/2B boundaries differ from other unit boundaries. It is characterized by a short-term variation (increase) of the mud/sand ratio, recording significant increase of A/S, possibly due to variation in sediment supply, interpreted here as climatic variation (dry episode).

The main changes in basin fill architecture are interpreted as major tectonic events. The onset of the Trutnov Formation deposition is interpreted as a major tectonic reactivation at the Autunian/Saxonian (Lower/Upper Rotliegend, ca. Sakmarian/Artinskian) boundary, when the extensional regime changed to a strike-slip regime accompanied by a transpressional uplift of the central part of the KPB (Fig. 13 A, C, D). The unconformity between Units 1 and 2 and the onset of high sandy sedimentation at the central part of the basin is interpreted as the later progradation of the coarse-grained material during the period of mostly inactive faults. The deposition of low-sinuosity sandstone dominated fluvial sediments over the mudstone dominated playa deposits must have been caused by a steepening of depositional gradient and was probably accompanied by a change in climate to more humid conditions (Fig. 13 B), which can most easily explain the increase in sediment supply to the basin.

7.3. Kinematic hypothesis

Deposition in the Trutnov Náchod Basin was governed by two major dextral strike-slip faults (Hronov-Poříčí FZ and Pilníkov FZ), which formed releasing the stepover pull-apart basin (sensu Dooley and McClay, 1997; see Figs. 13 C and D). The Trutnov Fm. has two main depocentres: the northern one in the Trutnov-Úpice area (up to 400 m thick), and a southern depocenter in the Náchod area (up to 600 m thick). The lower thickness (less than 300 m) in the central part of the basin in the Červený Kostelec area points to lower subsidence in this part of the basin (Prouza and Tásler, 2001; Fig. 3). Such basin fill geometry corresponds to the stepover pull-apart basin model of Rodgers (1980) and Dooley and McClay (1997), which demonstrated the splitting of a depocenter and the migration of two depocenters from the basin centre in later stages of the pull-apart development, where there is high overstep on major boundary strike-slip faults.

Present-day geometry of the main faults is affected by further postpermian dextral shearing between Elbe and Intra-Sudetic fault zones in Mesozoic and north-south compression in Cenozoic (Voigt, 1997; Uličný, 2001; Uličný et al., 2002) causing further clockwise rotation.

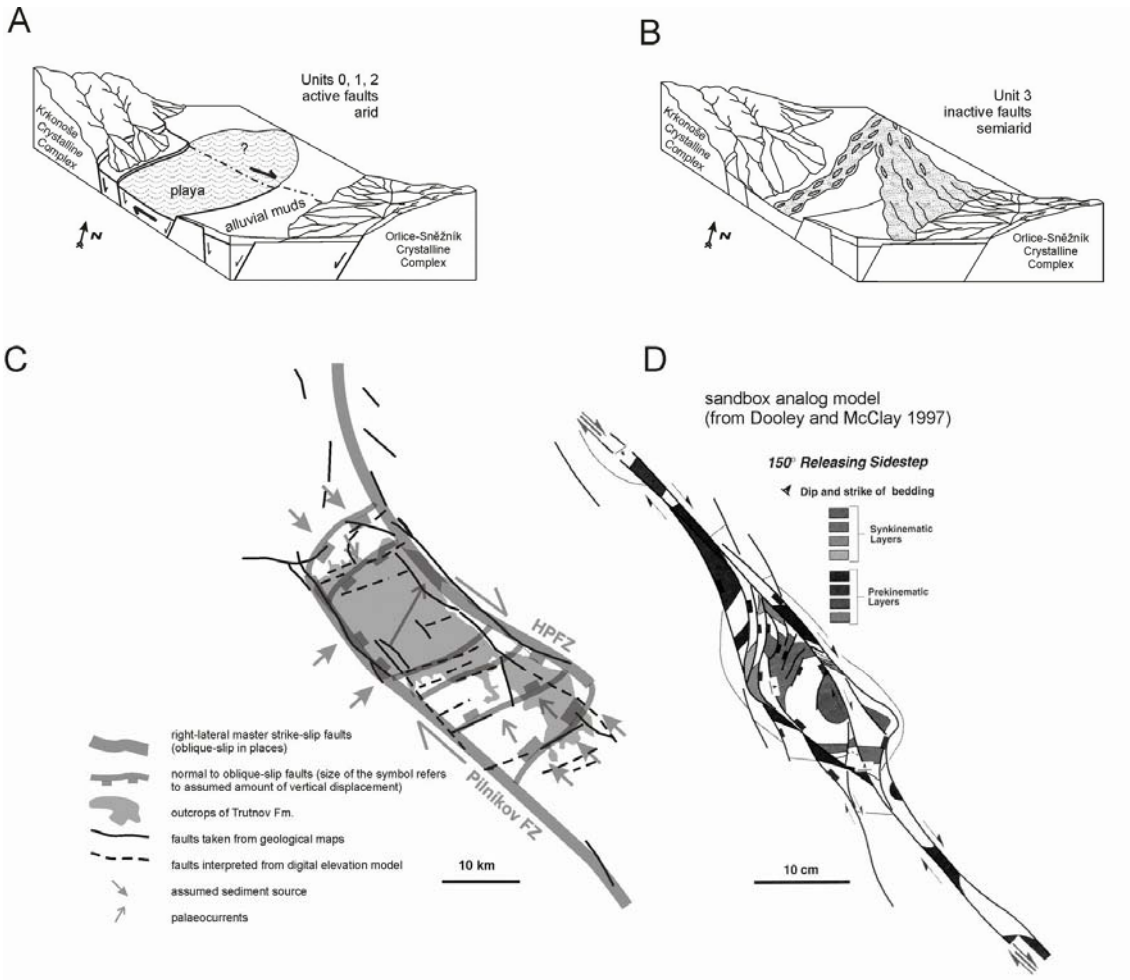

Figure 13. (A) A tectonosedimentary sketch of the TNSB illustrating active faulting forming a narrow alluvial fan fringe along the marginal fault in the north in an arid setting and (B) the progradation of aluvial conglomerates and fluvial sandstones during later stages of mostly inactive faults and more humid conditions. (C) A kinematic model of the TNSB as a pull-apart basin governed by NW striking dextral right stepping Hronov-Poříčí and Pilníkov fault zones. (D) The results of the sand box model for comparison; Releasing sidestep with initial overlap of driving faults. From Dooley and McClay (1997).

8. Conclusions

1. The depositional environment of the Trutnov Formation conglomerates is interpreted as a distal alluvial fan dominated by fluvial processes.

2. The Trutnov Formation sandstones are interpreted as a low-sinuosity fluvial system, with the following main characteristics: high variations in discharge and the preservation of unstable rock fragments, the abundance of calcretes / dolocretes suggest seasonal to ephemeral flow and arid to semi-arid climatic conditions. The induration of palaeosurfaces by calcretes / dolocretes locally influenced the channel geometry by limiting the lateral and vertical extent of channel incision.

3. Scattered outcrops were correlated with each other and with well logs using the heavy mineral analysis and outcrop gamma-ray logging. Five main genetic stratigraphic units were distinguished (Unit 1A – Unit 3).

4. Units 0, 1 and 2 are characterized by the deposition of playa facies in the north, alluvial mudstones/siltstones in the basin centre and alluvial conglomerates in the south. Unit 3 is formed by alluvial conglomerates in the north and south, respectively, and fluvial sandstone facies in the basin centre. Subunits 3A, 3B and 3C, distinguished within unit 3, represent fining-up/muddying-up cycles. The Unit 1/2, 2A/2B and 2B/2C boundaries are manifested in the outcrop-scale as erosional surfaces. The recognition of different source areas for the units and subunits, as well as the correlation in the well-log data across the basin, is evidence for the basin-wide nature of these surfaces.

5. The higher rate of accommodation creation in the south is inferred from the higher thicknesses of Units 0 – 2. The regional basin-wide unconformity below Unit 3 records negative accommodation. To allow for subsequent accumulation, stratigraphic base level must have risen and the A/S ratio increased during the deposition of Unit 3. Sorting, the occurrence of interchannel fine sediments, channel preservation and thickness decrease upwards within Unit 3, point to further a decrease of the A/S ratio. Other features, such as the upwards increase of carbonate

cementation, erosional features and grain size within unit 3, are interpreted as climate change from semiarid – semihumid to more arid conditions.

6. The abrupt onset of Unit 2 conglomerates on playa mudstones of Unit 1C in the north can be amplified by climatic change from arid to more humid conditions in the source area causing an increase in sediment supply. This interpretation is supported by the arid/semiarid conditions of Units 1A – 1C, the perennial character (more humid) of the lower part of Unit 2 and the ephemeral character of the fluvial system (back to arid/semiarid) at the top of Unit 2.

7. The main changes in basin fill architecture are interpreted as major tectonic events. The onset of the Trutnov Formation deposition is interpreted as a major tectonic reactivation at the Autunian/Saxonian (Lower/Upper Rotliegend, ca. Sakmarian/Artinskian) boundary, when the extensional regime changed to a strike-slip regime accompanied by a transpressional uplift of the central part of the KPB. The unconformity between Units 2 and 3 and the onset of high sandy sedimentation at the central part of the basin is interpreted as the later progradation of the coarse-grained material during the period of mostly inactive faults. The deposition of low-sinuosity sandstone dominated fluvial sediments over the mudstone dominated playa deposits must have been caused by a steepening of the depositional gradient and was probably accompanied by a change of climate to more humid conditions, which can most easily explain the increase in sediment supply to the basin.

8. The TNSB is interpreted as a pull-apart basin, the deposition of which was governed by two major dextral strike-slip faults (Hronov-Poříčí FZ and Pilníkov FZ) forming a releasing stepover.

Acknowledgements

This study represents a part of the PhD research by K. Martínek, financially supported by the Grant Agency of the Czech Republic, Grant No. 205/99/0739 to D. Uličný. The authors would like to thank Vladimír Prouza of the Czech Geological Survey, Prague, for his advice and sharing his experience from research in the Krkonoše Piedmont Basin. Lenka Špičáková provided her unpublished field documentation from the Starý Rokytník quarry. We are grateful to Zdeněk Táborský and František Veselovský, Czech Geological Survey, for heavy mineral separation and determination. We also thank the company Správa a údržba silnic, Trutnov, for permission to conduct research on their property. We also wish to thank to Dana Čápová, Czech Geological Survey – Geofond, for kind permission to use well-log data. Many thanks to Richard Withers for the English review.

References

Alexander, J., Leeder M.R., 1987. Active tectonic control on alluvial architecture. In: Ethridge, F.G., Flores, R.M. Harvey, M.D. (Eds), Recent Developments in Fluvial Sedimentology. SEPM Spec. Publ. vol. 39, pp. 243-252.

Aleksandrowski, P., Kryza, R., Mazur, S., and Źaba, J. (1997). Kinematic data on major Variscan strike-slip faults and shear zones in the Polish Sudetes, northeast Bohemian Massif: Geological Magazine, v. 134, p. 727-739.

Allen, P.A., Hovius N., 1998. Sediment supply from landslide-dominated catchments: implications for basin-margin fans. Basin Research, 10 (1), 19-35.

Allen, J.R.L., Banks, N.L., 1972. An interpretation and analysis of recumbent-folded deformed cross-bedding. Sedimentology 19, 257-283.

Blair, T.C., 1987. Tectonic and hydrologic controls on cyclic alluvial fan, fluvial, and lacustrine rift-basin sedimentation, Jurrasic-lowermost Cretaceous Todos Santos Formation, Chiapas, Mexico. J. Sedim. Petrol. 57, pp. 845-862.

Blair, T.C., 1999. Sedimentary processes and facies of the waterlaid Anvil Spring Canyon alluvial fan, Death Valley, California. Sedimentology 46 (5), 913-940.

Blair T.C.and Bilodeau, 1998. Development of tectonic cyclothems in rift, pull-apart, and foreland basins: Sedimentary response to episodic tectonism. Geology 16, 517-520.

Blum, M.D. and Törnquist, T.E. 2000. Fluvial responses to climate and sealevel change: A review and a look forward. Sedimentology, v. 47, p. 2–48.

Blum, M.D., Toomey, R.S., Valastro Jr, S. 1994. Fluvial response to late Quaternary climatic and environmental change, Edwards Plateau, Texas. Palaeogeography,-Palaeoclimatology,-Palaeoecology. 108(1-2), pp 1-21.

Brandmayr M., Dallmeyer R. D., Handler R. and Wallbrecher E., 1995. Conjugate shear zones in the Southern Bohemian Massif (Austria): implications for Variscan and Alpine tectonothermal activity. Tectonophysics 248, 97-116.

Bridge, J.S., 1993. Description and interpretation of fluvial deposits: a critical perspective. Sedimentology 40, 801-810.

Bridge, J.S., Mackey, S.D., 1993. A revised alluvial stratigraphy model. In: Marzo, M., Puigdefábregas, C. (Eds.), Alluvial Sedimentation, Spec. Publ. Int. Assoc. Sediment. vol. 17, pp. 319-336.

Bridge, J.S., 2003. Rivers and Floodplains. Blackwell, Oxford, pp. 1-491.

Burbank, D.W., Pinter, N., 1999. Landscape evolution: the interactions of tectonics and surface processes. Basin Research 11 (1), 1-6.

Chaloupský, J., 1989. Geologie Krkonoš a Jizerských hor. (in Czech) Academia, Praha, pp. 288.
Dooley T, McClay K, 1997. Analog modeling of pull-apart basins. AAPG Bulletin, 81 (11), 1804-1826.
Fishbaugh, D.A., Kvale, E.P. and Archer, A.W., 1989. Association of tidal and fluvial sediments within Lower Pennsylvanian rocks, Turkey Run State Park, Parke County, Indiana. A Guidebook for 1989 AAPG Eastern Section Meeting and Field Trip, pp. 1-44. Bloomington.
Gawthorpe, R.L., Leeder, M.R., 2000. Tectono-sedimentary evolution of active extensional basins. Basin Research 12 (3-4), 195-218.
Gebhardt U, Schneider J, Hoffmann N, 1991. Modelle zur Stratigraphie und Beckentwicklung im Rotliegenden der Norddeutschen Senke. Geol. Jb., A 127, 405 – 427, Hannover.
Gibling, M.R., Rust, B.R., 1990. Ribbon sandstones in the Pennsylvanian Waddens Cove Formation, Sydney Basin, Atlantic Canada: the influence of siliceous duricrusts on channel-body geometry. Sedimentology 37, 45-65.
Harwood, G., 1988. Microscopical techniques II: Principles of sedimentary petrography. In Tucker, M. (Ed.): Techniques in sedimentology. pp.108-174, Blackwell, Oxford.
Henk A, 1993. Late orogenic basin evolution in the Variscan internides – the Saar-Nahe Basin, southwest Germany. Tectonophysics, 223 (3-4), 273-290.
Hovius, N., 1998. Controls on sediment supply by large rivers. Special Publications SEPM vol. 59, pp. 3-16.
Jones S.J., Frostick L.E., Astin T.R. (2001) Braided stream and flood plain architecture: the Rio Vero Formation, Spanish Pyrenees. Sedimentary Geology 139, 229 - 260.
Katzung G., 1991. Developmental stages of Carboniferous-Permian molasses reflecting Late Hercynian evolution in northern Central Europe. Giornale di Geologia, ser. 3, vol. 53/1, 229 – 240, Bologna.
Kozur H. (1988). The Age of the Central European Rotliegendes. Z.geol.wiss., 16, 9, 907 – 915.
Kraus, M.J., 1987. Integration of Channel and Floodplain Suites, II. Vertical Relations of Alluvial Palesols. Journal of Sedimentary Petrology 57 (4), 602-612.
Leeder, M.R., Harris T., Kirkby M.J., 1998. Sediment supply and climate change: implications for basin stratigraphy. Basin Research 10 (1), 7-18.
Lucas, SG, Schneider, JW, Cassinis G, 2006. Non-marine Permian biostratigraphy and biochronology: an introduction. In: Lucas, SG, Schneider, JW, Cassinis G (eds) 2006. Non-Marine Permian Biostratigraphy and Biochronology. Geological Society, London, Special Publications, 265, 1–14.
Mange M., Turner P., Ince D., Pugh J. and Wright D. (1999) A new perspective on the zonation and correlation of barren strata: an integrated heavy mineral and paleomagnetic study of the Sherwood Sandstone Group, east Irish Sea Basin and surrounding areas. J. Petroleum Geology, 22, 3, pp. 325-348.
Martinsen, O.J., Ryseth, A., Helland-Hansen, W., Flesche, H., Torkildsen, G., Idil, S., 1999. Stratigraphic base level and fluvial architecture: Ericson Sandstone (Campanian), Rock Springs Uplift, SW Wyoming, USA. Sedimentology 46 (2), 235-259.
Mastalerz K., 1990. Lacustrine successions in fault-bounded basins: 1. Upper Antracosia Shale (Lower Permian) of the North Sudetic Basin, SW Poland. Annales Societatis Geologorum Poloniae, 60, 75 – 106.
Mattern F, 2001. Permo-Silesian movements between Baltica and Western Europe: tectonics and 'basin families' . Terra Nova 13 (5), 368-375.
Mattern F, 1996. The Elbe zone at Dresden – a Late Paleozoic pull-apart intruded shear zone. Z. dt. geol. Ges 147/1, 57 – 80, Stuttgart.
McCann, T., 1998. Sandstone composition and provenance of the Rotliegend of the NE German Basin. Sedimentary Geology 116 (3-4), 177-198.
Meyers, K. J., Bristow, C. S., 1989. Detailed sedimentology and Gamma-ray log characteristics of a Namurian deltaic successiion II: Gamma-ray logging. In: Whateley, M.K.G., Pickering, K.T. (Eds.): Deltas: sites and Traps for Fossil Fuels. Geol. Soc. Spec. Publ. No. 41, pp. 81-88.
Martínek, K., Štolfová, K., in press. Provenance study of Permian-Triassic non-marine sandstones of the Krkonoše Piedmont Basin: exotic marine limestone pebbles, heavy minerals and garnet mineralogy. Bulletin of Geosciences.
Miall, A.D., Arush, M., 2001. Cryptic sequence boundaries in braided fluvial successions. Sedimentology 48, 971-986.
Miall, A.D., 1985. Architectural-element analysis: a new method of facies analysis applied to fluvial deposits. Earth-Science Reviews 22, 261-308.
Morton A.C., Hallsworth, C.R., 1999. Processes controlling the composition of heavy mineral assemblages in sandstones. Sedimentary Geology 124 (1-4), 3-29.
Morton A., Knox R. W. O´B. and Hallsworth C. (2002) Correlation of reservoir sandstones using quantitative heavy mineral analysis. Petroleum Geoscience, 8, pp. 251-262.
Nemec, W., Steel, R.J., 1984. Alluvial and coastal conglomerates; their significant features and some comments on gravelly mass-flow deposits. In: Koster E.H., Steel R.J. (Eds.), Sedimentology of gravels and conglomerates. Memoir - Canadian Society of Petroleum Geologists, vol. 10, pp. 1-31.
Nichols, R. J., 1995. The liquification and remobilization of sandy sediments. In: Hartley, A., Prosser, D.J. (Eds.), Characterization of Deep Marine Clastic Systems , Geol. Soc. London Spec. Publ. vol. 94, pp. 63-76.

North American Commission on Stratigraphic Nomenclature, 1983. North American Stratigraphic Code. AAPG Bulletin, 67, 841-875.

Opletal, M., 1980. Geologie Orlických hor. (in Czech) Ústř. ústav geologický, Praha, pp. 202.

Preston J, Hartley A, Hole M., Buck S., Bond J., Mange M. and Still J. (1998) Integrated whole rock trace element geochemistry and heavy mineral chemistry studies: aids to the correlation of continental red-bed reservoirs in the Beryl Field, UK North Sea. Petroleum Geoscience, 4, pp. 7-16.

Prouza, V., Tásler, R., 2001. Podkrkonošská pánev. In: Pešek, J. (Ed.): Geologie a ložiska svrchnopaleozoických limnických pánví České republiky. Český geologický ústav, Praha, pp. 128-166.

Ramos, A. Sopena, A., 1983. Gravel bars in low-sinuosity streams (Permian and Triassic, central Spain). Spec. Publs. Int. Ass. Sediment. vol. 6, pp. 301-312.

Rodgers D., 1980. Analysis of pull-apart basin development produced by en-echelon strike-slip faults. In: Ballance P. F. and Reading H. G. (Eds.): Sedimentation in Oblique-slip Mobile Zones. IAS Spec. Publ. 4, pp. 27-42, Blackwell.

Rosen M. R., 1994. The importance of groundwater in playas: A review of playa classification and the sedimentology and hydrology of playas. Geological Society of America Special Paper, 289, pp 1-18.

Roscher, M, Schneider, JW, 2005. An annotaded correlation chart for continental Late Pennsylvanian and Permian Basins and the marine scale. In: Lucas SG, Ziegler KE, eds, The Nonmarine Permian, New Mexico Museum of Natural History and Science Bulletin No. 30., 282 – 290.

Roscher, M, Schneider, JW, 2006. Permo-Carboniferous climate: Early Pennsylvanian to Late Permian climate development of central Europe in a regional and global context. In: Lucas, SG, Schneider, JW, Cassinis G (eds) 2006. Non-Marine Permian Biostratigraphy and Biochronology. Geological Society, London, Special Publications, 265, 95–136.

Sánchez-Moya, Y., Sopena, A., Ramos, A., 1996. Infill architecture of a non-marine half-graben Triassic basin (central Spain). J. Sedim. Res. 66 (6), 1122-1136.

Scherer C.M.S., Lavina E.L.C., Dias Filho D.C., Oliveira F.M., Bongiolo D.E., Aguiar E.S. (2007) Stratigraphy and facies architecture of the fluvial–aeolian–lacustrine Sergi Formation (Upper Jurassic), Recôncavo Basin, Brazil. Sedimentary Geology 194, 169–193.

Schneider JW, 2001. Rotliegendstratigraphie – Prinzipen und Probleme. Beitr. Geol. Thuringen, N.F. 8, 7 – 42, Jena.

Schneider JW,, Rossler R, Gaitzsch B, 1994. Time lines of the Variscanvolcanism – a holostratigraphic synthesis. Zbl. Geol. Palaont., Teil I, H. 5/6, 477 – 490.

Schneider JW, Schretzenmayr S, Gaitzssch, 1998. Rotliegend Reservoirs at the Margin of the Southern Permian Basin. Excursion Guide. Leipziger Geowissenschaften, band 7, 15 – 44.

Shanley, K.W., McCabe, P.J., 1994. Perspectives on the sequence stratigraphy of continental strata. AAPG Bulletin 78 (4), 544-568.

Smith, A., 1990. The sedimentology and accretionary styles of an ancient gravel-bed stream: the Budleigh Salterton pebble beds (Lower Triassic), southwest England. Sedimentary Geology 67, 199-219.

Stemmerik, L., Ineson, J.R., Mitchell, J.G., 2000. Stratigraphy of the Rotliegend Group in the Danish part of the Northern Permian Basin, North Sea. Journal of the Geological Society 157, 1127-1136, Part 6.

Sweet, M.L., 1999. Interaction between aeolian, fluvial and playa environments in the Permian Upper Rotliegend Group, UK southern North Sea. Sedimentology, 46 (1), 171-187.

Talbot M.R., Holm K., Williams, M.A.J., 1994. Sedimentation in low-gradient desert margin systems: A comparison of the Late Triassic of northwest Somerset (England) and the late Quarternary of the east-central Australia. GSA Special Paper 289, pp. 97-117.

Tandon, S.K., Friend, P.F., 1989. Near-surface shrinkage and carbonate replacement processes, Arran Cornstone Formation, Scotland. Sedimentology 36, 1113-1126.

Uličný , D. 2001. Depositional systems and sequence stratigraphy of coarse-grained deltas in a shallow-marine, strike-slip setting: the Bohemian Cretaceous Basin, Czech Republic. Sedimentology 48, 599-628.

Uličný, D., Martínek, K., Grygar, R., 2002. Syndepositional Geometry and Post-Depositional Deformation of the Krkonoše Piedmont Basin: A Preliminary Model. Proceedings of the 7th Meeting of the Czech Tectonic Studies Group, Zelazno, Poland, May 9-12, 2002, Geolines 14, 101-102.

Voigt T, 1997. Evidences for Late Mesozoic-Cenozoic strike-slip faults in the Elbezone (Germany). Freiberger Forschungsheft, C468, 279-287. (in German)

Wojewoda J., Mastalerz K., 1989. Ewolucija klimatu oraz allocyklicnosc i autocyklicznosc sedymentacji na przykladzie osadow kontynentalnych gornego karbonu i permu w Sudetach. Przeglad Geologyczny, 4, 432, 173 – 180.

Wright, V.P., Platt, N.H., Wimbledon, W.A., 1988. Biogenic laminar calcretes: evidence of root-mat horizons in palaeosols. Sedimentology 35, 603-620.

Ziegler, M. A., 1989. North German Zechstein facies patterns in relation to their substrate. Geologische Rundschau 78 (1), 105-127.

Ziegler, P. A., 1990. Geological Atlas of Western and Central Europe Shell International Petroleum Maatschappij, The Hague.

Chapter 3

Provenance study of Permian non-marine sandstones of the Krkonoše Piedmont Basin: exotic marine limestone pebbles, heavy minerals and garnet composition

[1]Karel Martínek and [2]Kateřina Štolfová

1) Institute of Geology and Palaeontology, Charles University, Albertov 6, 128 43 Prague 2, Czech Republic, karel@natur.cuni.cz
2) School of Geological Sciences, University College Dublin, Belfield, Dublin 4, Ireland

Bulletin of Geosciences, in press

Motto:
If you want to learn about nature, to appreciate nature, it is necessary to understand the language that she speaks in.

Richard P. Feynman

Abstract

This study focuses on identifying major source areas in several intervals mainly in the Permian of the Krkonoše Piedmont Basin and integrates it with existing sedimentological data. Pebbles in Asselian – Guadalupian conglomerates of alluvial fan, nearshore lacustrine and lacustrine fan-delta deposits, which were deposited close to the northwestern and southeastern basin margin, respectively, correspond almost exclusively to local material from adjacent crystalline complexes.The heavy mineral associations of the sandstone matrix of these conglomerates support this interpretation. Crystalline units of the south-western part of the Krkonoše-Jizera Crystalline Complex and Orlice-Sněžník Crystalline Complex, respectively, are considered as the most favourable source.

Two main possible source areas for the fluvial Asselian deposits (Vrchlabí Formation) of the south-western part of the basin were found. Pebbles of late Devonian – early Carboniferous marine limestones probably come from the central part of the hypothetical Jítrava Hradec Basin. The garnet composition in sand detrital material points to leucogranites and pegmatites of the north-eastern Moldanubian Zone, the Přibyslavice area, as the possible source areas.

Guadalupian fluvial deposits reveal a wide range of sources, which can be attributed to the recycling of detrital material from Cisuralian and Carboniferous deposits. Garnet compositions indicate Moldanubian granulites, garnet clinopyroxenites, leucogranites and pegmatites as a possible source. We infer that Moldanubian granulites and garnet clinopyroxenites were exposed to an erosion level in the Early Permian at the latest.

Keywords: provenance, Krkonoše Piedmont Basin, Permian, Triassic, heavy minerals, pebble composition, detrital garnet composition

Introduction

Conglomerate pebble composition can be a good indicator of adjacent source areas in basin studies, but it usually does not provide information on more distant sources of detrital material. A heavy mineral association (HMA) from sandstones and a sandstone conglomerate matrix can indicate more distant sources. In areas with complex source rock lithologies (igneous, low-grade, medium-grade metamorphics, volcanics), the HMA can often contain mixed provenance information, which is not easy to interpret. An effective method for discriminating the specific source areas could be integrating palaeocurrent data with a detailed mineral chemistry determination using an electron microprobe (e.g. Morton 1985, Owen 1987, Morton 1991). Garnets with a potentially wide range in composition show significant differences in composition among different types of garnet-bearing lithologies (Čopjaková et al. 2005). Another advantage of garnet for provenance studies is its relative stability during diagenesis (Morton & Hallsworth 1999).

The aims of this study include determining the source areas of the Vrchlabí and Trutnov formations based on pebble composition, heavy mineral assemblages, and detrital garnet composition. Additionally, previously acquired palaeocurrent data obtained by conventional sedimentological methods are integrated. The composition of detrital garnets from fluvial Early Triassic deposits of Bohdašín Formation is also discussed.

Geological setting

The Krkonoše Piedmont Basin formed as part of a system of extensional / transtensional, intermontane basins during the post-Variscan period (Asturian – Triassic, Fig. 1). There has been systematic geological research of the Late Carboniferous – Triassic basin fill during the last several decades. This research was mainly based on geological mapping and several structural boreholes were also made. The lithostratigraphic concept of the basin was established by Tásler et al. (1981), Tásler & Prouza (1985 unpublished report), and a summary of this research was presented by Prouza & Tásler (2001). The provenance of selected sedimentary units was determined by Prouza & Tásler (2001) based mainly on the pebble composition of conglomerates. They suggest sources of clastic material of 1) Stará Paka Sandstone (Vrchlabí Formation) eroded from the underlying Semily Formation (the presence of cherts and tuffs of Ploužnice Horizon), 2) Horní Město Member (Trutnov Formation) transported from the north (the pebbles composed almost entirely of Krkonoše-Jizera Crystalline Complex rocks – crystalline limestone (dominant, up to 90%), quartzite, lydite, gneiss, micashist, granitoid; Upper Palaeozoic volcanites and sediments are rare), 3) Náchod Conglomerates (Trutnov Formation) transported from the south (based on the presence of pebbles of Orlice-

Sněžník Crystalline Complex – phyllite, granite, granite porphyry, crystalline limestone, quartzite). Pebble composition provides basic information on the provenance of local, coarse-grained, shortly transported material and did not allow distant source areas to be determined. Novák et al (1983, unpublished report) analysed heavy minerals of the Vrchlabí Formation from borehole ZŽ-1, they found a poor and not very variable association with a predominance of zircon, tourmaline, monazite with sporadic occurence of magnetite, apatie, garnets and Cr spinel, assuming low grade metamorphic and acid igneous source rocks. Sedimentological research has been conducted recently (Blecha et al. 1999, Martínek et al. 2006, Uličný & Martínek 2002 unpublished report), but palaeocurrent analysis give just limited information on provenance because of the limited amount of suitable outcrops and the difficulties in correlating important outcrops. Basin-wide unconformities (Fig. 2) and changes in the thicknesses of sedimentary units indicate substantial shifting of depocentres at the Stephanian B/C and Cisuralian/Guadalupian boundaries, which led to changes in basin configuration. At the Stephanian B/C boundary the depocentres are shifting from the south to the north, which was noted e.g. by Pešek (1994, 2005) as a common feature in Central and Western Bohemian basins, and interpreted as a switching of the major displacement from southern to northern marginal faults still in an extensional half-graben setting (Martínek et al. 2006, Uličný et al. 2002). At the Cisuralian/Guadalupian (Lower/Upper Rotliegend) boundary a major tectonic rearrangement of the basin, probably from an extensional to a strike-slip regime, occurred (Uličný et al. 2002).

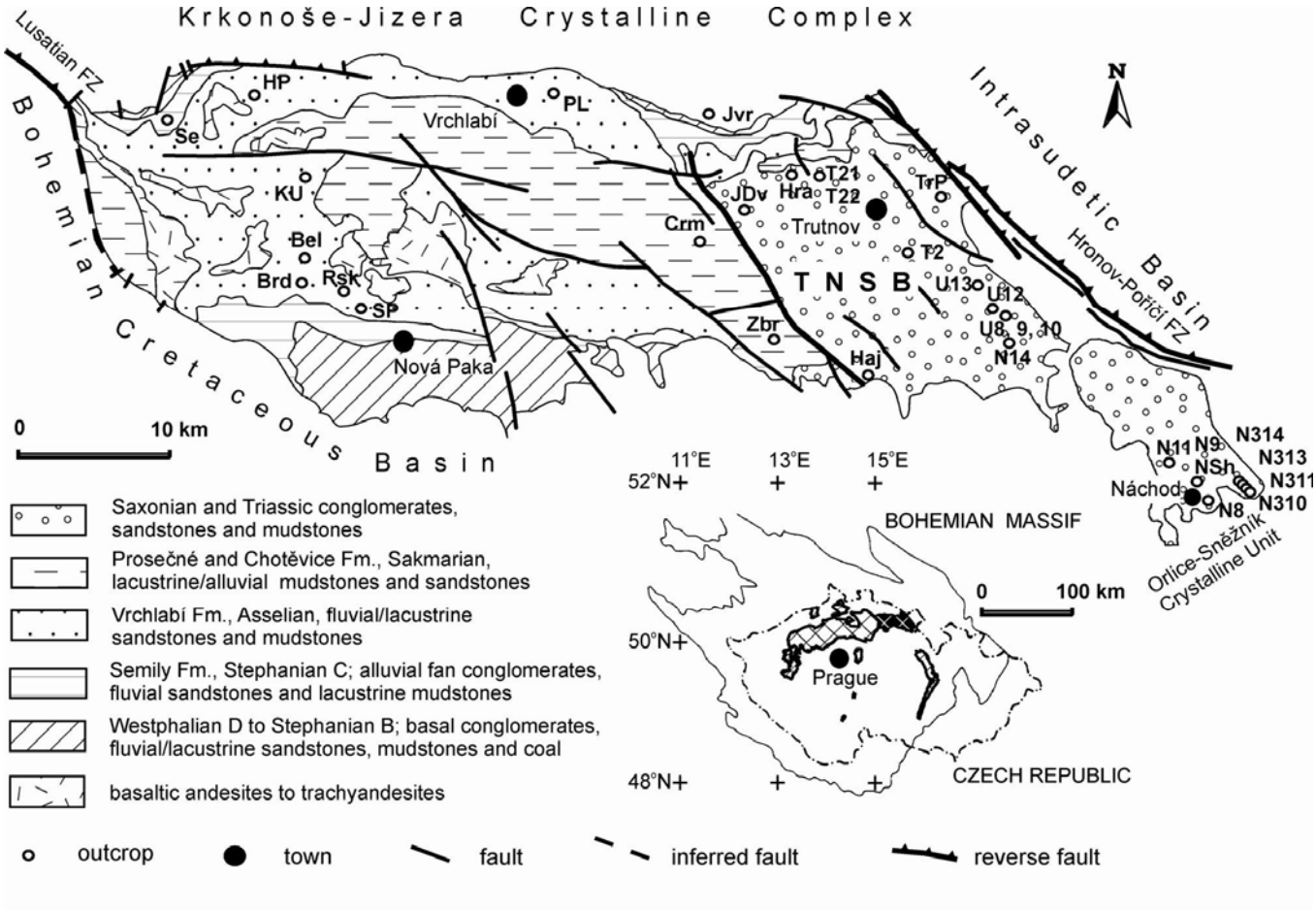

Figure 1. Simplified geological map of the Krkonoše Piedmont Basin (KPB) with sample locations. Inset map: outline of non-marine Permo-Carboniferous basins (hash) and KPB (black hash). Outcrop samples: Boz – Bozkov, HP – Honkův potok, Se – Semily, KU – Kundratice, Bel – Bělá, Brd – Brodky, Rsk – Roškopov, SP – Stará Paka Railway Station, Plz – Ploužnice, NP – Zlámaniny near Nová Paka, VrF – Vrchlabí - phyllites, VrS – Vrchlabí – Semily Formation, PL – Prostřední Lánov, Crm – Čermná, Zvc – Zvičina, Zbr – Záboří, Jvr – Javorník, Mrs – Maršov, Žac – Žacléř, JDv – Janský Dvůr, Hra – Hrádeček, T21 and T22 – Pekelský vrch, TrP – Trutnov Poříčí, Žlt –Žaltman, T2 – Trutnov – Starý Rokytník, U13 – Suchovršice, U8, 9, 10, 12 – Úpice, N14 – Havlovice, Haj – Hajnice, N11 – Dolní Radechová, N9, NSh, N8 – Náchod, N310, N311, N313, N314 – Náchod Běloves, Pkl – Peklo.

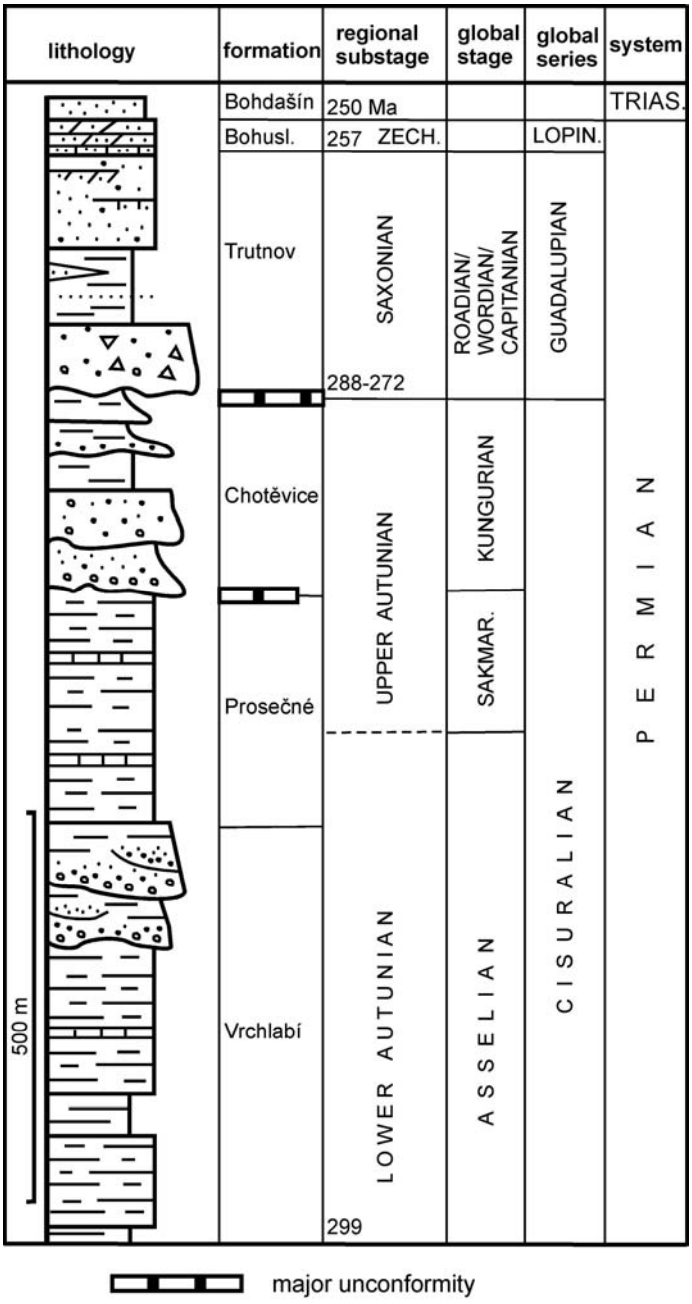

Palaeocurrent analysis of the fluvial sandstones of the Vrchlabí Formation (Asselian) at the south-western part of the basin (Stará Paka and surroundings) reveals dominant NNE trending palaeocurrent vectors (Štolfová 2004). Fluvial sandstones of the Trutnov Formation (Guadalupian), deposited after major unconformity in the eastern part of the basin, show a low spread of palaeocurrent vectors trending to the north and northeast (Martínek 2003). Very similar north-eastern trends of fluvial sandstones of the Trutnov Formation were observed in the adjoining south-western part of the Intrasudetic Basin (Lojka 2003). This is in agreement with Prouza & Tásler (2001) who suggested a single depositional area covering the eastern part of the Krkonoše Piedmont Basin (Trutnov Náchod Subbasin) and Intrasudetic Basin during the Guadalupian.

Figure 2. Stratigraphical chart of the Krkonoše Piedmont Basin based on the borehole Pé-1 in the centre of the basin (Asturian – Autunian) and on the compiled stratigraphy of the Trutnov Náchod Subbasin (Saxonian – Triassic, Prouza & Tásler 2001). Time values in Ma from Haq (2007).

Methods

The individual methods used in provenance studies have different significance and are influenced by a number of factors that complicate the recognition of provenance. Therefore a complex approach included integrating the modal composition of sandstones and the typology of quartz grains of sandstones (23 samples from Vrchlabí Formation, 42 samples from Trutnov Formation), pebble composition data (15 beds of 5 outcrops from the Vrchlabí Formation, 9 beds of 8 outcrops from the Trutnov Formation were inspected), heavy mineral analysis (67 samples), and garnet composition (5 rock samples, which correspond to 43 grains and 150 spot analyses).

Modal composition was studied using standard petrological optical microscopy with semiquantitative estimates of each component. Pebble composition was determined at outcrops using lithology identification of all pebbles of 1 square meter of vertical outcrop section of each bed. Heavy mineral assemblages provide the main database, which was further processed to separate provenance-specific features and to eliminate other factors. The main sample set was taken from outcrops of the Vrchlabí and Trutnov formations, several samples were also taken from the surrounding units: Kumburk, Semily, Prosečné, and Bohdašín formations (Asturian – Triassic), Krkonoše-Jizera and Orlice-Sněžník crystalline complexes and from the Intrasudetic Basin (Namurian C – Asturian). Sample location is indicated in Fig. 1, their age in Table 1. Heavy mineral samples were processed by the laboratories of the Czech Geological Survey, Prague. Heavy minerals were separated from the sand fraction below 0.5 mm (70 g samples) using heavy liquids (tetrabromethane C2H2Br4, 2.95 g/cm3) from disintegrated, washed and dried sandstone samples (2 - 5 kg hand specimens). Individual minerals were determined using a standard petrologic optical microscope; X-ray diffraction and electron microprobe analyses were carried out where necessary for proper mineral identification. The chemical composition of garnet was determined by electron microanalysis. Analyses were carried out at the Laboratory of Electron Microscopy and Microanalysis (Charles University in Prague) using a CamScan S4 scanning electron microscope with an energy dispersive analytical system Oxford instruments LINK ISIS 300. The beam current was 7 nA. Accelerating voltage was 20 kV. Acquisition time was 170 seconds. The energy resolution of the EDS spectra was 72 eV. A ZAF procedure was used to quantify the spectra. Mg, Al, Si, Ca, Ti, Cr, Mn, Fe and V were analysed with following detection limits: MgO (0.21 wt %), Al2O3 (0.19 wt %), SiO2 (0.18 wt %), CaO (0.10 wt %), TiO2 (0.08 wt %), V2O5 (0.13 %), Cr2O3 (0.08 wt %), MnO (0.08 wt %), FeO (0.13 wt%). The SPI Supplies 53 Minerals Standard Set #02753-AB was used for routine quantitative calibration.

Results

Modal and pebble composition

We focused mainly on the pebble and modal composition of the Vrchlabí Formation fluvial deposits, where exotic limestone pebbles were found and where information on the source areas was scarce. The source areas are expected south of the basin, according to palaeocurrents (Štolfová 2004), and are mostly covered by Late Cretaceous deposits.

The provenance analysis of fluvial deposits of the Vrchlabí Formation is based on the modal composition of sandstones, the pebble composition of conglomerates and the typology of the quartz grains. Identification of rock composition is based on a hand specimen and a thin section study. Conglomerates are oligomictic to polymictic in nature with pebble and cobble sizes ranging from 0.5 to 16 cm. Pebbles of quartzite, para- and orthogneiss, lydites and acid volcanics are common. Clasts of metamorphic rocks are well rounded, generally better than the other pebbles. Sandstones are mainly composed of quartz grains (58 - 82 vol. %) with variable rounding and levels of preservation. The grains are sub-angular to sub-oval and commonly replaced by calcite cement. Quartz grains are interpreted in terms of four possible origins: plutonic, low-grade metamophic, high-grade metamorphic and volcanic (Basu et al. 1975). Plagioclase and K-feldspar usually range from 2 to 12 vol %. The individual samples show low variability. Carbonate cement and plutonic quartz are found in all samples, the original mud-rich matrix is rarely preserved. The presence of biotite, which breaks down easily due to its mechanical and chemical instability, points to a very close source area, possibly the adjacent Zvičina Crystalline Unit. Metamorphic rock fragments, mostly altered phyllites, quartzitic phyllites and quartzites, are probably derived from a Carboniferous source; they are very similar to material from the Krkonoše-Jizera and Zvičina crystalline complexes (Kachlík 2004 pers. comm.). Acid volcanic rock fragments probably have their origin in the southern part of the Krkonoše Piedmont Basin.

In the outcrops of the Stará Paka Railway Station locality, five pebbles of shallow marine limestone were found in fluvial sandstones. These pebbles occur in several beds and their size ranges from 3 to 5 cm in diameter. They contain a lot of bioclasts, both intact and fragmented, of open marine and shallow water carbonate origin. The rich faunal assemblage includes foraminifers, ostracods, brachiopods, molluscs, sponge spicules and less abundant crinoids, echinoderms and calcispheres (Fig. 3). Limestone is highly recrystallized, originally probably biomicritic. Interestingly some of the elongated bioclasts, which are interpreted as algae, are silicified and infilled by bitumen.

The preserved benthic foraminifers have a more complex test shape than those known from Early and Middle Devonian strata (Pojarkov 1969). However, the test shapes are not as complex as those typical for fusulinids of the Late Carboniferous and Permian times (Tappan & Loeblich 1988, Kalvoda 1990, Kalvoda 2002). Hence we conclude that the foraminifers probably fall within the Late Devonian (late Famennian) to Early Carboniferous (Tournaisian – Visean) age interval. Other abundant fossils such as ostracods, brachiopods, molluscs and calcispheres are difficult to identify precisely because of the diagenetic overprint of the limestones, mainly neomorphism, and are therefore poor indicators of exact limestone age. The identification of algae remnants, with solid bitumen inclusions and the occurrence of spheroidal or oval fossils, which have a thick outer wall, remain problematic. The diverse assemblage of organisms and their abundance points to a normal salinity environment. The occurrence of the benthic foraminifers and other organisms listed above suggests an open marine shelf or epicontinental sea environment in a tropical or subtropical climate.

Modal and pebble composition of other samples of the Trutnov Formation point to local crystalline rock sources, which are known from previous works (summarized in Prouza & Tásler 2001). Therefore these results are not presented and discussed in this study.

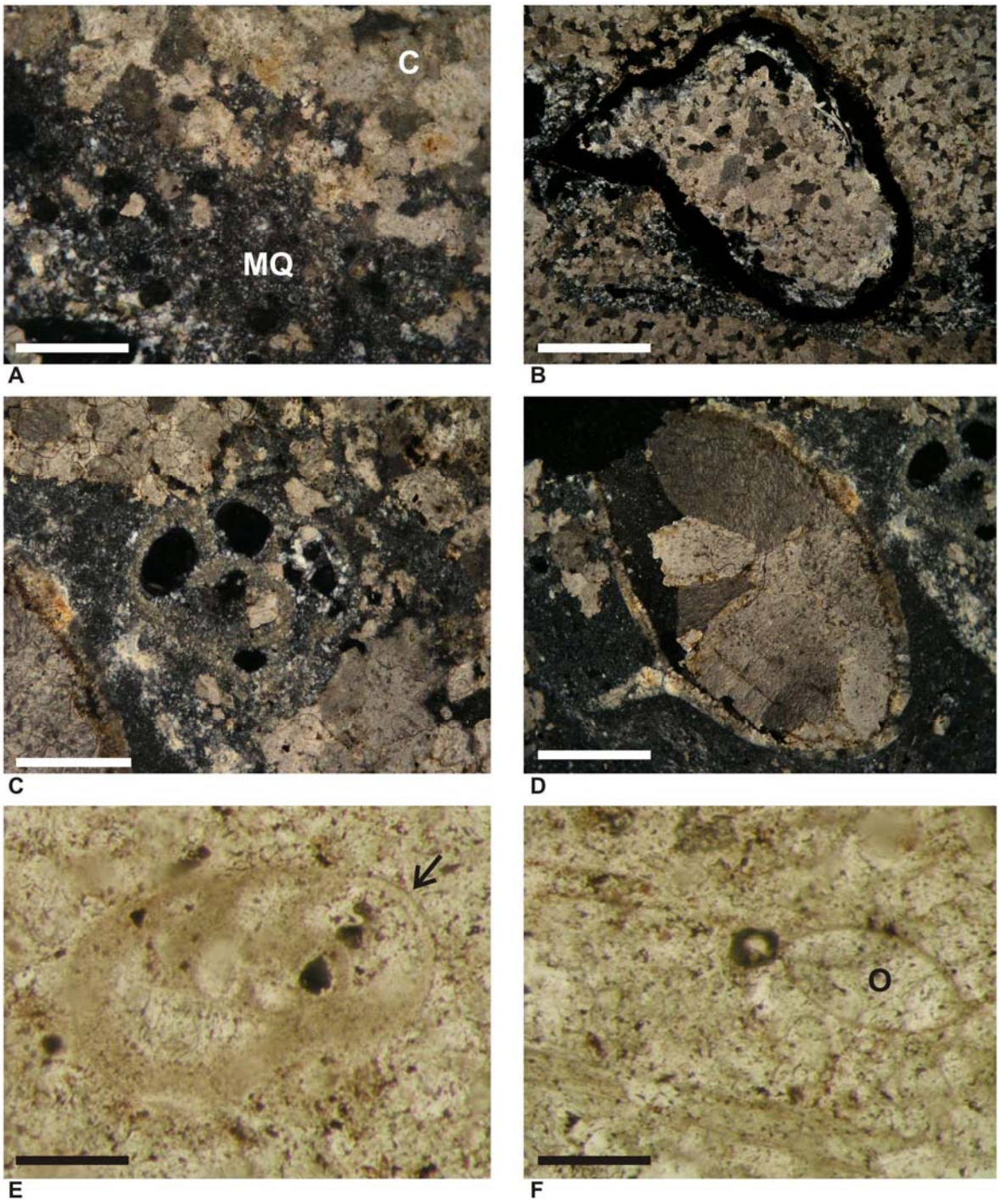

Figure 3. Photomicrographs of limestone pebbles from Vrchlabí Formation, locality Stará Paka Railway Station. A) Limestone silicification. Microquartz (MQ) replacing calcite spar (C). Crossed nicols, scale bar 0.5 mm. B) Bioclast or intraclast is rounded by organic matter (black). Crossed nicols, scale bar 0.2 mm. C) Foraminifers has more cells than foraminifers from Lower and Middle Devonian age. They form more complicated forms, which is more typical for foraminifers from Carboniferous or uppermost Devonian. Crossed nicols, scale bar 0.4 mm. D) Shell of mollusc or brachiopod is filled by calcite spar, whereas foraminifer is partly silicified (top right). Crossed nicols, scale bar 0.5 mm. E) Photomicrograph shows detail of another foraminifer, at her right side the shell wall is well preserved (arrow). Parallel nicols, scale bar 0.8 mm. F) Ostracod shell (O) and elongated fragments of unknown origin (algae?). Parallel nicols, scale bar 1.2 mm. G) Calcispheres (arrow) are partly recrystallized, but the radial concentric structure still can be seen. Crossed nicols. H) Probable plant remnants (algae?), which are partly infilled by organic matter. Cirlular bioclasts occuring among them are probably calcispheres. Parallel nicols.

Heavy mineral suite

Heavy minerals are subject to a varying rate of alteration and desintegration during weathering in the source area, transport to the basin, weathering during periods of alluvial storage on the floodplain, diagenesis during burial and weathering at the outcrop. These processes significantly affect the proportions of individual heavy minerals found in the sedimentary record, which can differ from the proportions of accessory minerals in the source area. Haughton et al. (1991), Morton & Hallsworth (1994, 1999) discussed the factors influencing heavy mineral composition and Morton & Hallsworth (1999) and Morton & Hallsworth (1994) isolated provenance-sensitive features, and avoided parameters that are influenced by other factors. The mineral indices proposed by these authors can eliminate transport/weathering/diagenetic modifications. Such an approach is successful in identifying provenance. The results obtained are summarized in Fig. 4, where detrital heavy minerals are plotted.

The major components of heavy mineral association found in most samples are zircon, apatite, tourmaline and garnet. These minerals could originate from a wide range of possible source rocks: metamorphic, plutonic, volcanic, either from the adjacent Krkonoše-Jizera Crystalline Complex or many other source rocks south of the basin. Cretaceous marine deposits cover some potential source areas south of the basin. The provenance-specific minerals presented in Fig. 4 are not abundant in all samples. For example, in conglomerates deposited close to the basin margin (Náchod and Horní Město conglomerates) rock fragments (quartzite, phyllite, highly altered – Fe-oxidized – phyllite) and Fe oxides predominate in the heavy fraction. The interpretation of the relative proportions of the individual heavy minerals in the samples, where the sum of these selected provenance-specific minerals is less than 5 – 10 % of the total HM fraction, must be very careful. There may be significant errors in calculating the relative proportions of minerals. Several distinct heavy mineral associations (HMA), which are also supported by distinct heavy mineral (HM) indices, were found (Fig. 5). Stephanian C samples from the north-western part of the basin have an association of monazite-tourmaline-gahnite that is similar to Cisuralian samples from the north-western and north-central parts of the basin, while Cisuralian samples from the south-western part of the basin (near Stará Paka, samples SPxyz, Fig. 5A) have a different association dominated by pyroxene-ilmenite-rutile-tourmaline-garnet. Sakmarian samples Crm and Zbr belong to the Prosečné Formation, they have a very poor mineral association dominated by tourmaline. The lower part of Guadalupian deposits is characteristic by an ilmenite-rutile-tourmaline association, while upper Guadalupian deposits have an ilmenite-rutile-tourmaline-garnet association. Kyanite and staurolite were also found sporadically. They occur in the fluvial sandstones of the Trutnov and Vrchlabí formations.

The RuZi (100 x TiO2 group/TiO2 group + zircon), GZi (100 x garnet/garnet + zircon) and ATi (100 x apatite/apatite + tourmaline) HM indices of Morton & Hallsworth (1999) give other provenance specific information. On the GZi/ATi plot (Fig. 5) the distinct composition for the Horní Město and Náchod Conglomerates, the Čistá Sandstone, the upper part of the Havlovice Sandstone, the Prosečné Formation and the last group with similar heavy mineral composition including Kumburk Fm., Semily Fm., Stará Paka Sst, Rudník member, and the lower part of Havlovice Sst. were recognized.

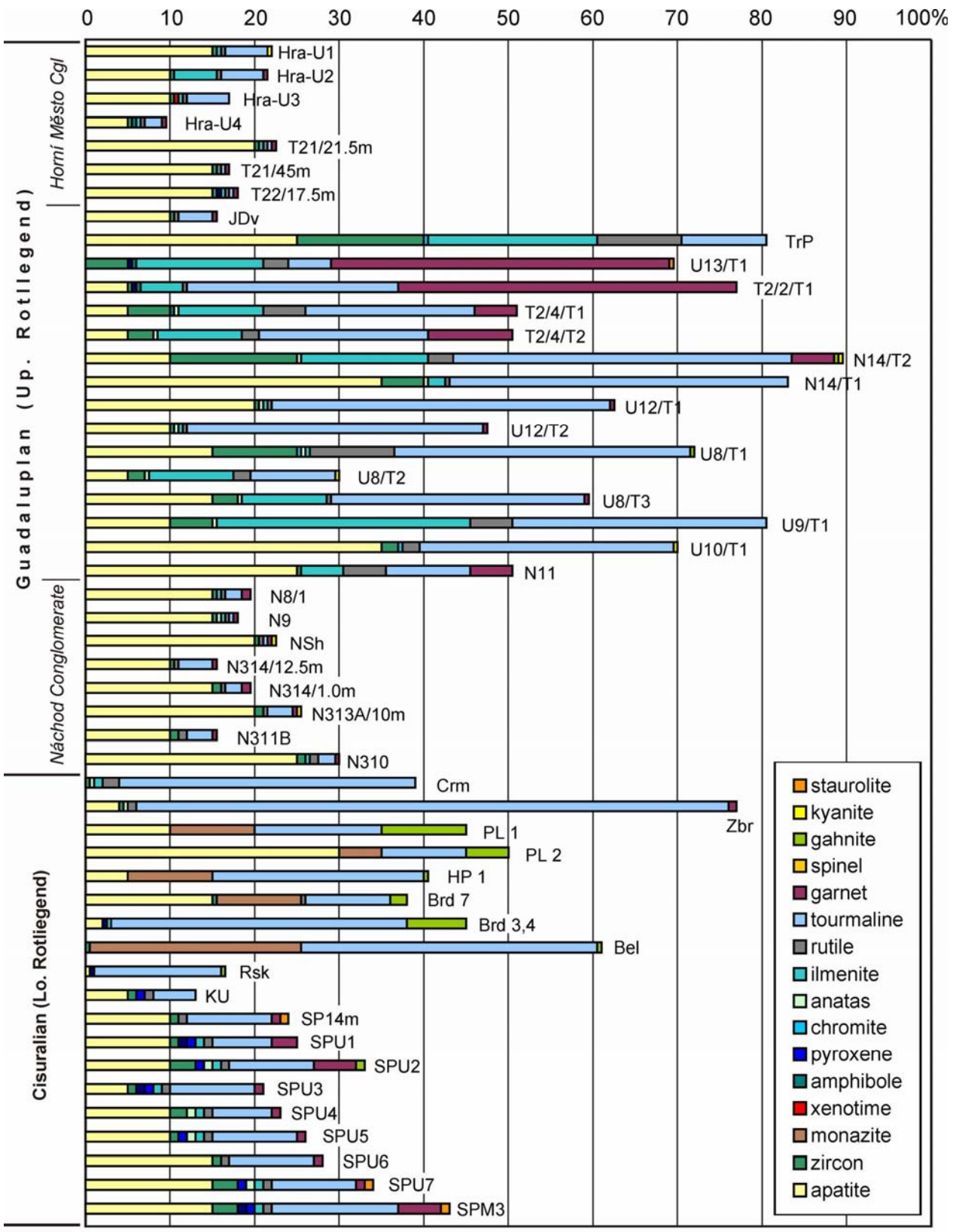

Figure 4. Detrital heavy minerals. Only heavy minerals considered as primary, derived from source rocks are presented. Rock fragments, carbonates, muscovite, biotite/phlogopite, and diagenetic and other secondary minerals are not included. Carboniferous – Triassic rocks represent sandstones and a sandstone matrix of conglomerates, sampled crystalline rocks include low grade metamorphics.

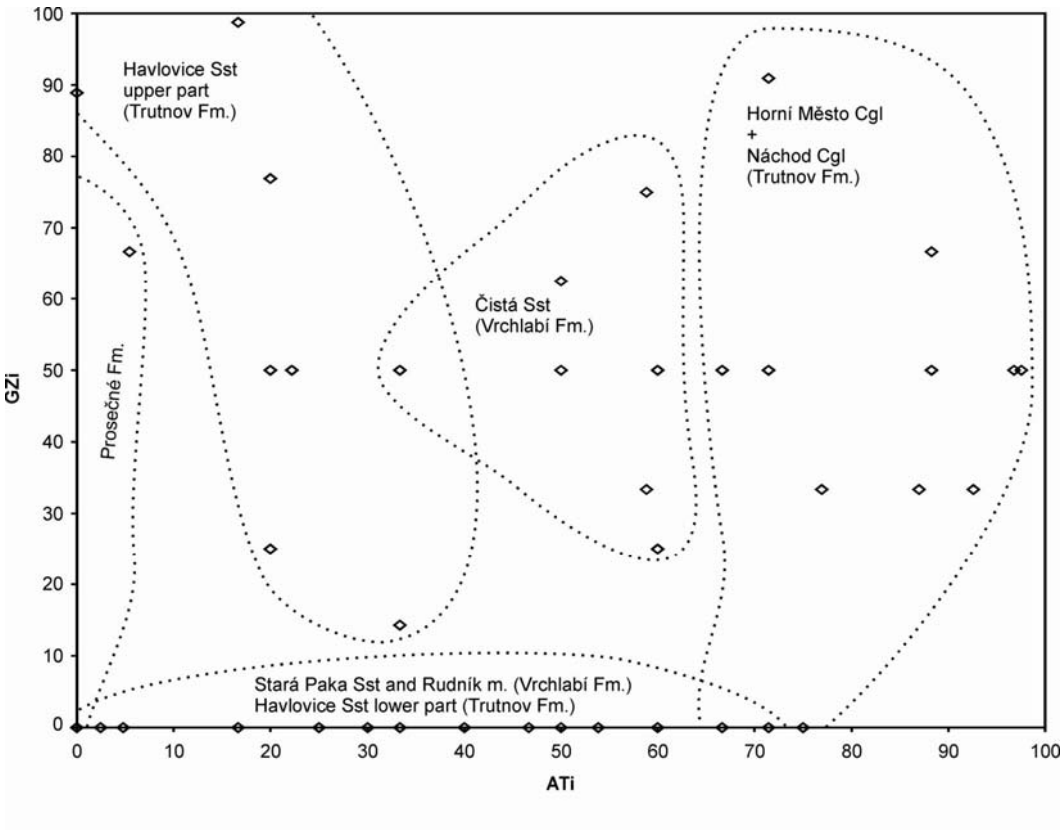

Figure 5. The heavy mineral indices of Morton & Hallsworth (1999) point to distinct source rocks of individual lithostratigraphical units.

Garnet composition

An effective method for discriminating specific source areas is detailed mineral chemistry determination using an electron microprobe (Morton 1985, Owen 1987, Morton 1991). Garnet composition was successfully used for the provenance study of clastic material of the Early Carboniferous foreland Culm Basin deposits of the Moravo-Silesian Zone at the eastern margin of the Bohemian Massif (Čopjaková et al. 2005). The results of garnet electron microprobe analyses from the Krkonoše Piedmont Basin (Permian – Triassic) are summarized in Figs 6 – 7. Garnet separation was carried out on 15 samples representing the main stratigraphic units. Unfortunately, many samples contain garnets of small size and they are highly weathered, only 5 samples contained garnets suitable for electron microprobe analysis. They include one sample of Asselian and Triassic, respectively, and three samples of Guadalupian age.

Sample SPU-1 (Fig. 7, one grain was analysed) comes from the fluvial sandstones of the Vrchlabí Formation, Asselian, the Stará Paka railway station locality, the same from which Devonian/Carboniferous marine limestone pebbles were described. Dominant spessartine (0.7) composition with very low almandine (0.15), grossular (0.05) and pyrope (0.01) components and the absence of zonality is characteristic.

Samples U13 (Figs. 6 and 7, six grains were analysed) are from the upper part of the fluvial sandstone unit of the Trutnov Formation (Guadalupian, locality Suchovršice-Adamov near Úpice), Unit 3B sensu Uličný & Martínek (2002 unpublished report). Most garnet grains are dominated by almandine (0.45 – 0.65), have high pyrope (0.25 – 0.45), low grossular (less than 0.1) and very low spessartine components (less than 0.05). Zonality is absent. Anomalous very high almandine (0.70) and low pyrope (0.09) grain (U13-T1-2); and very high xMg garnet also occurs (U13-T1-4, up to 0.50 pyrope).

Samples T2-3-T1 (Figs. 6 and 7, 13 grains analysed) are from fluvial sandstones of the Trutnov Formation (Trutnov – Starý Rokytník, Unit 3B). Most grains (8) are of almandine (0.65 – 0.8) – pyrope (0.25 – 0.05) composition with variable grossular (0.05 – 01) and spessartine (0.15 – less than 0.05). Two spessartine (0.4 – 0.45) - almandine (0.35 – 0.38) dominated grains have a grossular component of 0.1 – 0.2. Three grains are pyrope (0.6 - 0.38) - almandine (0.1 - 0.38) dominated with grossular of 0.15 – 0.25, one of these grains (T2-3-T1-45) has 0.6 pyrope and 0.1 uvarovite (Cr garnet). Garnets T2-3-T1-06 and T2-3-39 have preserved a prograde chemical zonality with a high xMg value in the rim (0.35 – 0.45 pyrope, 0.3 – 0.6 almandine, 0.2 – 0.1 grossular).

Sample T21-21-1 (Fig. 7, one grain was analysed) comes from the Trutnov Formation's, Horní Město Conglomerates, alluvial fan deposits forming a narrow (up to 1 km) fringe along the northern margin of the Trutnov Náchod Subbasin (north of Vlčice and Trutnov). Conglomerate pebbles are composed of local material from the Krkonoše-Jizera Crystalline Complex (Prouza & Tásler 2001), but the garnet sample is from a sandstone matrix, which can contain material from more distal sources. In addition, a major unconformity at the base of the Trutnov Formation was accompanied by significant tectonic rearrangement of the basin (Uličný et al. 2002), which caused uplift and erosion of older strata. Clasts of Stephanian C age within the Trutnov Formation are reported by Prouza & Tásler (2001). A dominant almandine (0.6) – spessartine (0.2) composition with low xMg, Ca and the absence of zonality was found.

In samples HAJN (Figs. 6 and 7, locality Hajnice, Bohdašín Formation, Early Triassic, fluvial red bed "Buntsandstein" facies, 22 grains) almandine (0.7 – 0.55) – pyrope (0.2 – 0.45) garnets with variable grossular (0.05 – 0.15) and very low spessartine (less than 0.05) prevail (14 grains). Five grains are almandine (0.6 – 0.8) dominated with a low grossular (0.05 - 0.1) and variable spessartine (0 – 0.2) component. Two grains are pyrope (0.42 – 0.45) dominated with almandine (0.35 – 0.38), grossular (0.21 – 0.23) and very low spessartine (less than 0.05). Most pyrope-almandines have flat profiles. In garnets Hajn3 and Hajn23 a weak prograde zonality can be observed. There is a slight increase in xMg from the core to the rim (see Figs. 7 and 8). Only grain HAJN18 has a higher pyrope (0.45) component (0.35 almandine, 0.2 grossular).

Although there is a wide variety in garnet composition among the studied samples, some could be grouped according to similarities in composition. The high xMg garnet of U13-T1-4 (up to 0.50 pyrope) is similar to T2-3-T1-37, T2-3-T1-39 and HAJN18 (pyrope 0.45, almandine 0.35, grossular 0.2). Almandine-pyrope garnets of T2-3-T1 (0.65 – 0.45 almandine, 0.45 – 0.25 pyrope) have a composition similar to sample U13. A dominant almandine (0.6) – spessartine (0.2) composition with high Mn and low xMg, Ca and the absence of zonality is characteristic for the samples T21-21-1, T2-3-T1-32 and SPU-1.

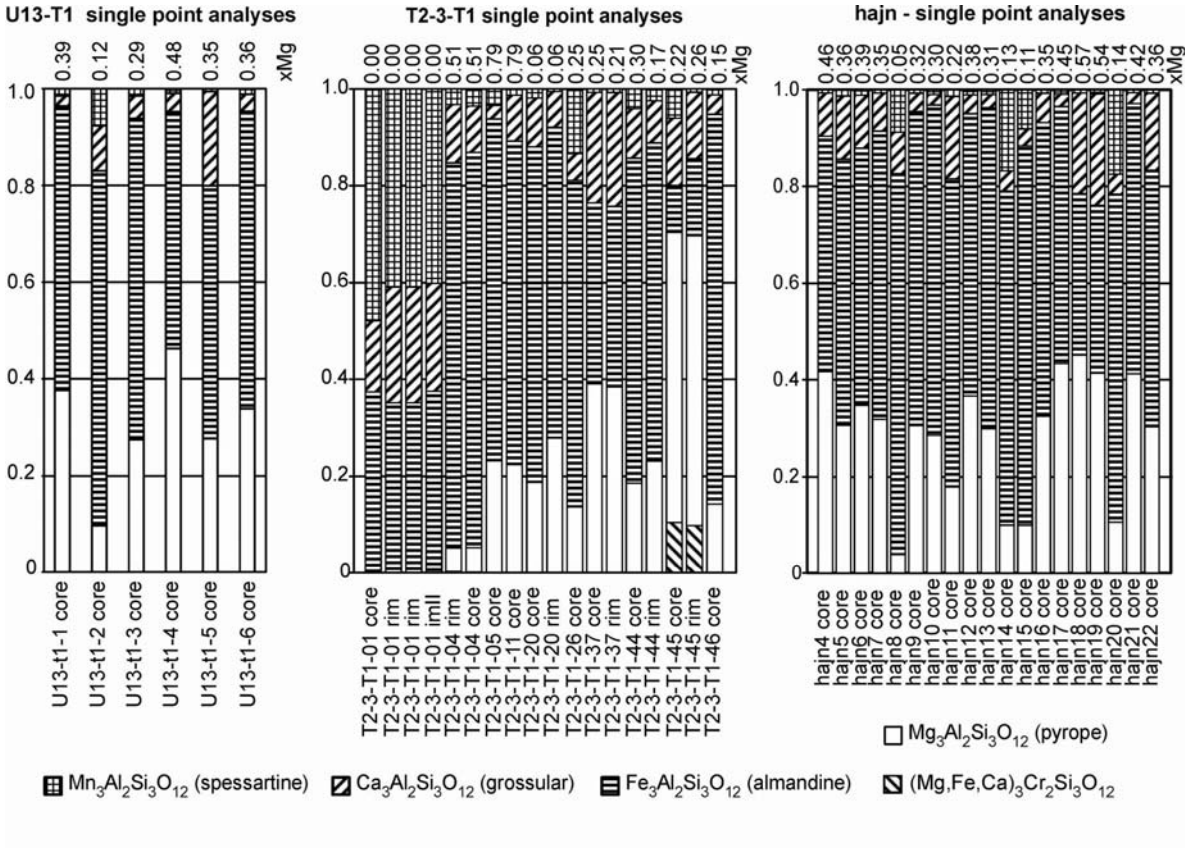

Figure 6. Garnet composition revealed from single point analyses of the grains in samples U13-T1, Úpice, Trutnov Formation, Early Permian (Upper Rotliegend); T2-3-T1, Trutnov – Starý Rokytník, Trutnov Formation; hajn, Hajnice, Bohdašín Formation, Triassic.

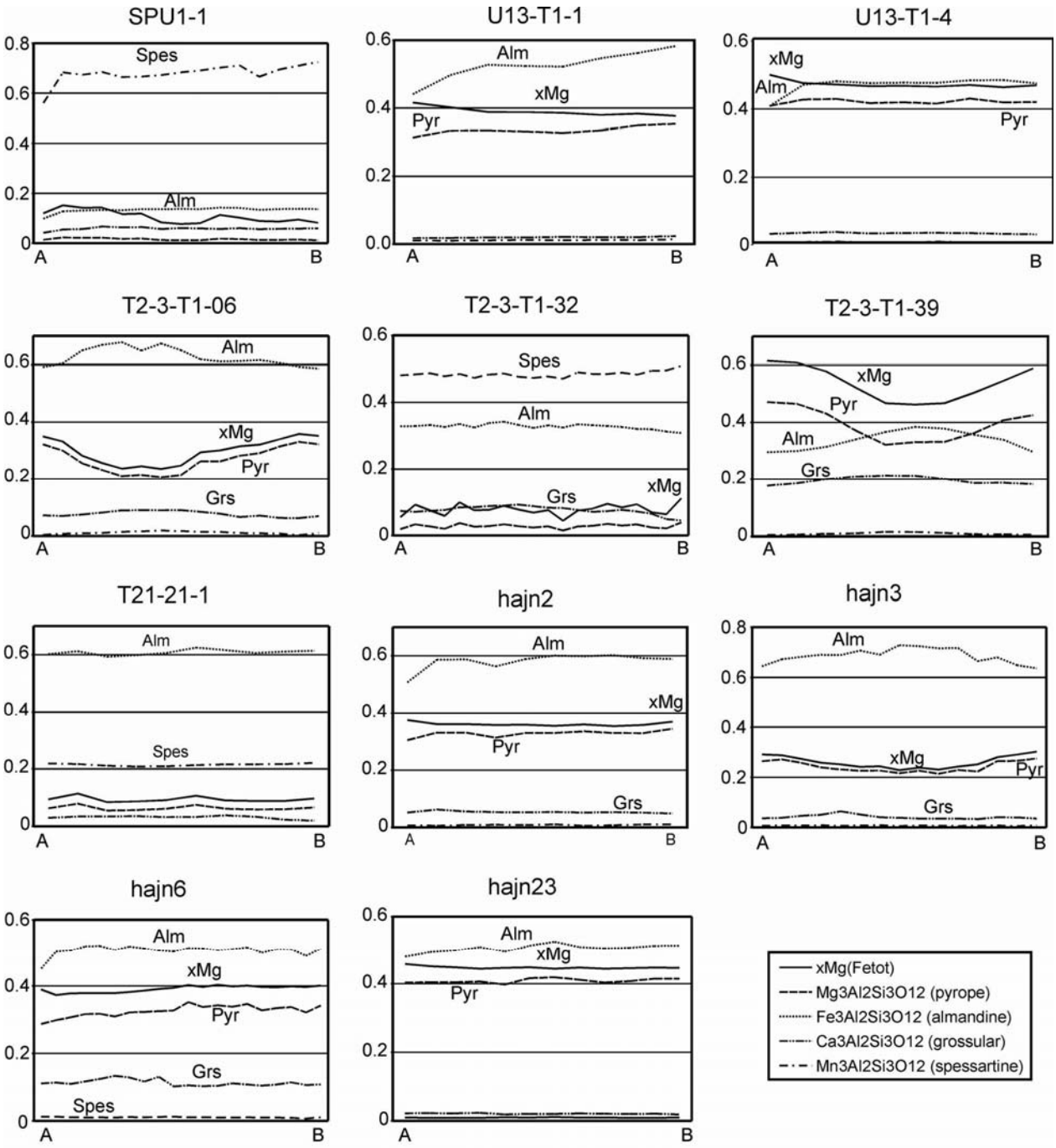

Figure 7. Profiles through garnet grains, zonality is discussed in the text. xMg values are calculated as Mg/(Mg+Fe). Location of profiles is shown on Fig. 8. Sample SPU1, Stará Paka, Vrchlabí Formation, Early Permian (Lower Rotliegend); U13-T1, Úpice, Trutnov Formation, Early Permian (Upper Rotliegend); T2-3-T1, Trutnov – Starý Rokytník, Trutnov Formation; T21-21.5m, Pekelský vrch, Trutnov Formation; hajn, Hajnice, Bohdašín Formation, Triassic.

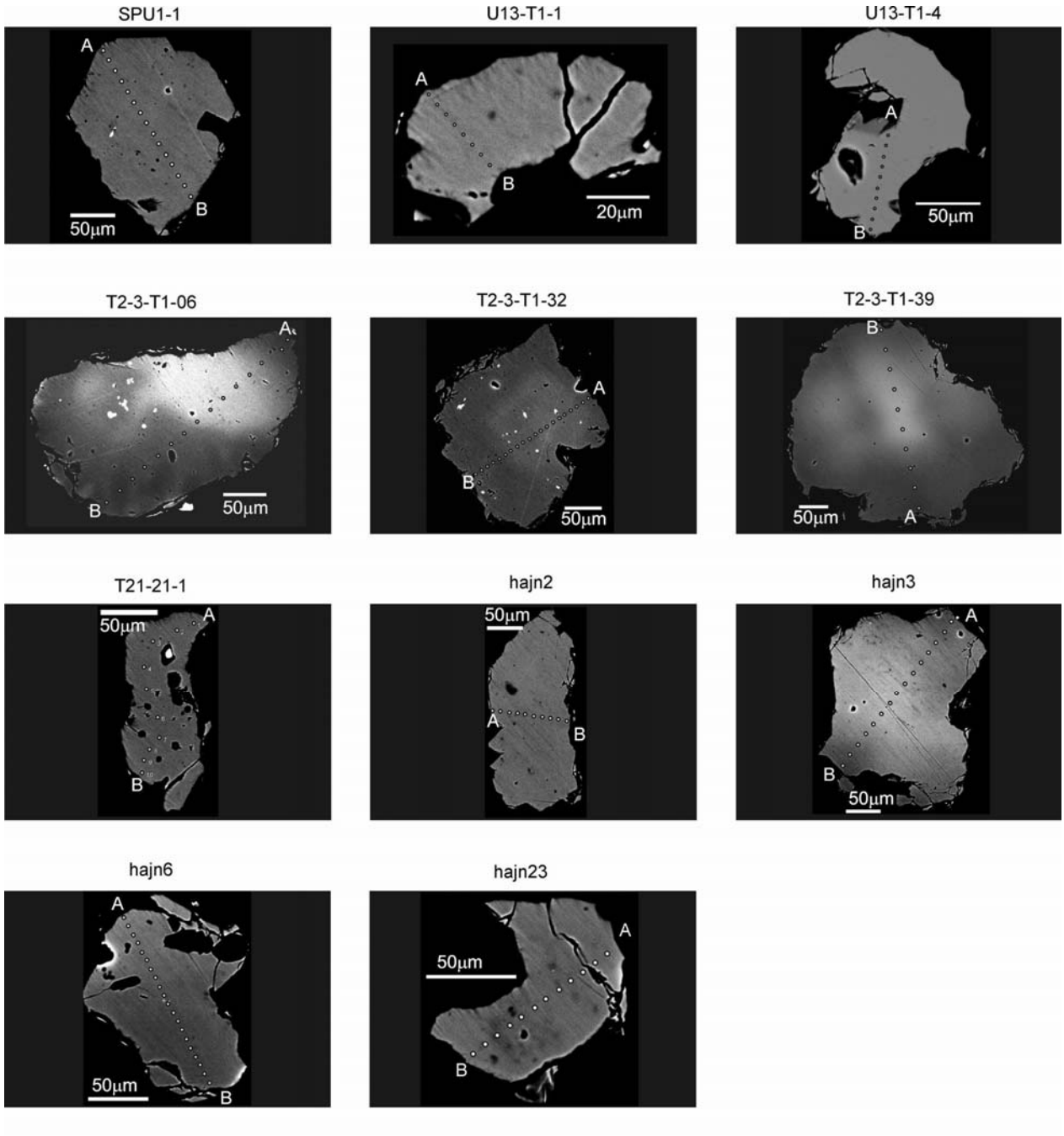

Figure 8. SEM photographs show typical garnet grains with location of profiles (see Fig. 7). Sample SPU1, Stará Paka, Vrchlabí Formation, Early Permian (Lower Rotliegend); U13-T1, Úpice, Trutnov Formation, Early Permian (Upper Rotliegend); T2-3-T1, Trutnov – Starý Rokytník, Trutnov Formation; T21-21.5m, Pekelský vrch, Trutnov Formation; hajn, Hajnice, Bohdašín Formation, Triassic.

Discussion

In this study, based on the provenance-specific clastic material found in the samples studied, we discuss possible source areas for particular stratigraphic units. It also leaves the discussion open for other possible source areas, where direct evidence is missing. The conglomerates of alluvial fan deposits, which were deposited close to the basin margin, contain almost exclusively local material in the pebbles (e.g. Semily Formation near Semily; Lánov conglomerates near Vrchlabí, Vrchlabí Formation; Horní Město Conglomerates near Trutnov, Trutnov Formation; Náchod Conglomerates near Náchod, Trutnov Formation). Our findings are in agreement with the interpretations of Prouza & Tásler (2001).

Provenance of exotic limestone pebbles

We describe, for the first time, the occurrence and composition of exotic marine limestone pebbles within the fluvial sandstones of the Vrchlabí Formation. Palaeocurrent data indicate a sediment supply from the south or southwest of the Krkonoše Piedmont Basin. As stated above the most likely age of this limestone is Upper Devonian or Lower Carboniferous. We consider the deposits of the Jítrava Hradec Basin (sensu Čech et al. 1989) to be the most favourable source of pebbles. This hypothetical sedimentary basin is known only from relics in which marine deposits of Late Devonian and Early Carboniferous age occur. Deposits are preserved only in the Ještěd area (near Jítrava) and in several boreholes near Hradec Králové. Upper Devonian to Lower Carboniferous in situ marine limestone was encountered in the Nepasice borehole near Hradec Králové. Stromatoporoids, foraminifers and algae of probable Upper Famenian age (Zukalová 1976) were found in the limestone samples taken from the base of the carbonate sequence. A specimen of rugose coral was also found and its age is Late Famennian (Galle 1976). In the Nepasice borehole, the limestone sequence has some features in common with the development of the Ještěd area, but its appearance and fossil content is most similar to the Devonian of Moravia, namely the Moravian Karst facies (Chlupáč & Zikmundová 1976). It can be also correlated to Dzikowiec in the Klodzko region (Gluszek & Tomas 1994). The limestones of the Jítrava area are of Famennian age and contain trilobite and conodont fauna, they are organic matter rich in places and they may represent a mid to deeper shelf marine environment (Chlupáč 1964, Chlupáč 1997, Budil 2007 personal communication). Although the fossil content of the limestone pebbles from the Stará Paka Railway Station locality does not correspond either with the Nepasice nor the Jítrava occurrence (Kalvoda 2004 personal communication), the age of deposits corresponds well. The source of limestone pebbles could be in the central part of the Jítrava Hradec Basin, where, unfortunately, the sedimentary record of this age is not known. This area is extensively covered by Pennsylvanian non-marine and Late Cretaceous marine deposits, but Devonian/Carboniferous deposits could have also been eroded during the Mississipian/Pennsylvanian tectonostratigraphic rearrangement of the area.

Inferences from heavy minerals

The stratigraphic significance of HMA and their usage for outcrop correlation purposes within the Trutnov Formation is discussed elsewhere (Uličný & Martínek 2002 unpublished report). This study is focused on the interpretation of possible source areas. The HM composition of most samples is highly complex and it is not easy to extract provenance specific information. Boundaries of the main lithostratigraphic units are marked with changes in HMA (Fig. 5A and 5B). The similarity in the association of monazite-tourmaline-gahnite in the Stephanian C samples from the north-western part of the basin and Cisuralian samples from north-western and north-central parts of the basin point to the existence of a similar source area for this part of the basin during the Stephanian C and Cisuralian. Samples are mostly from basin margin clastics (alluvial fan, nearshore lacustrine, lacustrine fan-delta facies). Monazites are not very significant, they are abundant in granitoids and orthogneisses. Gahnite was not described so far from either the marbles nor metapelites of the Krkonoše-Jizera Crystalline Complex, but some calc-silicate rocks of contactmetamorphism zones are possible candidates; gahnite is known from the Staré Město Crystalline Complex and the Moldanubian Zone. Tourmaline is abundant in the phyllites and shists of the Krkonoše-Jizera and Zvičina crystalline complexes. Source areas could possibly be some units of the south-western part of the Krkonoše-Jizera Crystalline Complex or overlying, already eroded, units. Cisuralian samples from the south-western part of the basin have a different association dominated by pyroxene-ilmenite-rutile-tourmaline-garnet. Samples come from fluvial facies of the Vrchlabí Formation, for which palaeocurrents indicate transport from the south. Source areas of the fluvial sandstones could be more distant. More information is needed to determine particular units of the central and southern Bohemian Massif as possible source areas, (see discussion of garnet composition below). The poor mineral association dominated by tourmaline of the Sakmarian samples (Crm and Zbr belonging to the Prosečné Formation) could be explained in terms of poor preservation of less stable heavy minerals. Unstable heavy minerals were probably disintegrated and weathered due to a prolonged exposure on the floodplain. The Prosečné Formation is characterised by a low-gradient alluvial-lacustrine system with low subsidence rates and a semi-arid climate (Martínek 1995, Prouza & Tásler 2001) and long-time exposure of sediments on the floodplain is expected. The stratigraphy of garnet-free and garnet-rich units of the Guadalupian is discussed in Uličný & Martínek (2002 unpublished report) in detail. It could be concluded that a major change in source areas is expected at the mid-Guadalupian basin-wide unconformity. Changes in HM composition of various stratigraphic units point to tectonic and tectonostratigraphic changes in source areas, which correlate with tectonosedimentary changes within the basin. At least the Cisuralian/Guadalupian boundary, but probably also Stephanian B/C and mid-Guadalupian unconformities, have such a nature. Minerals pointing to more distant sources are kyanite and staurolite. These minerals occur in the fluvial sandstones of the Trutnov and Vrchlabí formations, which have palaeoflows to the north and northeast. Kyanite and staurolite do not occur either in the adjacent Krkonoše or Zvičina Crystalline complexes. The closest occurrence of such minerals is in the Orlice-Sněžník granulites or Moldanubian metamorphics.

Inferences from garnet composition

Garnet SPU-1 with a dominant spessartine (0.7) composition with very low almandine (0.15), grossular (0.05) and pyrope (0.01) components and an absence of zonality is interpreted as probably coming from a magmatic source; garnets from leucocratic granites and pegmatites can have a similar composition. Mn rich garnets are described e.g. by Breiter (2005) from orthogneisses, pegmatites and granites near Přibyslavice, the NE part of the Moldanubian Zone (7 – 15 wt. % MnO). Alternatively, very similar garnet (0.6 Spess, 0.15 Gross, 0.15 Alm) with an absence of zoning also occurs in the blueschists of the eastern part of the Krkonoše-Jizera Crystalline Complex in Sněžný potok near Žacléř (Žáčková 2006 pers. comm.) but palaeocurrent data show an opposite direction, which eliminates this source from further discussion.

Most U13-T1 garnet grains are dominated by almandine (0.45 – 0.65), have high pyrope (0.25 – 0.45) and very low spessartine and grossular components (less than 0.05). Such a composition and the absence of zonality (similar to sample HAJN) is interpreted as possibly coming from a granulite source. Tajčmanová et al. (2006) described garnets from felsic granulites of the Strážek Unit, NE Moldanubian Zone (approx. 90 km SE of Krkonoše Piedmont Basin), of the eastern Bohemian Massif, with a similar composition (0.55 – 0.85 Alm, 0.1 – 0.3 Pyr, Spes and Grs less than 0.05) and an absence of zonality. Similar bright garnets, with a composition of 0.30 - 0.64 Alm, 0.14 – 0.40 Pyr, 0.05 – 0.27 Grs, were described by Fiala & Kopecký (1964) from Carboniferous sandstones of the borehole Třtěno Tř-1 near Louny, the Kladno-Rakovník Basin, and interpreted by these authors as coming from felsic granulites. The garnets from the Křišťanov Granulite of Farský Hill, southern Bohemian Moldanubian Zone (approx. 200 km south of Krkonoše Piedmont Basin) have a lower pyrope component (0.18-0.20 Pyr, 0.66-0.73 Alm, 0.1-0.02 Grs and 0.02 Sps, Verner 2006 pers. comm.), similar to samples U13-T1-3a and 3b. Anomalous very high xMg garnet also occurs here (U13-T1-4, up to 0.50 pyrope), its composition is similar to T2-3-T1-39 and HAJN18. They can come from Moldanubian garnet pyroxenites, e.g. an occurrence in Bezděčín near Tábor (approx. 160 km south of the basin) has garnets with 0.44 Pyr, 0.37 Alm and 0.16 Grs (Machart & Paděra 1982).

Most of the garnet grains of the sample T2-3-T1 are of dominant almandine-pyrope and pyrope-almandine composition. Those without zonality could be interpreted as coming from granulites south of the basin. Garnet T2-3-T1-06 has preserved a prograde chemical zonality. A high xMg value in the rim points to a possible high-grade metamorphic source. The preservation of zonality can be interpreted as being due to lower P/T conditions (amphibolite facies) or just a short exposure of the garnet at granulite facies conditions. Garnet T2-3-T1-39 has prograde zonality and a high pyrope component, but a high almandine component too. This composition is rare and can be compared with garnet clinopyroxenites, which are associated with eclogites and ultramafic rocks in Moldanubian Zone. The high Mn garnet T2-3-T1-32 with an absence of zonality is interpreted as possibly coming from a magmatic source, leucocratic granites and pegmatites can have a similar composition. The Cr-pyrope grain T2-3-T1-45 with 0.5 – 0.6 Pyr, 0.1 – 0.15 Alm, 0.1 – 0.15 Grs and a 0.1 uvarovite component has an affinity to violet Cr-pyropes from Podsedice (near Lovosice, western Bohemia, 0.75 Pyr, 0.12 Alm, 0.09 – 0.12 Uvr, Sps and Grs less than 0.01), which originate in pyrope lherzolite on peridotite bodies in basement gneisses and which have been recycled several times to Permo-Carboniferous, late Cretaceous and Pleistocene deposits and Neogene volcanic breccia (Seifert & Vrána 2005). The composition of particular grains in this sample is rather variable pointing to source areas south, southeast and southwest of the basin. These areas are not necessarily considered as primary sources of detritic material. Several phases of recycling of older sedimentary units (Carboniferous-Cisuralian) is expected at the major intervals of the basin tectonic rearrangements indicated, e.g., by basin-wide unconformities (Stephanian B/C, Cisuralian/Guadalupian).

Garnet T21-21-1 has a dominant almandine (0.6) – spesartine (0.2) composition with high Mn, low xMg, Ca and the absence of zonality, interpreted as possibly coming from a magmatic source, leucocratic granites, orthogneisses and migmatites. The sample is similar to garnets T2-3-T1-26, U13-T1-2 and HAJN14, but the sample comes from a sandstone matrix of Horní Město Conglomerates and is located close to the northern margin of the basin. The pebbles originated from the Krkonoše-Jizera Crystalline Complex but the sandstone matrix may contain material recycled from older strata (Carboniferous, Cisuralian).

Most HAJN garnets are almandine rich and have flat profiles, in garnets 3 and 23 a weak prograde zonality can be observed. There is a slight increase in xMg from the core to the rim. High xMg (0.3 – 0.4, but also 0.45 and 0.55), a grossular component in the range of 2 – 12 % (up to 20%) and a very low spessartine component are characteristics. The homogeneous garnet chemistry, low spessartine and a high xMg component point to a high-grade metamorphic origin corresponding to granulite facies. The differences in the grossular component content can be explained by variable pressure conditions, including decompression history.

In most samples almandine-pyrope garnets with high-grade metamorphic features dominate. They are probably coming from southern or north-eastern Moldanubian granulites. The high pyrope garnets may have a possible source area in southern Moldanubian pyroxenite bodies. The dominant southward sources for Permian deposits are in agreement with the palaeoflows. The high-grade metamorphic rocks of the Moldanubian Zone were already exhumed during the Early Permian. Assuming that Moldanubian garnets were recycled from Carboniferous, it can be inferred that the Moldanubian Zone was exposed to erosion during the Late Carboniferous, as indicated by the data from Kulm in central Moravia (Dvořák 1973, Hartley & Otava 2001, Kotková et al. 2007).

Near Vestřev (12 km southwest of Trutnov) an abundant detrital pyrope occurs in Quaternary alluvial gravels, which was exploited for jewellery (Řídkošil et al. 1997). The pyrope composition (0.75 Pyr, 0.13 Alm, 0.04-0.07 Uvar, and 0.01-0.04 Grs) is characteristic of garnet peridotites, but the original source of pyrope near Vestřev is uncertain. No pyrope was found in the nearby Permian sandstones; a possible derivation from Permian volcanic rocks, which could bring pyrope-rich basement rocks, remains to be examined. We can also speculate that pyrope could have been derived from some post-Permian deposits, which are not currently preserved. In the Kolín area, 40 km south of the studied basin, there are at present relatively abundant local sources of pyrope, which contain characteristically oriented acicular rutile inclusions (Běhal et al. 2000, Vrána 2008). It is nearly certain, that the pyrope peridotites near Kolín were not exposed to erosion during the Permian, as it would be difficult to understand the presence of granulite- and pyroxenite-derived garnets in the studied samples interpreted as coming in part from southern Bohemia and the absence of Kolín pyropes. Another problem, which remains open, is the presence of unusual almandine-spessartine garnets enriched in grossular (T2-3-T1-01). We have not found a possible source rock for such a garnet composition.

Conclusions

Pebbles in Asselian – Guadalupian conglomerates of alluvial fan, nearshore lacustrine and lacustrine fan-delta deposits, which were deposited close to the northwestern and southeastern basin margin, respectively, correspond almost exclusively to local material from adjacent crystalline complexes.The heavy mineral associations of the sandstone matrix of these conglomerates support this interpretation. Crystalline units of the south-western part of the Krkonoše-Jizera Crystalline Complex and Orlice-Sněžník Crystalline Complex, respectively, are considered as the most favourable source.

The two main possible source areas for the fluvial Asselian deposits of the south-western part of the basin were found. Pebbles of late Devonian – early Carboniferous marine limestones come probably from the central part of the hypothetical Jítrava Hradec Basin, while the source of sand detrital material could be located in leucogranites and pegmatites of the north-eastern Moldanubian Zone, Přibyslavice area.

Guadalupian fluvial deposits reveal a wide range of sources, which can be attributed to the recycling of detrital material from Cisuralian and Carboniferous deposits. Garnet compositions indicate Moldanubian granulites, garnet clinopyroxenites, leucogranites and pegmatites as possible source.

Moldanubian granulites and garnet clinopyroxenites were exposed to erosion in the Early Permian at the latest.

Acknowledgements

We wish to thank J. Košler and V. Janoušek for sharing their ideas, J. Konopásek for his suggestions, discussions and help with garnet composition interpretations. The research was performed as a part of the PhD thesis of K. Martínek with the support of the Grant Agency of the Czech Academy of Sciences, grant No. IAB3111305 to K. Martínek and the Grant Agency of the Czech Republic, grant No. 205/99/0739 to D. Uličný. We are grateful to Z. Táborský, F. Veselovský and R. Lojka, of the Czech Geological Survey, for heavy mineral separation and determination, J. Míková for garnet separation and R. Procházka for electron microprobe analyses. Many thanks to R. Withers for the English review. K. Štolfová thanks J. Kalvoda, V. Kachlík and D. Bosence for their suggestions and contribution to the palaeogeographic topics. Special thanks to K. Holcová for her help with lab processing, her discussions and suggestions concerning micropalaeontology, to V. Kachlík for his information on accessory minerals in crystalline complexes. We thank also to P. Čejchan, O. Fatka and P. Budil for discussions on the calcispheres and Palaeozoic of Jítrava and to Peter Haughton for discussion of selected provenance aspects. We gratefully acknowledge the reviewers S. Vrána, J. Schneider, R. Čopjaková, the editor Š. Manda and anonymous reviewers for improving the manuscript.

References

BASU, A., YOUNG, S.W., SUTTNER, L.J., JAMES W.C. & MACK, G.H. 1975. Re-evaluation of of the use of undulatory extinction and polycrystallinity in detrital quartz for provenance interpretation. *Journal of Sedimentary Petrology 45***,** 873-882.

BĚHAL, Z., NOVÁK, F., PAULIŠ, P. & PEJŠA, J. 2000. Historická naleziště českého granátu (pyropu) na Kolínsku a jejich mineralogie. *Práce muzea v Kolíně, řada přírodovědná 4,* 3-32.

BLECHA, M., MARTÍNEK K. & MIHALJEVIČ M. 1999. Sedimentary and geochemical record of the ancient Kalná Lake, Lower Permian, Krkonoše Piedmont Basin, Czech Republic. *Acta Universitatis Carolinae 43(4),* 657 – 665.

BREITER K. 2005. Peraluminické granitoidy sv. Moldanubika. (in Czech) *Excursion guide, 2nd meeting of the Czech Geological Society, Slavonice,* 114-136.

CHLUPÁČ, I. 1964. Nový nález fauny ve slabě metamorfovaném paleozoiku Ještědského pohoří. (in Czech with German summary) *Časopis pro mineralogii a geologii 9(1),* 27-35.

CHLUPÁČ, I. 1997. Poznámky k rozšíření devonu a stavbě metamorfovaného paleozoika v jižní a střední části Ještědského pohoří. (in Czech) *Zprávy o geologických výzkumech v roce 1997,* 19 – 22.

CHLUPÁČ, I. & ZIKMUNDOVÁ, J. 1976. The Devonian and Lower Carboniferous in the Nepasice bore in East Bohemia. *Věstník Ústředního Ústavu Geologického 51,* 269-277.

ČOPJAKOVÁ R., SULOVSKÝ P. & PATERSON B.A. 2005. Major and trace elements in pyrope-almandine garnets as sediment provenance indicators of the Lower Carboniferous Culm sediments, Drahany Uplands, Bohemian Massif. *Lithos 82 (1-2).* 51-70.

ČECH S., HAVLÍČEK V. & ZIKMUNDOVÁ J. 1989. The Upper Devonian and Lower Carboniferous in north-eastern Bohemia (based on the boreholes in the Hradec Králové area). *Věstník Ústředního Ústavu Geologického 64,* 65 – 75.

DVOŘÁK J. 1973. Synsedimentary tectonics of the Palaeozoic of the Drahany Upland (Sudeticum, Moravia, Czechoslovakia). *Tectonophysics 17, 4,* 359-383.

FIALA J. & KOPECKÝ L. 1964. Ke genezi pyropu a jiných granátů v třetihorní sopečné brekcii Velkého vrchu a Malého vrchu u Třtěna. (in Czech) *Věstník Ústředního Ústavu Geologického 39,* 267-273.

GALLE, A. 1976. Rugose coral Petraiella in the Famennian (Upper Devonian) of Bohemia. *Věstník Ústředního Ústavu Geologického 51,* 279.

GLUSZEK, A. & TOMAS, A., 1994. Age of the Nowa Wies Formation (Bardzkie Mts., Middle Sudetes, SW Poland). *Annales Societatis Geologorum Poloniae 62*, 293-308.

HAQ, B.U. 2007. The Geological Time Table. 6th revised ed., Elsevier.

HARTLEY A. J. & OTAVA J. 2001. Sediment provenance and dispersal in a deep marine foreland basin. the Lower Carboniferous Culm Basin, Czech Republic. *Journal of the Geological Society, London 158,* 137-150.

HAUGHTON, P.D.W., TODD, S.P. & MORTON, A.C. 1991. Sedimentary provenance studies. 1-13. *In* MORTON, A.C., TODD, S.P. & HAUGHTON, P.D.W. (eds). *Developments in Sedimentary Provenance Studies. Geological Society Special Publications 47.*

HOLCOVÁ, K. 2003. Foraminiferal assemblages in acid residues from the 'Cisarska rokle' Gorge at Srbsko (the Lower/Middle Devonian boundary interval, Barrandian area) and their paleoenvironmental significance. *Bulletin of Geosciences 78, 4,* 393-403.

KOTKOVÁ, J., GERDES, A., PARRISH, R.R. & NOVÁK, M. 2007. Clasts of Variscan high-grade rocks within Upper Viséan conglomerates – constraints on exhumation history from petrology and U-Pb chronology. *Journal of Metamorphic Geoogy 25,* 781-801.

KALVODA, J. 1990. Foraminiferal zonation of the Upper Devonian and Lower Carboniferous in Moravia (Czechoslovakia). *Časopis Moravského zemského muzea v Brně, Vědy přírodní 75*, 71-93.

KALVODA, J. 2002. Late Devonian-Early Carboniferous foraminiferal fauna: zonations, evolutionary events, paleobiogeography and tectonic implications. *Folia Facultatis Scientiarium Naturalium Universitatis Masarykianae Brunensis, Geologia 39,* 1-213.

KUKAL, Z. 1984. Granitoidové plutony byly hlavním zdrojem živců permokarbonských sedimentů. *Časopis Mineralogie Geologie 29,* 193-196.

LOJKA, R. 2003. *Sedimentologie aluviálních uloženin a původ klastického materiálu trutnovského souvrství ve vnitrosudetské pánvi. 113 pp*. (in Czech) *Master thesis, Charles University, Prague, Czech Republic.*

MACHART J. & PADĚRA K. 1982. Websterit a griquait ze serpentinitu od Bezděčína u Tábora (jižní Čechy). (in Czech) *Časopis pro mineralogii a geologii 27, 1,* 95-102.

MARTÍNEK K. 1995. *Sedimentární facie a interpretace prostředí sedimentace svrchního prosečenského souvrství podkrkonošské pánve a geochemie sedimentů kalenského obzoru. 60 pp.* (in Czech) *Master thesis, Charles University, Prague, Czech Republic.*

MARTÍNEK K. 2003. Climatic vs. tectonic controls on the fluvial/alluvial Trutnov Fm., Lower Permian, Bohemian Massif: integrated well-log, outcrop and heavy mineral study. *22nd IAS Meeting of Sedimentology, Opatija – September 17-19, 2003, Abstracts Book, p. 61, Zagreb.*

MARTÍNEK K., BLECHA M., DANĚK V., FRANCŮ J., HLADÍKOVÁ J., JOHNOVÁ R. & ULIČNÝ D. 2006. Record of palaeoenvironmental changes in a Lower Permian organic-rich lacustrine succession. Integrated sedimentological and geochemical study of the Rudník member, Krkonoše Piedmont Basin, Czech Republic. *Palaeogeography, Palaeoclimatology, Palaeoecology 230,* 85-128.

MORTON, A.C. 1985. A new approach to provenance studies. electron microprobe analysis of detrital garnets from Middle Jurassic sandstones of the northern North Sea. *Sedimentology 32,* 553-566.

MORTON, A.C. 1991. Geochemical studies of detrital heavy minerals and their application to provenance research, 31-45. In MORTON, A.C., TODD, S.P. & HAUGHTON, P.D.W. (eds). *Developments in Sedimentary Provenance Studies, Geology. Society Special Publications 47.*

MORTON A.C. & HALLSWORTH C.R. 1994. Identifying provenance-specific features of detrital heavy mineral assemblages in sandstones. *Sedimentary Geology 90,* 241-256.

MORTON A.C. & HALLSWORTH C.R. 1999. Processes controlling the composition of heavy mineral assemblages in sandstones. *Sedimentary Geology 124,* 3-29.

OWEN, M.R. 1987. Hafnium content of detrital zircons, a new tool for provenance study. *Journal of Sedimentary Petrology 57,* 824-830.

PEŠEK J. 1994. *Carboniferous of Central & Western Bohemia (Czech Republic).* 60 pp. Czech Geological Survey, Prague.

PEŠEK J. 2005. Hiatuses between the base of the Pennsylvanian and the base of the Triassic in the Bohemian Massif (Czech Republic). *Bulletin of Geosciences 80,* 67-78.

PETRÁNEK, J. 1978. Byly variské plutony Českého masívu tak rychle obnaženy, že se staly zdrojem materiálu karbonských arkóz ? *Časopis Mineralogie Geologie 23,* 381-387.

PETRÁNEK, J. 1984. Karbonské arkózy, variské granitoidy a subsekventní vulkanismus. *Časopis Mineralogie Geologie 29,* 197-210.

POJARKOV 1969: *Razvitije i razprostranenije devonskich foraminifer.* Nauka, Moscow, 172 pp.

PROUZA V. & TÁSLER R. 2001. Podkrkonošská pánev. 128-166. In PEŠEK J. ET AL. (eds). *Geologie a ložiska svrchnopaleozoických limnických pánví České republiky.* ČGÚ, Praha.

ŘÍDKOŠIL, T., LANGROVÁ, A. & KAŠPAR, P. 1997. Gemologické studium pyropu z Podsedic a Vestřevi. *Sborník okresního muzea Českého ráje Turnov,* 47-51.

SEIFERT A. & VRÁNA S. 2005. Bohemian garnet. *Bulletin of Geosciences 80, 2,* 113-124.

ŠTOLFOVÁ, K. 2004. *Architectural element analysis of fluvial sandstones, Vrchlabí formation, Krkonoše piedmont basin, NE Czech Republic. tectonic and climatic controls.* 78 pp. *Master thesis, Charles University, Prague, Czech Republic.*

TAJČMANOVÁ L., KONOPÁSEK J. & SCHULMANN K. 2006. Thermal evolution of the orogenic lower crust during exhumation within a thickened Moldanubian root of the Variscan belt of Central Europe. *Journal of Metamorphic Geology 24 (2).* 119-134.

TAPPAN, H. & LOEBLICH A.R.jr. 1988. Foraminiferal evolution, diversification, and extinction. *Journal of Paleontology 62 (5),* 695-714.

TÁSLER R., HAVLENA V. & PROUZA V. 1981. Nové litostratigrafické členění centrální a západní části podkrkonošské pánve. *Věstník Ústředního Ústavu Geologického 56,* 129-143.

ULIČNÝ, D., MARTÍNEK, K. & GRYGAR, R. 2002. Syndepositional Geometry and Post-Depositional Deformation of the Krkonoše Piedmont Basin. A Preliminary Model. *Proceedings of the 7th Meeting of the Czech Tectonic Studies Group, Zelazno, Poland, May 9-12, 2002, Geolines 14,* 101-102.

VRÁNA, S. 2008. Mineral inclusions in pyrope from garnet peridotites, Kolín area, central Czech Republic. *Journal of Geoscience 53, 1, 17 - 30.*

ZUKALOVÁ, V. 1976. Upper Devonian stromatoporoids, foraminifers and algae in borehole Nepasice (eastern Bohemia). *Věstník Ústředního Ústavu Geologického 51,* 281-284.

Table 1
Distribution of heavy minerals based on a semiquantitative determination (in % from total heavy fraction).

Table 2.
Representative electron microprobe analyses of garnet composition (results in wt. %).

tables 1 and 2 included only in electronic version of this document on CD-ROM

Thesis conclusions

Four facies associations recognized within the Rudník member are interpreted as: a) anoxic offshore deposits (pelagic, finely laminated black shales, carbonate/black shale laminites and carbonates), b) suboxic to oxic offshore deposits (pelagic to hemipelagic laminated grey, variegated to red mudstones and carbonates), c) nearshore and mudflat deposits (nearshore sandstones, sandstone/mudstone heterolithics, carbonates, mudflat mudstones) , and d) gravity driven deposits (turbidite sandstones, distal turbidite silty mudstones, debrite conglomerates).

The lateral distribution of sedimentary facies with high gradient facies (turbidites, debris flows) and the thickest offshore facies succession distributed along the present-day northern basin margin, and much thinner offshore facies successions and low-gradient facies (mudstone and carbonate dominated), found in the south and south-west of the basin, point to the asymmetry of Rudník Lake deposits.

The apparent asymmetry of the basin fill and the distribution of sedimentary facies reveal an original half-graben basin geometry. Subsidence along the northern basin margin fault was the main factor controlling large-scale facies architecture of the Vrchlabí Formation (Asselian) within the basin. A substantial increase in subsidence rate was probably responsible for the formation of the large (300 – 500 km^2), relatively deep and long-lived lacustrine system of the Rudník Lake.

The observed seasonal lamination is in agreement with climate models for the Early Permian.

The Rudník Lake was a complex lacustrine system with well-developed offshore and nearshore zones, a stratified water column, periods of high and mainly algal bioproductivity and eutrophication which favoured the accumulation of large amounts of hydrogen-rich kerogen in the sediments: TOC is up to 23% and HI > 500 mg/g.

Major lake level fluctuations of the Rudník lacustrine system, recorded by shallowing-up facies units in most sections throughout the basin, were followed by significant changes in lake water salinity, reflected by changes in boron content in the clay fraction of mudstones. The highstands were periods of hydrologically more open conditions and lower salinity, indicated by the low boron values. The lowstands, on the other hand, were characterized by higher salinity and higher boron values. This is interpreted as a response to an increase in the evaporation/precipitation ratio in a hydrologically closed lake.

Lake level fluctuations of the Rudník Lake can also be traced in the monotonous offshore facies-dominated section, where no sedimentological evidence of lake-level changes exists. Evidence of such changes is documented by variations in $\delta^{18}O$ and $\delta^{13}C$ values of primary calcite, $\delta^{13}C$ and Hydrogen Index (HI) of organic matter. In the first case, an upward-increase of $\delta^{18}O$, $\delta^{13}C_{calcite}$ and HI and a decrease of $\delta^{13}C_{TOC}$ in vertical sections are interpreted as a result of increased bioproductivity and lake-level lowering. It probably represents a change in climate from relatively humid to a warmer and more arid period. In the second case, the increase in $\delta^{13}C_{calcite}$ and HI, and decrease in $\delta^{13}C_{TOC}$ followed by stable and relatively low $\delta^{18}O$ values reflect an increase in bioproductivity during a period of high lake level and probably a hydrologically more open regime. This can be interpreted as the transition to warmer conditions during a stable, humid climate period.

The depositional environment of the Trutnov Formation conglomerates is interpreted as a distal alluvial fan dominated by fluvial processes. The Trutnov Formation sandstones are interpreted as a low-sinuosity fluvial system, with the following main characteristics: high variations in discharge and the preservation of unstable rock fragments, the abundance of calcretes / dolocretes suggesting seasonal to ephemeral flow and arid to semi-arid climatic conditions. The induration of palaeosurfaces by calcretes / dolocretes locally influenced the channel geometry by limiting the lateral and vertical extent of channel incision.

Scattered outcrops were correlated with each other and with well logs using the heavy mineral analysis and outcrop gamma-ray logging. Five main genetic stratigraphic units were distinguished (units 0 – 3). Units 0, 1 and 2 are characterized by the deposition of playa facies in the north, alluvial mudstones/siltstones in the basin centre and alluvial conglomerates in the south. Unit 3 is formed by alluvial conglomerates in the north and south, respectively, and fluvial sandstone facies in the basin centre. Subunits 3A, 3B and 3C, distinguished within unit 3, represent fining-up/muddying-up cycles. The Unit 2/3, 3A/3B and 3B/3C boundaries are manifested in the outcrop-scale as erosional surfaces. The recognition of different source areas for the units and subunits, as well as the correlation in the well-log data across the basin, is evidence for the basin-wide nature of these surfaces.

The higher rate of accommodation creation in the south is inferred from the higher thicknesses of Units 0 – 2. The regional basin-wide unconformity below Unit 3 records low accommodation. To allow for subsequent accumulation, stratigraphic base level must have risen and the A/S ratio increased during the deposition of Unit 3. Sorting, the occurrence of interchannel fine sediments, channel preservation and thickness decrease upwards within Unit 3, point to further a decrease of the A/S ratio. Other features, such as the upwards increase of carbonate cementation, erosional features and grain size within unit 3, are interpreted as climate change from semiarid – semihumid to more arid conditions.

The abrupt onset of Unit 3 conglomerates on playa mudstones of Unit 2 in the north can be amplified by climatic change from arid to more humid conditions in the source area causing an increase in sediment supply. This interpretation is supported by the arid/semiarid conditions of units 0 – 2, the perennial character (more humid) of the lower part of Unit 3 and the ephemeral character of the fluvial system (back to arid/semiarid) at the top of Unit 3.

The main changes in basin fill architecture are interpreted as major tectonic events. The onset of the Trutnov Formation deposition is interpreted as a major tectonic reactivation at the Autunian/Saxonian (Lower/Upper Rotliegend, ca. Sakmarian/Artinskian) boundary, when the extensional regime changed to a strike-slip regime accompanied by a transpressional uplift of the central part of the Krkonoše Piedmont Basin (KPB). The unconformity between Units 2 and 3 and the onset of high sandy sedimentation at the central part of the basin is interpreted as the later progradation of the coarse-grained material during the period of mostly inactive faults. The deposition of low-sinuosity sandstone dominated fluvial sediments over the mudstone dominated playa deposits must have been caused by a steepening of the depositional gradient and was probably accompanied by a change of climate to more humid conditions, which can most easily explain the increase in sediment supply to the basin.

The TNSB is interpreted as a pull-apart basin, the deposition of which was governed by two major dextral strike-slip faults (Hronov-Poříčí FZ and Pilníkov FZ) forming a releasing stepover.

Pebbles in Asselian – Guadalupian conglomerates of alluvial fan, nearshore lacustrine and lacustrine fan-delta deposits, which were deposited close to the northwestern and southeastern basin margin, respectively, correspond almost exclusively to local material from adjacent crystalline complexes.The heavy mineral associations of the sandstone matrix of these conglomerates support this interpretation. Crystalline units of the south-western part of the Krkonoše-Jizera Crystalline Complex and Orlice-Sněžník Crystalline Complex, respectively, are considered as the most favourable source.

The two main possible source areas for the fluvial Asselian deposits of the south-western part of the basin were found. Pebbles of late Devonian – early Carboniferous marine limestones come probably from the central part of the hypothetical Jítrava Hradec Basin, while the source of sand detrital material could be located in leucogranites and pegmatites of the north-eastern Moldanubian Zone, Přibyslavice area.

Guadalupian fluvial deposits reveal a wide range of sources, which can be attributed to the recycling of detrital material from Cisuralian and Carboniferous deposits. Garnet compositions indicate Moldanubian granulites, garnet clinopyroxenites, leucogranites and pegmatites as possible source.

Moldanubian granulites and garnet clinopyroxenites were exposed to erosion in the Early Permian at the latest.

Prohlášení

Prohlašuji, že jsem nepředložil práci ani její podstatnou část k získaní jiného nebo stejného akademického titulu jinde.

Statement

I declare, I have not submitted neither thesis nor its part to obtain other academic degree or the same degree elsewhere.

Prague, 18 November 2008

.....
Mgr. Karel Martínek